Critical Reviews in Biochemistry and Molecular Biology, 39:21–68, 2004

ISSN: 1040-9238
DOI: 10.1080/10409230490440541

Taylor & Francis
Taylor & Francis Group

Fe(II)/α-Ketoglutarate-Dependent Hydroxylases and Related Enzymes

Robert P. Hausinger

Department of Microbiology and Molecular Genetics and Department of Biochemistry and Molecular Biology, Michigan State University, East Lansing, Michigan, USA

Fe(II)/α-ketoglutarate (αKG)-dependent hydroxylases catalyze an amazing diversity of reactions that result in protein side-chain modifications, repair of alkylated DNA/RNA, biosynthesis of antibiotics and plant products, metabolism related to lipids, and biodegradation of a variety of compounds. These enzymes possess a β-strand "jellyroll" structural fold that contains three metal-binding ligands found in a His^1-X-Asp/Glu-X$_n$-His^2 motif. The co-substrate, αKG, chelates Fe(II) using its C-2 keto group (binding opposite the Asp/Glu residue) and C-1 carboxylate (coordinating opposite either His^1 or His^2). Oxidative decomposition of αKG forms CO_2 plus succinate and leads to the generation of an Fe(IV)-oxo or other activated oxygen species that hydroxylate the primary substrate. The reactive oxygen species displays alternate reactivity in related enzymes that catalyze desaturations, ring expansions, or ring closures. Other enzymes resemble the Fe(II)/αKG-dependent hydroxylases in terms of protein structure or chemical mechanism but do not utilize αKG as a substrate. This review describes the reactions catalyzed by this superfamily of enzymes, highlights key active site features revealed by structural studies, and summarizes results from spectroscopic and other approaches that provide insights into the chemical mechanisms.

Keywords hydroxylase, dioxygenase, α-ketoglutarate, ferrous ion, metalloenzyme

Editor: James A. Imlay.

Address correspondence to Robert P. Hausinger, 6193 Biomedical Physical Science, Michigan State University, East Lansing, MI 48824-4320, USA. E-mail: hausinge@msu.edu

Abbreviations: **ACC**: 1-aminocyclopropane-1-carboxylate; **αKG**: alpha-ketoglutarate; **ANS**: anthocyanidin synthase; **AtsK**: alkyl sulfatase; **CarC**: carbapenem synthase; **CAS**: clavaminate synthase; **CD**: circular dichroism; **2,4-D**: 2,4-dichlorophenoxyacetic acid; **DACS**: deacetylcephalosporin C synthase; **DAOCS**: deacetoxycephalosporin C synthase; **eIF-5A**: eukaryotic initiation factor 5A; **ENDOR**: electron nuclear double resonance; **EPR**: electron paramagnetic resonance; **ESEEM**: electron spin-echo envelop modulation; **FIH**: factor-inhibiting HIF (HIF-specific asparaginyl hydroxylase); **HIF**: hypoxia-inducible factor; **HPPD**: 4-hydroxyphenylpyruvate dioxygenase; **IPNS**: isopenicillin N synthase; **LMCT**: ligand-to-metal charge transfer; **MCD**: magnetic circular dichroism; **MLCT**: metal-to-ligand charge-transfer; **NO**: nitric oxide; **PDB**: protein database; **rR**: resonance Raman; **TauD**: taurine/αKG dioxygenase; **TfdA**: 2,4-D/αKG dioxygenase; **UV**: ultraviolet; **VHL**: von Hippel-Lindau tumor suppressor protein; **XAS**: X-ray absorption spectroscopy.

I. INTRODUCTION

This review of Fe(II)/α-ketoglutarate (αKG)-dependent hydroxylases and related enzymes begins (see Section II) by describing the amazing diversity of reactions catalyzed by members of this enzyme superfamily. Most representatives couple the oxidative decomposition of αKG (forming CO_2 and succinate) to the hydroxylation of a cosubstrate, as illustrated in Scheme 1 (the incorporated oxygen atom is shown in bold here and in the following schemes). The various types of primary substrates recognized by these enzymes include proteins, methylated nucleotides, lipids, and a wide range of small molecules that, depending on the enzyme, are used for synthesis or undergo decomposition. Other selected family members catalyze desaturation, ring expansion, ring formation, or other types of oxidative reactions. Also discussed are enzymes that function independently of αKG, yet that are related to the Fe(II)/αKG-dependent hydroxylases by sequence or mechanism. This superfamily of enzymes is united by their requirement for Fe(II), which is weakly bound by three amino acid side chains that typically occur in a His^1-X-Asp/Glu-X$_n$-His^2 motif (Table 1). When utilized as a substrate, αKG chelates the Fe(II) using its C-1 carboxylate and C-2 ketone, with additional binding stabilization provided by the C-5 carboxylate interacting with other side chains. Section III highlights the key active site features revealed by the rapidly expanding number of structural studies being carried out with this enzyme family (Table 2). Finally, insights into the mechanism of these enzymes from structural, spectroscopic, isotope incorporation, and

TABLE 1
Metal ligands and αKG-binding residues of selected Fe(II)/αKG-dependent hydroxylases and related enzymes

Enzyme	Ligand 1	Ligand 2	Spacing	Ligand 3	Spacing	αKG C-5 stabilization
Human prolyl 4-hydroxylase	His 412	Asp 414	68	His 483	9	Lys 493
Human lysyl hydroxylase	His 638	Asp 640	49	His 690	9	Arg 700
Human HIFα-specific prolyl hydroxylase-1	His 135	Asp 137	58	His 196	8	Arg 205
Human FIH	His 199	Asp 201	77	His 279	NA	Lys 214, Tyr 145, Thr 196
Escherichia coli AlkB	His 131	Asp 133	53	His 187	16	Arg 204
Streptomyces clavuligerus CAS	His 144	Glu 146	132	His 279	13	Arg 293, Thr 172
Streptomyces clavuligerus DAOCS	His 183	Asp 185	57	His 243	14	Arg 258, Ser 260
Erwinia carotovora CarC	His 101	Asp 103	147	His 251	11	Arg 263, Thr 130, Arg 253
Penicillium decumbens EpoA	His 131	Asp 133	40	His 174	10	Arg 185
Dactylosporium sp. proline 4-hydroxylase	His 109	Asp 111	103	His 215	10	Arg 226
Streptomyces sp. strain TH1 proline 3-hydroxylase	His 107	Asp 109	48	His 158	9	Arg 168, Ser 170, His 135
Petunia hydrida flavanone 3β-hydroxylase	His 220	Asp 222	55	His 278	9	Arg 288, Ser 290
Citrus unshiu flavonol synthase	His 221	Asp 223	53	His 277	9	Arg 287, Ser 289
Arabidopsis thaliana ANS	His 232	Asp 234	53	His 288	9	Arg 298, Tyr 217, Asn 215
Cucurbita maxima gibberellin 7-oxidase	His 182	Asp 184	53	His 238	9	Arg 248, Ser 250
Cucurbita maxima gibberellin 20-oxidase	His 243	Asp 245	53	His 299	9	Arg 309, Ser 311
Caranthus roseus desacetoxyvindoline-4-hydroxylase	His 308	Asp 310	55	His 366	9	Arg 376, Ser 378
Hyoscyamus niger hyoscyamine 6β-hydroxylase	His 217	Asp 219	54	His 274	9	Arg 284, Ser 286
Human trimethyllysine hydroxylase	His 201	Glu 203	146	His 350	13	Arg 364
Pseudomonas sp. AK1 β-butyrobetaine hydroxylase	His 209	Asp 211	138	His 350	11	Arg 362
Human β-butyrobetaine hydroxylase	His 202	Asp 204	142	His 347	12	Arg 360
Human phytanoyl-CoA hydroxylase	His 175	Asp 177	86	His 264	10	Arg 275
Salmonella typhimurium LpxO	His 155	Asp 157	44	His 202	9	Arg 212
Escherichia coli TauD	His 99	Asp 101	153	His 255	10	Arg 266, Thr 126
Pseudomonas putida S-313 AtsK	His 108	Asp 110	153	His 264	10	Arg 275, Thr 135
Pseudomonas stutzeri WM88 hypophosphite/αKG dioxygenase	His 116	Asp 118	87	His 206	10	Arg 217
Ralstonia eutropha TfdA	His 114	Asp 116	146	His 263	10	Arg 274
Pseudomonas syringae pv. *Phaseolicola* ethylene-forming enzyme	His 189	Asp 191	76	His 268	8	Arg 277
Escherichia coli Gab protein	His 160	Asp 162	129	His 292	12	Arg 305
Aspergillus (Emericella) nidulans IPNS	His 214	Asp 216	53	His 270	NA	NA
Tomato ACC oxidase	His 177	Asp 179	54	His 234	9	Arg 244

NA, not applicable.

biomimetic studies are described in Section IV. Notably, our current understanding of the hydroxylase mechanism represents a detailed refinement of a mechanistic proposal that was published over 20 years ago (Hanauske-Abel & Günzler, 1982). This review serves to update a series of previous surveys of this field (Abbott & Udenfriend, 1974; De Carolis & De Luca, 1994; Prescott, 1993; Prescott & Lloyd, 2000; Schofield & Zhang, 1999; Udenfriend & Cardinale, 1982) and to highlight directions for future investigations.

TABLE 2
Summary of structurally characterized Fe(II)/α-ketoglutarate-dependent hydroxylases and related enzymes

Enzyme	Molecules bound	Resolution (Å)	PDB code	Reference
Human FIH	Apoprotein	2.8	1IZ3	Lee *et al*., 2003
	Fe(II)	2.2	1MZE	Dann *et al*., 2002
	Fe(II) + αKG	2.4	1MZF	Dann *et al*., 2002
	Fe(II) + *N*-oxaloylglycine + HIFα C-terminal peptide	2.15	1H2K	Elkins *et al*., 2003
	Fe(II) + αKG + HIFα C-terminal peptide	2.25	1H2L	Elkins *et al*., 2003
	Zn(II) + *N*-oxaloylglycine + HIFα C-terminal peptide	2.5	1H2M	Elkins *et al*., 2003
	Fe(II) + αKG + HIFα C-terminal peptide	2.82	1H2N	Elkins *et al*., 2003
Streptomyces clavuligerus CAS	Apoprotein	1.63	1DS0	Zhang *et al*., 2000
	Fe(II) + αKG	1.08	1DS1	Zhang *et al*., 2000
	Fe(II) + αKG + N-α-acetyl-L-arginine	1.4	1DRY	Zhang *et al*., 2000
	Fe(II) + αKG + proclavaminic acid	2.1	1DRT	Zhang *et al*., 2000
	Fe(II) + αKG + deoxyguanidinoproclavaminic acid + NO	1.54	1GVG	Zhang *et al*., 2002
Streptomyces clavuligerus DAOCS	Apoprotein	1.3	1DCS	Valegård *et al*., 1998
	Fe(II)	1.5	1RXF	Valegård *et al*., 1998
	Fe(II) + αKG	1.5	1RXG	Valegård *et al*., 1998
	Fe(II) + succinate	1.5	1UO9	Valegård *et al*., 2004
	Fe(II) + αKG + ampicillin	1.5	1UNB	Valegård *et al*., 2004
	Fe(II) + penicillin G	1.6	1UOF	Valegård *et al*., 2004
	Fe(II) + αKG + penicillin G	1.7	1UOB	Valegård *et al*., 2004
	Fe(II) + deacetoxycephalosporin C	1.7	1UOG	Valegård *et al*., 2004
DAOCS R258Q	Fe(II) + α-keto-β-methyl-butanoate	1.5	1HJG	Lee *et al*., 2001b
DAOCS R258Q	Fe(II) + α-keto-β-methyl-pentanoate	1.6	1HJF	Lee *et al*., 2001b
DAOCS deltaR306	Fe(II) + αKG	2.1	1E5I	Lee *et al*., 2001a
DAOCS deltaR307A	Fe(II) + succinate + carbon dioxide	1.96	1E5H	Lee *et al*., 2001a
Erwinia carotovora CarC	Fe(II) + αKG	2.4	1NX4	Clifton *et al*., 2003
	Fe(II) + αKG + L-*N*-acetylproline	2.3	1NX8	Clifton et al., 2003
Streptomyces sp. strain TH1 proline 3-hydroxylase	Apoprotein	2.3	1E5R	Clifton *et al*., 2001
	Fe(II)	2.4	1E5S	Clifton *et al*., 2001
Arabidopsis thaliana ANS	Apoprotein + αKG	2.1	1GP4	Wilmouth *et al*., 2002
	Fe(II) + αKG + dihydroquercetin	2.2	1GP5	Wilmouth *et al*., 2002
	Fe(II) + αKG + dihydroquercetin + 30 min oxygen exposure	1.75	1GP6	Wilmouth *et al*., 2002
Escherichia coli TauD	Apoprotein	1.9	1OTJ	O'Brien *et al*., 2003
	Fe(II) + αKG + taurine	2.5	1GY9	Elkins *et al*., 2002
	Fe(II) + αKG + taurine	2.5	1OS7	O'Brien *et al*., 2003

(Continued on next page)

TABLE 2
Summary of structurally characterized Fe(II)/α-ketoglutarate-dependent hydroxylases and related enzymes
(Continued)

Enzyme	Molecules bound	Resolution (Å)	PDB code	Reference
Pseudomonas putida S-313 AtsK	Sodium ion	1.9	1OIH	Müller *et al*., 2004
	Na + αKG	2.07	1OIJ	Müller *et al*., 2004
	Fe(II) + αKG	2.2	1OII	Müller *et al*., 2004
	Fe(II) + αKG + 2-ethylhexyl-1-sulfate	2.05	1OIK	Müller *et al*., 2004
Escherichia coli Gab protein	Apoprotein	2	1JR7	Chance *et al*., 2002
Aspergillus (Emericella) nidulans	Mn(II)	2.5	1IPS	Roach *et al*., 1995
IPNS	Fe(II) + δ-(L-α-aminoadipoyl)-L-cysteinyl-D-valine	1.3	1BK0	Roach *et al*., 1997
	Fe(II) + δ-(L-α-aminoadipoyl)-L-cysteinyl-D-valine + NO	1.45	1BLZ	Roach *et al*., 1997
	Fe(II) + isopenicillin *N*	1.35	1QJE	Burzlaff *et al*., 1999
	Fe(II) + δ-(L-α-aminoadipoyl)-L-cysteinyl-L-*S*-cysteine	1.5	1QIQ	Burzlaff *et al*., 1999
	Fe(II) + δ-(L-α-aminoadipoyl)-L-cysteinyl-L-*S*-cysteine + oxygen	1.4	1QJF	Burzlaff *et al*., 1999
	Fe(II) + δ-(L-α-aminoadipoyl)-L-cysteinyl-D-α-hydroxyvaleryl ester	1.55	1HB1	Ogle *et al.*, 2001
	Fe(II) + δ-(L-α-aminoadipoyl)-L-cysteinyl-D-α-hydroxyvaleryl ester + oxygen 30 s	1.3	1HB2	Ogle *et al.*, 2001
	Fe(II) + δ-(L-α-aminoadipoyl)-L-cysteinyl-D-α-hydroxyvaleryl ester + oxygen 30 s	1.4	1HB3	Ogle *et al.*, 2001
	Fe(II) + δ-(L-α-aminoadipoyl)-L-cysteinyl-D-α-hydroxyvaleryl ester + oxygen 120 s	1.5	1HB4	Ogle *et al.*, 2001
	Fe(II) + δ-(L-α-aminoadipoyl)-L-cysteinyl-D-α-aminobutyrate	2.2	1OC1	Long *et al*., 2003
	Fe(II) + δ-(L-α-aminoadipoyl)-L-cysteinyl-D-α-aminobutyrate + NO	1.3	1OBN	Long *et al*., 2003
Pseudomonas fluorescens HPPD	Fe(II)	2.4	1CJX	Serre *et al*., 1999

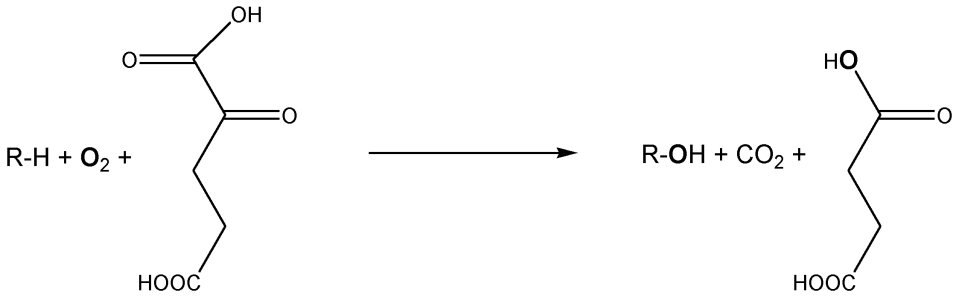

SCHEME 1.

II. REACTIONS OF Fe(II)/α-KETOGLUTARATE-DEPENDENT HYDROXYLASES AND RELATED ENZYMES

A. Protein Modification

At least four distinct Fe(II)/αKG-dependent hydroxylases utilize the side chains of proteins as substrates, resulting in the modification of proline, lysine, aspartic acid, and asparagine residues. Studies of these enzymes range from the earliest work on Fe(II)/αKG-hydroxylases through very recent investigations related to hypoxia-induced cellular signaling events.

Prolyl 4-hydroxylase, the first Fe(II)/αKG-dependent hydroxylase identified (Hutton *et al.*, 1966), catalyzes the reaction illustrated in Scheme 2 to yield the *trans*-4-hydroxyprolyl group. In mammals, this activity is essential to the formation of collagens, elastins, and several other proteins (Kivirikko & Pihlajaniemi, 1998). For example, type I collagen contains lengthy Gly-X-Y repeats with about 10% of the Y positions occupied by 4-hydroxyproline. The hydroxylated residue forms both inter- and intrachain hydrogen bonds, thus stabilizing the protein's unique triple-helical structure. In plants, prolyl 4-hydroxylase targets precursors of the extensions, repetitive proline-rich proteins, arabinogalactan-proteins, and other key components of the extracellular matrix and reproductive tissues (Kieliszewski & Lamport, 1994; Wu *et al.*, 2001). Genes encoding prolyl 4-hydroxylase have been cloned from human (Helaakoski *et al.*, 1989), plant (Hieta & Myllyharju, 2002), insect (Annunem *et al.*, 1999), nematode (Veijola *et al.*, 1994), and other sources, including *Paramecium bursaria Chlorella* virus-1 (Ericksson *et al.*, 1999), suggesting a role for 4-hydroxyproline in this algal-specific virus. In most cases, the enzyme is comprised of two distinct subunits, the hydroxylase α subunit and a protein disulfide isomerase β subunit which maintains solubility; however, algal and plant prolyl 4-hydroxylases are monomeric proteins (Hieta & Myllyharju, 2002; Kaska *et al.*, 1988). Results from site-directed mutagenesis studies of the human enzyme were interpreted to suggest that His 412, Asp 414, and His 483 coordinate Fe(II), Lys 493 binds the C-5 carboxylate of αKG (with the K493R variant retaining 15% of the wild-type enzyme activity), and His

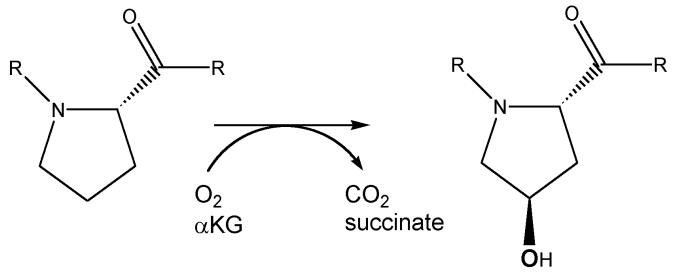

SCHEME 2.

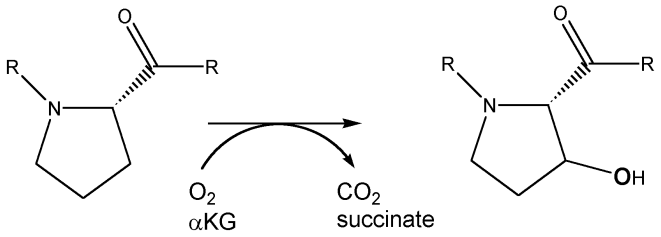

SCHEME 3.

501 having a critical but undefined role (Table 1) (Lamberg *et al.*, 1995; Myllyharju & Kivirikko, 1997). The peptide substrate-binding domain of human collagen prolyl 4-hydroxylase was crystalized (Pekkala *et al.*, 2003), but this domain is separate from the catalytic domain and no structure has been reported.

Much less information is available for prolyl 3-hydroxylase, an enzyme catalyzing the reaction shown in Scheme 3. This activity has been resolved from prolyl 4-hydroxylase (Tryggvason *et al.*, 1976) and partially purified from several sources (Risteli *et al.*, 1977; Tryggvason *et al.*, 1979); however, no subunit or sequence information is available. Procollagen is the only known natural substrate of this enzyme, with mature collagen containing 3-hydroxyproline levels up to 10% of the amount of 4-hydroxyproline (Kivirikko & Pihlajaniemi, 1998).

Lysyl hydroxylase is a medically important enzyme that catalyzes the reaction indicated in Scheme 4. The enzyme hydroxylates 0.5% to 7% of the X-Lys-Gly triplets of procollagen, with the modification serving as the attachment site for galactose or glucosylgalactose units (Kivirikko & Pihlajaniemi, 1998). In addition, many other proteins are known to contain this modified amino acid. Defects in lysyl hydroxylase activity are associated with the type VI variant of Ehlers-Danlos syndrome, leading to various connective tissue problems (e.g., joint hypermobility, skin hyperextensibility, and skin fragility). Three related isoforms of lysyl hydroxylase have been identified in humans (Hautala *et al.*, 1992; Passoja *et al.*, 1998; Valtavaara *et al.*, 1997,

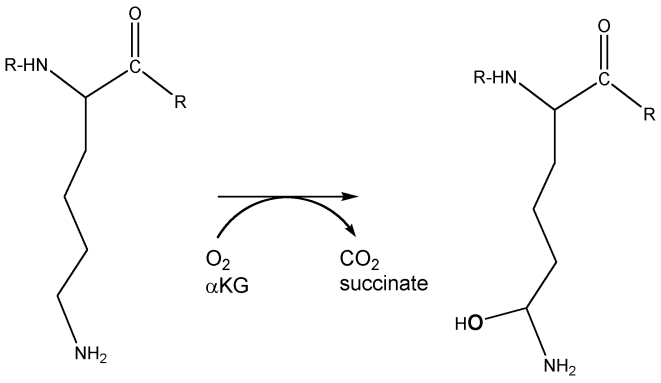

SCHEME 4.

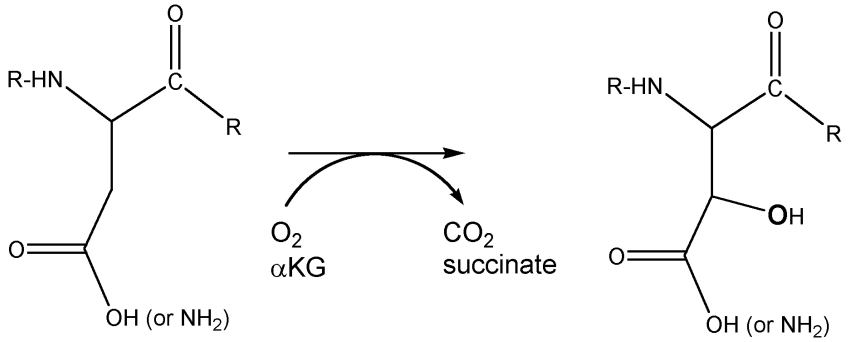

SCHEME 5.

1998). Site-directed mutagenesis studies were carried out on one of the human genes, and the results obtained with the variant homodimeric enzymes were interpreted to suggest that His 638, Asp 640, and His 690 (Table 1, residue numbers after processing of the protein) are metal ligands, Arg 700 stabilizes the C-5 carboxylate of αKG (with the K700R variant retaining about 10% activity), and His 688 plays an additional critical role (Passoja *et al.*, 1998; Pirskanen *et al.*, 1996).

A specific lysyl residue of eukaryotic initiation factor 5A (eIF-5A) undergoes a two-step modification, including hydroxylation, to produce hypusine (*N*-ε-(4-amino-2-hydroxybutyl) lysine) (Park *et al.*, 1993). The NAD-dependent enzyme deoxyhypusine synthase first transfers the butylamine group of spermine to the eIF-5A lysyl group in a reversible reaction (Park *et al.*, 2003), then deoxyhypusyl hydroxylase completes the transformation. Initial studies of the hydroxylase activity led to the conclusion that enzyme reactivity was independent of Fe(II) and αKG (Abbruzzese *et al.*, 1986); however, later inhibition studies with metal chelators provided evidence of an essential Fe(II) binding site (Abbruzzese *et al.*, 1991; Clement *et al.*, 2002). More recently, deoxyhypusyl hydroxylase has been purified and shown to be a member of the Fe(II)/αKG-dependent hydroxylases (George McLendon, personal communication). The role of this modified residue is unknown, but the eIF-5A protein is essential for cell proliferation.

Aspartyl (asparaginyl) β-hydroxylase modifies the β-carbon of specific aspartic acid or asparagine residues (Scheme 5) in the epidermal growth factor-like domains of a number of vitamin K-dependent proteins, coagulation factors, and complement factors. The modified residue forms a calcium-binding site, likely to be important for protein–protein interactions. Since its discovery in 1989 (Gronke *et al.*, 1989; Stenflo *et al.*, 1989), the monomeric enzyme was purified and characterized (Wang *et al.*, 1991) and the gene has been cloned and expressed from several sources, including humans (Jia *et al.*, 1992; Korioth *et al.*, 1994). Mutagenesis studies of the bovine gene led to the proposal that His 675 is one of the metal ligands, where substitution of this residue by Asp or Glu retains some activity (Jia *et al.*, 1994; McGinnis *et al.*, 1996). Notably, His 675 is not preceded by a His-X-Asp/Glu sequence, so the identity of additional metal ligands remains unclear. Also of interest, overexpression of human aspartyl (asparaginyl) β-hydroxylase in NIH-3T3 cells is associated with malignant transformation—for unknown reasons. (Ince *et al.*, 2000).

Although protein hydroxylases have been studied for decades, interest in this enzyme group has intensified since the discovery, in 2001, of their involvement in the hypoxic response. Oxygen deprivation, or hypoxia, occurs during tumor formation, diabetes, and other ischemic diseases, leading to hypoxia-inducible factor (HIF)-dependent transcription of a wide variety of genes. The two subunits of this heterodimeric transcription factor (HIFα and HIFβ) are constitutively synthesized, but HIFα is targeted for degradation in cells containing normal oxygen concentrations. Two enzymes catalyzing side-chain hydroxylation are involved in this process (Hewitson *et al.*, 2003).

A prolyl 4-hydroxylase plays a key role in targeting HIFα for degradation on the basis of evidence indicating that Pro 564 of HIFα is hydroxylated in an oxygen-, Fe(II)-, and αKG-dependent reaction (Ivan *et al.*, 2001; Jaakkola *et al.*, 2001). The hydroxylated HIFα forms a complex with the von Hippel-Lindau tumor suppressor protein (VHL), elongin B, and elongin C, resulting in polyubiquitinylation and destruction of the transcription factor subunit. The hypoxia-mimicking effects of cobalt and desferrioxamine are thus understood to result from inhibition of the prolyl 4-hydroxylase activity (Minchenko *et al.*, 2002). Similarly, a lack of VHL-directed degradation of HIFα explains the elevated expression of hypoxia-inducible genes caused by suppression of *Drosophila melanogaster* prolyl 4-hydroxylase by RNA interference (Bruick & McKnight, 2001). The structural basis for the hydroxylation-specific interaction was elucidated by two crystallography studies involving a complex comprised of a Pro 564-containing peptide of HIFα, VHL, and the two elongin proteins (Hon *et al.*, 2002; Min *et al.*, 2002). The hydroxyproline residue nicely fits into a gap of the

VHL core with optimized hydrogen bonding interactions. The VHL protein was shown to ubiquitinylate two independently-acting sites within HIFα (Masson *et al.*, 2001). EGL-9 protein in *C. elegans* was predicted to be an Fe(II)/αKG-dependent hydroxylase (Aravind & Koonin, 2001) and later shown to be a HIFα-specific prolyl 4-hydroxylase (Epstein *et al.*, 2001). A family of isoforms exists in humans—each containing the signature sequence of Fe(II)/αKG-dependent hydroxylases (Table 1) (Bruick & McKnight, 2001; Epstein *et al.*, 2001; Oehme *et al.*, 2002). No crystal structure has yet been reported for a HIFα-specific prolyl hydroxylase; however, two sets of coordinates have been deposited in the Protein Data Bank (PDB; access codes 1IZF and 1IZG), so this information may be forthcoming.

Superimposed on the hypoxia-inducible effects associated with the HIFα-specific prolyl 4-hydroxylase is a process involving hydroxylation of Asn 803. In the absence of hydroxylation the HIFα domain binds to the p300 protein with the target Asn deeply buried at the molecular interface (Dames *et al.*, 2002; Freedman *et al.*, 2002). Hydroxylation of Asn 803 in the carboxyl-terminal transactivation domain of HIFα prevents its interaction with the p300 transcription coactivator (Lando *et al.*, 2002). Interestingly, the stereospecificity of the hydroxylation reaction is distinct from that observed for the well-studied aspartyl/asparaginyl hydroxylases, resulting in the *threo*-isomer rather than the *erythro*-isomer (McNeill *et al.*, 2002a). A yeast two-hybrid approach was used to identify the HIFα-specific asparaginyl hydroxylase that was shown to be identical to the "factor-inhibiting HIF" (FIH), a protein known to interact with HIFα and VHL and to repress HIF transcriptional activity (Hewitson *et al.*, 2002; Mahon *et al.*, 2001). As summarized in Table 2, the structures of the apoprotein (Lee *et al.*, 2003), the Fe(II)- and αKG-bound form of FIH (Dann *et al.*, 2002), and the complex between FIH and a carboxyl-terminal domain of HIFα (Elkins *et al.*, 2003) were elucidated. The metal ligands are His 199, Asp 201, and His 279, whereas Tyr 145, Thr 196, and Lys 214 stabilize binding of the αKG C-5 carboxylate in a unique type of interaction (Table 1). The HIFα Asn 803 is ideally oriented to undergo the observed reaction at the FIH active site, but oxidation during crystallization was prevented by the use of anaerobic conditions.

B. Repair of Alkylated DNA/RNA

The newest function ascribed to the Fe(II)/αKG-dependent hydroxylases is repair of alkylation-damaged DNA and RNA. Cellular polynucleotides are alkylated by endogenous components, such as *S*-adenosylmethionine, and by reaction with two general classes of environmental and laboratory chemicals. S_N1 agents include methylnitrosourea and *N*-methyl-*N*′-nitro-*N*-nitrosoguanidine that react with the N^7 position of guanine, N^3 of adenine, O^6 of guanine, O^2 or O^4 of pyrimidines, and the nonphosphodiester oxygen atoms of the phosphate backbone. In contrast, S_N2 agents such as methylmethanesulfonate and dimethylsulfate react primarily with the N^1 position of adenine and N^3 of cytosine (Sedgwick & Lindahl, 2002). To overcome the mutagenic and toxic effects of these modifications, cells produce a variety of DNA repair enzymes. For example, *Escherichia coli* possesses two distinct 3-methyladenine DNA glycosylases, encoded by *tag* and *alkA*, that remove the offending alkyl groups along with the attached adenines to create abasic sites in the DNA product. Alternatively, *ogt* and *ada* encode O^6-methylguanine methyltransferases, while *ada* also encodes O^4-methylthymine methyltransferase and methylphosphotriester methyltransferase activities. These single-turnover proteins transfer the target methyl groups to their active site cysteine residues, thus inactivating their activities. While *tag* and *ogt* are constitutively expressed, methyl transfer to Cys 69 of the *ada* gene product converts it into an activator that increases expression of *alkA*, *ada*, *aidB* (somehow involved in protection against S_N1 agents), and *alkB*. As described below, *alkB* encodes an Fe(II)/αKG-dependent hydroxylase that directly repairs 1-alkyladenine and 3-alkylcytosine lesions in DNA or RNA (Schemes 6 and 7).

Nearly 20 years were required to identify the function of *alkB* following its initial description as an *E. coli* gene that modestly affects reactivation of methylmethanesulfonate-treated phage lambda (Kataoka *et al.*, 1983). The gene was cloned and sequenced (Kataoka & Sekiguchi, 1985) and the protein purified (Kondo *et al.*, 1986), but without any clarification of its role. Expression of *E. coli alkB* in human cells was shown to confer resistance to high concentrations of S_N2 alkylating agents (Chen *et al.*, 1994), demonstrating that the enzyme functions independently of other cellular components. In contrast to the weak effects observed for *alkB* mutants on reactivation of methylated double-stranded phage (lambda and M13), pronounced deficiencies were noted for reactivation of the methylmethanesulfonate-treated single-stranded DNA viruses (M13, f1, and G4) (Dinglay *et al.*, 2000) and a single-stranded RNA virus (Aas *et al.*, 2003). These results are most compatible with repair of 1-methyladenine and 3-methylcytosine lesions that are preferentially formed by methylation of single-strand polynucleotides. Critical insight into the role of this enzyme was derived from iterative sequence analyses that identified AlkB as a member of the Fe(II)/αKG-dependent dioxygenase superfamily (Aravind & Koonin, 2001). This suspicion was confirmed by studies demonstrating direct repair of methylated DNA by AlkB in an Fe(II)-dependent process that consumes oxygen plus αKG and produces succinate plus formaldehyde (Trewick *et al.*, 2002), thus resulting in release of replication blocks (Falnes *et al.*, 2002). Subsequently, direct

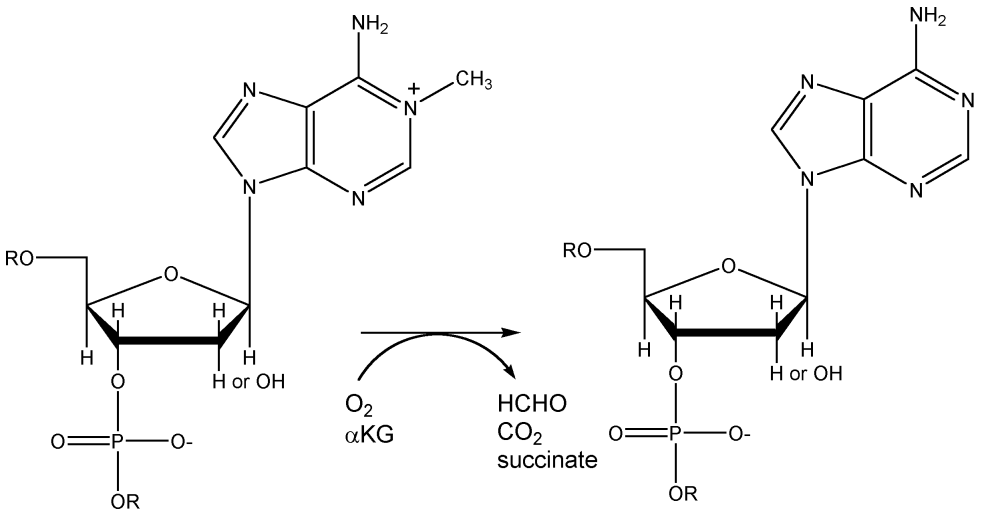

SCHEME 6.

repair of methylated RNA lesions was established (Aas *et al.*, 2003). *In vitro* investigations reveal that the sites repaired by AlkB include 1-methyladenine and 3-methylcytosine in DNA (Trewick *et al.*, 2002) or RNA (Aas *et al.*, 2003), as well as adducts containing ethyl (Duncan *et al.*, 2002), hydroxyethyl, propyl, and hydroxylpropyl groups (Koivisto *et al.*, 2003). Trewick *et al.* (2002) noted that αKG decomposition is partially uncoupled from DNA repair, accounting for the observed ascorbate requirement for AlkB activity (described further in Section IV part I). Only this uncoupled reaction is observed when using the small molecules 1-methyladenosine, 1-methyl-2′-deoxyadenosine, 3-methylcytidine, and 3-methyl-2′-deoxycytidine (Welford *et al.*, 2003). In contrast, demethylation is achieved by the enzyme when using the oligonucleotide trimer d(Tp1meApT) or 5′ phosphorylated 1-me-dAMP (Koivisto *et al.*, 2003). The bacterial enzyme contains the likely metal- and αKG-binding residues His 131, Asp 133, His 187, and Arg 204 (Table 1). Each of the putative metal ligands was individually changed to cysteine by site-directed mutation of the corresponding codons, and the variant proteins were shown to undergo thiol:disulfide exchange reactions with disulfide-containing DNA (synthesized with thiol-substituted cytosine and derivatized with diaminoethane disulfide to create the mixed disulfide) to covalently attach AlkB to the DNA (Mishina & He, 2003). These studies demonstrate that DNA has access to the AlkB active site, but they do not provide any information related to the normal binding mode of this substrate. Although no crystallographic results have been reported yet, a theoretical model of the enzyme structure has been reported (Henshaw *et al.*, 2004).

Eight human homologues of *alkB* have been identified (termed *hABH1* through *hABH8*) (Duncan *et al.*, 2002;

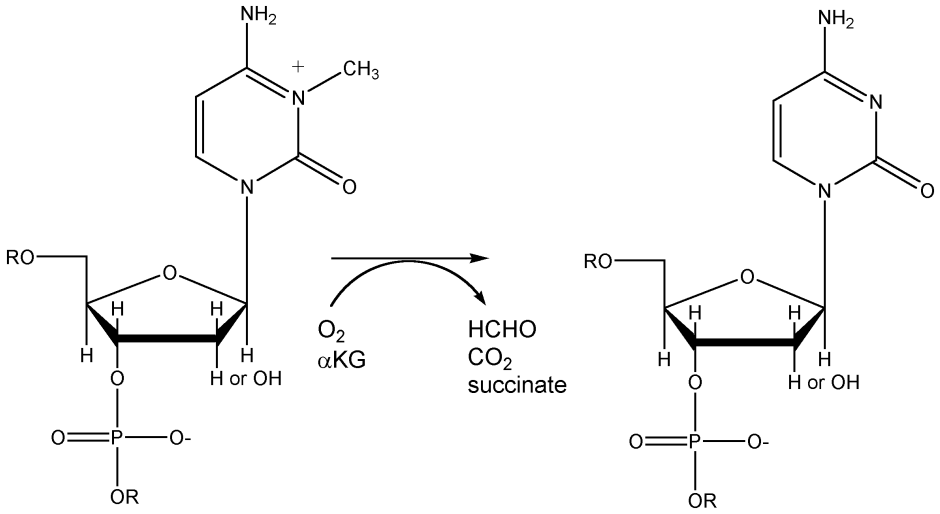

SCHEME 7.

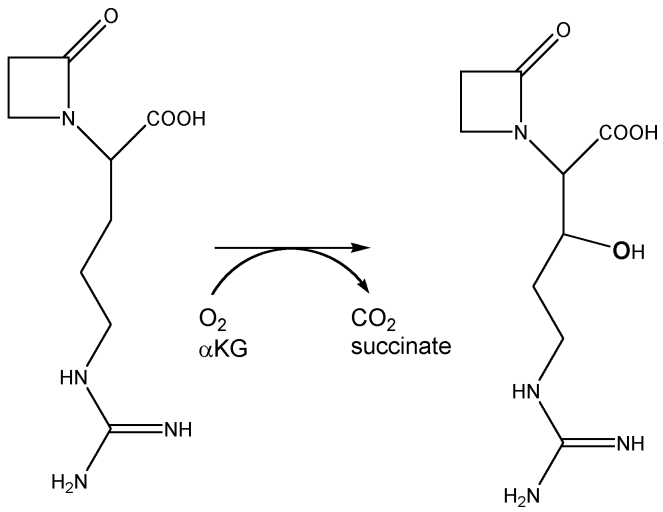

SCHEME 8.

Kurowski *et al.*, 2003). Curiously, a clone containing *hABH1* initially was reported to complement an *E. coli alkB* mutant (Wei *et al.*, 1996), but other researchers could not reproduce this result (Duncan *et al.*, 2002) and the purified gene product was inactive for repair of methylated DNA or RNA (Aas *et al.*, 2003; Duncan *et al.*, 2002). Both *hABH2* and *hABH3* complement an *alkB* mutant and encode enzymes capable of repairing 1-methyladenine, 3-methylcytosine, and 1-ethyladenine lesions in DNA (Duncan *et al.*, 2002). In addition, ABH3 (but not ABH2) repairs alkylated RNA (Aas *et al.*, 2003). In addition, ABH2 and ABH3 (but not ABH1) can form crosslinks to disulfide-containing DNA when these proteins are modified to replace a metal ligand residue with a cysteine; thus confirming their similarities to AlkB (Mishina *et al.*, 2004). No biochemical studies have been reported for the remaining five homologues (Kurowski *et al.*, 2003). A three-dimensional model was constructed for the core of ABH3, but no crystal structures are reported for any of these human proteins.

C. Biosynthesis of Antibiotics

Fe(II)/αKG-dependent dioxygenases function during the biosynthesis of a diverse range of antibiotics. In addition to catalyzing a variety of hydroxylation reactions, some family members catalyze desaturation, ring expansion, ring formation, and other types of chemical transformations. The positions of these enzymes in antibiotic pathways vary from the generation of precursors to the modification of more complete intermediates. The following paragraphs describe biochemical studies on the better-studied representatives of the Fe(II)/αKG-dependent dioxygenases involved in antibiotic synthesis; however, it is important to note that sequence analyses are consistent with similar enzymes participating in a number of other pathways (e.g., those generating mitomycin C, nikkomycin, syringomycin, and viomycin (Chen *et al.*, 2000; Mao *et al.*, 1999; Yin *et al.*, 2003; Zhang *et al.*, 1995)).

Clavaminate synthase (CAS) catalyzes three separate oxidative steps in the synthesis of clavulanic acid and exemplifies the versatility of Fe(II)/αKG-dependent dioxygenases (Lloyd *et al.*, 1999b). The enzyme hydroxylates the β-lactam illustrated in Scheme 8, in a reaction comparable to other Fe(II)/αKG-dependent hydroxylases. Proclavaminate amidinohydrolase then hydrolyzes the guanidino group to yield proclavaminic acid, and clavaminate synthase catalyzes sequential cyclization and desaturation reactions as shown in Scheme 9. Most studies of clavaminate synthase have been carried out using the two isozymes from *Streptomyces clavuligerus* (Busby *et al.*, 1995; Marsh *et al.*, 1992), but the single *Streptomyces antibioticus* CAS isozyme also was purified and shown to exhibit the trifunctional activities (Janc *et al.*, 1995). Results from site-directed mutagenesis studies suggest that His 145 and His 280 are likely to be metal ligands in CAS isozyme 2 from *S. clavuligerus* (Khaleeli *et al.*, 2000). The crystal structure of Fe(II)- and αKG-bound CAS isozyme 1 in the presence of N-α-acetyl-L-arginine or proclavaminic acid (under anaerobic conditions, Table 2) confirms that the

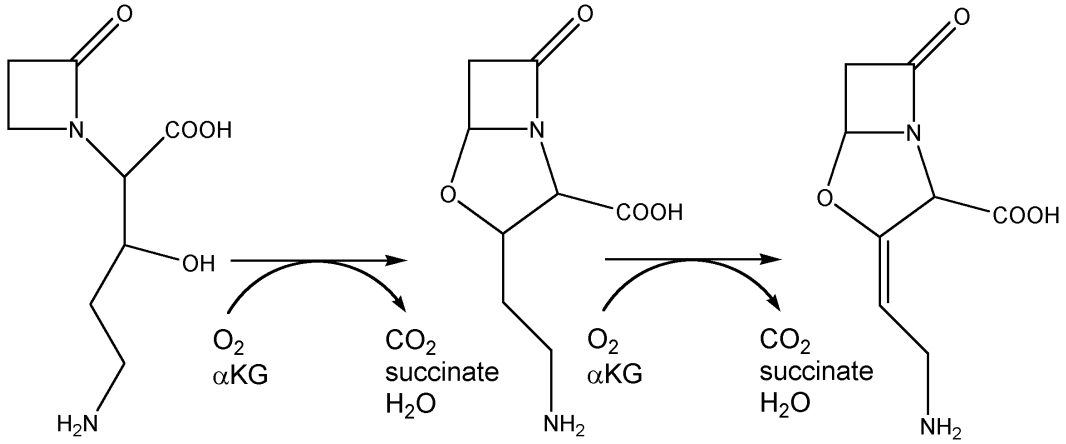

SCHEME 9.

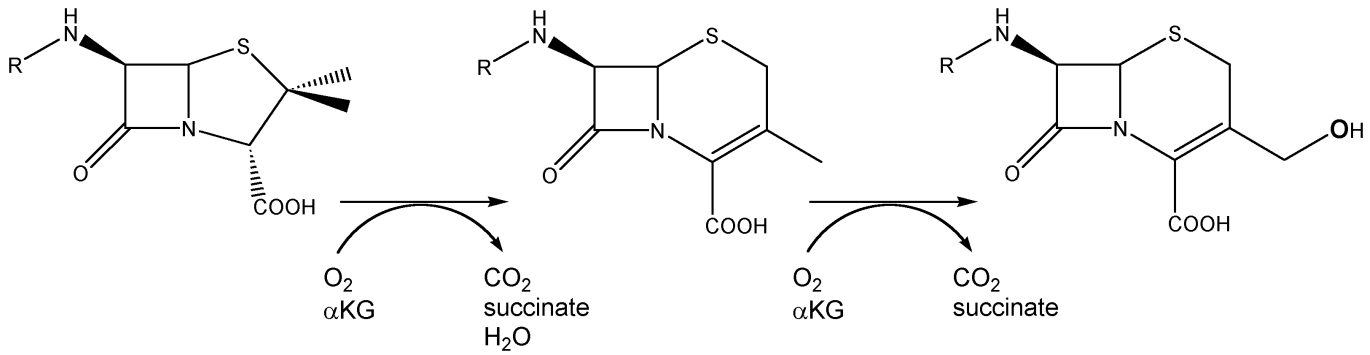

SCHEME 10.

corresponding histidines and a glutamic acid (His 144, Glu 146, and His 279) bind Fe(II) (Zhang *et al.*, 2000). In addition, the structure reveals that the C-5 carboxylate of αKG interacts with Arg 293 and Thr 172 (Table 1). Subtle differences in the binding modes of the two substrates likely relate to their distinct hydroxylase versus ring-forming/desaturase reactivities.

Deacetoxycephalosporin C synthase (DAOCS) and deacetylcephalosporin C synthase (DACS) are Fe(II)/αKG-dependent dioxygenases that catalyze sequential reactions starting with penicillin N in cephalosporin synthesis, as depicted in Scheme 10. A single enzyme carries out the ring expansion and hydroxylase reactions in *Cephalosporium acremonium* according to gene cloning and enzyme isolation studies (Baldwin *et al.*, 1987; Dotzlaf & Yeh, 1987; Samson *et al.*, 1985). In contrast, separate but related enzymes are found in *Streptomyces clavuligerus*. The second enzyme, DACS, was purified from *S. clavuligerus*, found to be a monomer, kinetically characterized, and shown to exhibit slight expandase activity (Baker *et al.*, 1991). The gene was cloned encoding *S. clavuligerus* DAOCS, the first enzyme in the sequence, allowing recombinant enzyme to be produced and extensively characterized (Dotzlaf & Yeh, 1989; Kovacevic *et al.*, 1989). This protein undergoes a monomer-to-trimer equilibrium according to gel filtration chromatography and light-scattering analyses (Lloyd *et al.*, 1999a). Results from extended X-ray absorption fine structure spectroscopy provide evidence for two histidine ligands to the six-coordinate metal site in the absence or presence of αKG (Lloyd *et al.*, 1999a). Crystallographic investigations of anaerobic samples were used to confirm the trimeric nature of the protein, identify the metal ligands as His 183, Asp 185, and His 243, and reveal interactions between the αKG C-5 carboxylate and Arg 258 as well as Ser 260 (Tables 1 and 2) (Valegård *et al.*, 1998). The R258Q variant uses αKG poorly because it lacks the ability to form a salt bridge to the C-5 carboxylate of this substrate; however, the mutant DAOCS exhibits enhanced reactivity with aliphatic α-ketoacids—a process termed "chemical co-substrate rescue" by the authors (Lee *et al.*, 2001b). An array of active site variants has been investigated, providing evidence that Arg 160, Arg 162, and Arg 266 are important for binding penicillin N (Lipscomb *et al.*, 2002) and that changes to several other residues can affect catalysis (Lee *et al.*, 2002). For example, substitution of a single amino acid side chain was shown to control whether the enzyme catalyzes ring expansion, methyl group hydroxylation, or both reactions (Lloyd *et al.*, 2004). Additional DAOCS crystallographic studies have revealed critical features of substrate and product binding, as described in Section III.

Carbapenem synthase (CarC) catalyzes an Fe(II)/αKG-dependent desaturation reaction, similar to CAS and DAOCS, and additionally exhibits an epimerization reaction at the tertiary carbon atom that joins the two rings in the bicyclic structure (Scheme 11). The best-characterized example of this enzyme, derived from *Erwinia carotovora*, is 23% identical to CAS (McGowan *et al.*, 1996). Crystal structures were obtained for the enzyme in the presence of Fe(II) plus αKG and with the substrate analogue L-*N*-acetylproline (Table 2) (Clifton *et al.*, 2003). The structural results show that His 101, Asp 103, and His 251 are metal ligands while Arg 263, Thr 130, and Arg 253 are used to stabilize the C-5 carboxylate of αKG (Table 1).

Another family member appears to catalyze a step in the semisynthetic pathway of the antibiotic fosfomycin (Watanabe *et al.*, 1999). *Penicillium decumbens* was shown to possess an epoxidase activity, encoded by *epoA*, which converts chemically synthesized *cis*-propenylphosphonic acid to the broad-spectrum antibiotic (Scheme 12). The natural function of this enzyme is unclear. The sequence of the gene product contains His 131, Asp 133, His 174, and Arg 185 (the standard Fe(II)/αKG-dependent hydroxylase motif; Table 1) and otherwise resembles the sequence of proline 4-hydroxylase. No activity was detected in cell extracts, but it is unclear whether αKG was included in the assay mixture.

Proline hydroxylases provide a paradigm of Fe(II)/αKG-dependent hydroxylases that participate in antibiotic synthesis by producing hydroxylated precursors. The

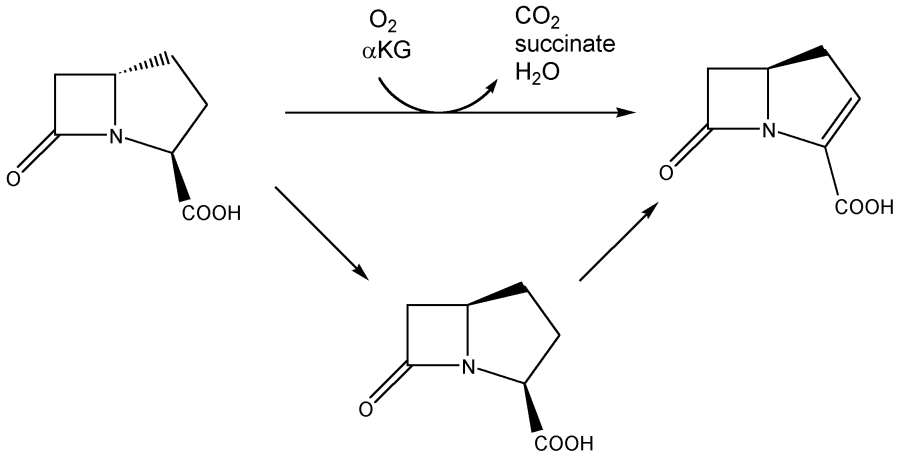

SCHEME 11.

proline 4-hydroxylase from *Streptomyces griseoviridus* uses the free amino acid, as shown in Scheme 13, rather than a protein side chain, as described earlier, to produce *trans*-4-hydroxyproline that is subsequently incorporated into the antibiotic entamycin (Lawrence *et al.*, 1996). Analogous enzymes occur in selected other strains of *Streptomyces*, *Amycolatopsis*, and *Dactylosporangium*, with the gene being cloned (Table 1) and enzyme characterized from one of the latter species (Shibasaki *et al.*, 1999). Similarly, proline 3-hydroxylase activity (Scheme 14) was detected in two *Bacillus* strains and two *Streptomyces* strains, including *S. canus* ATCC 12647—a producer of the peptide antibiotic telomycin (Mori *et al.*, 1996). Of note, the product in this case is the *cis* isomer of 3-hydroxyproline. The gene-encoding proline 3-hydroxylase was cloned and the enzyme characterized from *Streptomyces* sp. strain TH1 (Mori *et al.*, 1997). This enzyme is a monomer like the proline 4-hydroxylase, but distinct from the heteromeric prolyl 4-hydroxylase. The fungus *Glara lozoyensis* possesses two distinct enzymes that produce *trans*-3-hydroxyproline or *trans*-4-hydroxyproline (Petersen *et al.*, 2003), but no sequence information is available for the two isozymes. The structures of *Streptomyces* sp. strain TH1 proline 3-hydroxylase apoprotein and the anaerobic, Fe(II)-bound form reveal His 107, Asp 109, and His 158 as metallocenter ligands, while Arg 168, Ser 170, and His 135 are likely to bind αKG (Tables 1 and 2) (Clifton *et al.*, 2001).

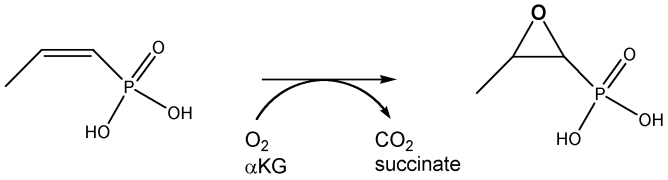

SCHEME 12.

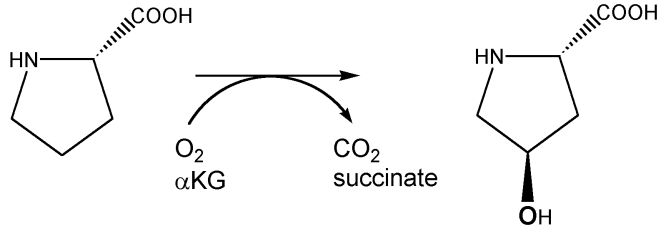

SCHEME 13.

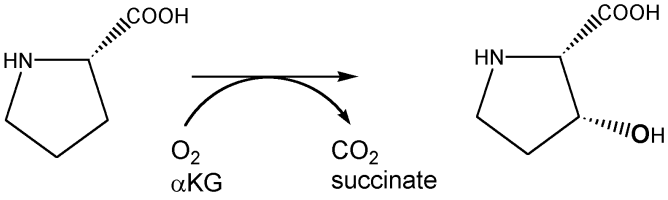

SCHEME 14.

It is reasonable to suggest that Fe(II)/αKG-dependent hydroxylases might provide precursors or otherwise contribute to the synthesis of many additional antibiotics (Chen *et al.*, 2001). For example, a gene in *Streptomyces verticillus* was proposed to encode a histidine hydroxylase, responsible for production of β-hydroxyhistidine in bleomycin, a cancer chemotherapy agent (Calcutt & Schmidt, 1994). Streptothricin synthesis utilizes 3-hydroxyarginine (Martinkus *et al.*, 1983), possibly synthesized by an enzyme analogous to CAS. An alternative arginine hydroxylase might participate in synthesis of the peptide antibiotic K-582, which contains 4-hydroxyarginine (Kawauchi *et al.*, 1983). On the other hand, without studies of the purified enzymes and sequence information one must be cautious in assigning roles to Fe(II)/αKG-dependent hydroxylases during antibiotic synthesis. For

example, investigations carried out with cell extracts of *Streptomyces fradiae* led to the suggestion that two Fe(II)/αKG-dependent hydroxylases participate in the synthesis of the antibiotic tylosin (Omura *et al.*, 1984). Both of the reactions were stated to require αKG and oxygen, and CO_2 production was shown to be stoichiometric with formation of one product. Nevertheless, more recent genetic analyses and DNA sequencing studies (summarized in Cundliffe *et al.*, 2001)) reveal that these reactions are carried out by cytochrome P450-type enzymes.

D. Biosynthesis of Plant Products

Plants synthesize a remarkable variety of compounds by use of Fe(II)/αKG-dependent dioxygenases. The following paragraphs focus on the use of such enzymes during biosynthetic transformations of flavonoids, gibberellins, and alkaloids. The flavonoids include flavones, isoflavones, flavonols, anthocyanins, and other compounds that provide color to plants, protect them from ultraviolet (UV)-induced photodamage, act as signaling molecules in plant-microbe interactions, serve as defense molecules against pathogens, and exhibit a myriad of other plant roles (Bohm, 1998) while also acting as antioxidants, antimalarial medicines, and possible anticancer agents in humans (Bohm, 1998; Le Marchand, 2002). Gibberellins are tetracyclic diterpene phytohormones that regulate growth and development (Hedden, 1999; Hedden & Kamiya, 1997; Hedden & Phillips, 2000). The structurally complex alkaloids include important drugs that have experimental and therapeutic importance. In addition to participating in biosynthesis of these three types of compounds (described below), Fe(II)/αKG-dependent dioxygenases are likely to play additional roles in plants, such as the *Fusarium verticillioides FUM9* gene product that functions in the synthesis of the polyketide mycotoxin fumonisin (Seo *et al.*, 2001).

Flavanone 3β-hydroxylase catalyzes one of the key steps of flavonoid biosynthesis (top reaction in Scheme 15) in which flavanones (such as naringenin depicted here) are converted to *trans*-dihydroflavonols (such as the dihydrokaempferol illustrated). The enzyme from *Petunia hybrida* was purified in 1986 and shown to be an Fe(II)/αKG-dependent hydroxylase (Britsch & Grisebach, 1986). The gene encoding this enzyme has been cloned and sequenced from petunia (Britsch *et al.*, 1992) and several other plants (Britsch *et al.*, 1993; Charrier *et al.*, 1995; Pelletier & Shirley, 1996), and recombinant *P. hybrida* enzyme was purified (Lukacin *et al.*, 2000b). Results derived from mutagenesis studies (Table 1) of the recombinant *P. hybrida*

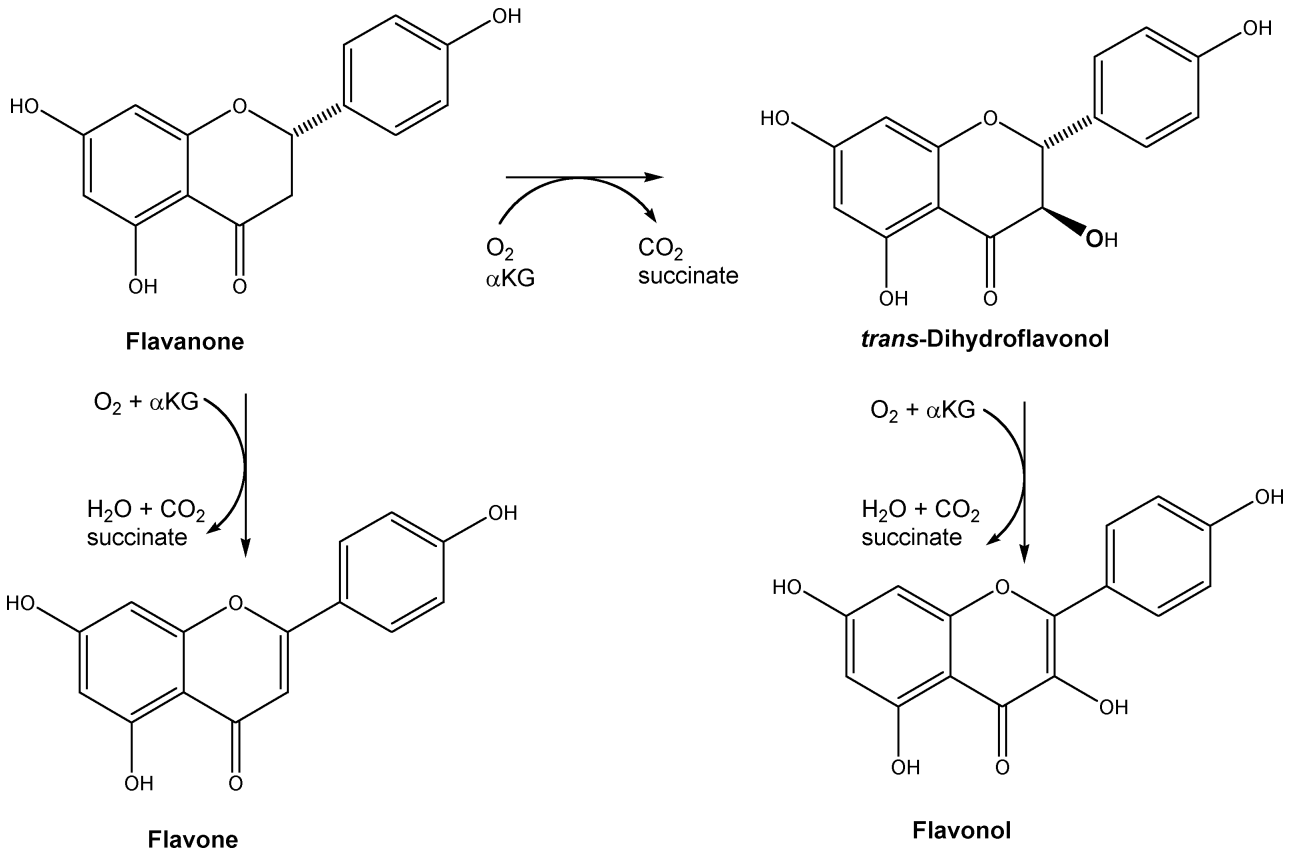

SCHEME 15.

gene are consistent with His 220, Asp 222, and His 278 being metal ligands, while Arg 288 and Ser 290 assist in binding αKG (although some activity is observed with the H220Q, D222N, R288K, R288Q, S290T, S290A, and S290V variants; Lukacin & Britsch, 1997; Lukacin *et al.*, 2000a).

Flavone synthase I also utilizes flavanones as substrates, but this enzyme catalyzes the Fe(II)/αKG-dependent dehydration reaction to introduce a double bond between C-2 and C-3 (producing apigenin for the reaction shown on the left in Scheme 15). The enzyme was purified and the gene cloned from parsley (Britsch, 1990; Martens *et al.*, 2001). No 2-hydroxynaringenin is detected during the reaction, and addition of this compound does not inhibit the reaction or lead to product; thus, 2-hydroxyflavanones are not dissociable intermediates in the reaction (Martens *et al.*, 2003). An alternative P450-type enzyme catalyzes this reaction in many plants and is denoted *flavone synthase II*.

Flavonol synthases catalyze a reaction analogous to that of flavone synthases but use dihydroflavonols as their substrates (e.g., converting dihydrokaempferol to kaempferol, as shown on the right in Scheme 15). The gene-encoding flavonol synthase was first isolated from petunia petals (Holton *et al.*, 1993) but has since been cloned and expressed from several sources including *Arabidopsis thaliana* (Prescott *et al.*, 2002). Antisense expression of the petunia gene in the plant leads to reduced flavonol levels (Holton *et al.*, 1993). The Fe(II)/αKG-dependent enzyme was purified from *Citrus unshiu* and extensively characterized by kinetic and mutagenesis methods (Wellman *et al.*, 2002). The flavonol synthase metal ligands are proposed to include His 221, Asp 223, and His 277, while Arg 287 is suggested to participate in αKG binding (Table 1). In addition to possessing flavonol synthase activity, the recombinant *C. unshiu* protein also exhibits flavanone 3β-hydroxylase activity (Lukacin *et al.*, 2003). A chimeric enzyme comprised of the *P. Hybrida* flavanone 3β-hydroxylase with its C-terminal 52 residences replaced by the corresponding region of *C. unshiv* flavonol synthase exhibited exclusively flavanone 3β-hydroxylase activity, indicating that this region does not define the selectivity of enzyme (Wellman *et al.*, 2004).

The synthesis of anthocyanins, involving the Fe(II)/αKG-dependent anthocyanidin synthase (ANS), offers an alternative route of processing of *trans*-dihydroflavonols. This pathway includes ketone reduction of the *trans*-dihydroflavonol by dihydroflavonol reductase, conversion of the resulting leucoanthocyanidin to anthocyanidin (Scheme 16), and hydroxyl group glycosylation to form anthocyanin (Nakajima *et al.*, 2001; Springob *et al.*, 2003). Surprisingly, *in vitro* studies with purified ANS reveal quercetin and dihydroquercetin as the major products, a finding that is consistent with formation of flav-2-en-3,4-diol as the *in vivo* product (Turnbull *et al.*, 2003). This intermediate transforms to anthocyanidin under acidic conditions. Genes encoding ANS proteins have been cloned from several sources, but direct evidence for a gene encoding this Fe(II)/αKG-dependent activity was first obtained using recombinant enzyme from mint, *Perilla fructescens* (Saito *et al.*, 1999). The enzyme from *Arabidopsis thaliana* was structurally characterized under anaerobic conditions in the presence of Fe(II), αKG, and substrate (Tables 1 and 2) (Wilmouth *et al.*, 2002). These studies reveal His 232, Asp 234, and His 288 as the metal ligands, Arg 298, Asn 215, and Tyr 217 as being involved in αKG binding, and the presence of two substrate binding sites (containing dihydroquercetin). In addition, a structure was determined for crystals that were exposed to oxygen for 30 min; the results are consistent with one substrate molecule being converted to quercetin and the αKG decomposing to succinate.

Another Fe(II)/αKG-dependent dioxygenase involved in flavonoid biosynthesis is an enzyme catalyzing 6-hydroxylation of methylated flavonols (Scheme 17). This enzyme, isolated from *Chrysosplenium americanum* was purified, kinetically characterized, and shown to utilize quercetin derivatives in the order trimethylated > dimethylated > tetramethylated > methylated > nonmethylated (but still retaining 10% of the activity observed with trimethylated substrate) (Anzellotti & Ibrahim, 2000). Significantly, this is one of only two Fe(II)/αKG-dependent hydroxylases known to insert an oxygen atom into a C–H bond of a carbon atom located in an aromatic ring. The second such reaction (involving the flavonoid-like compound

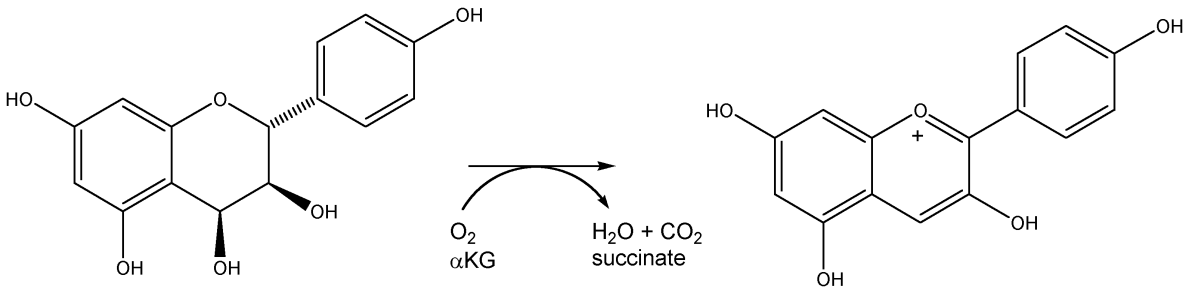

SCHEME 16.

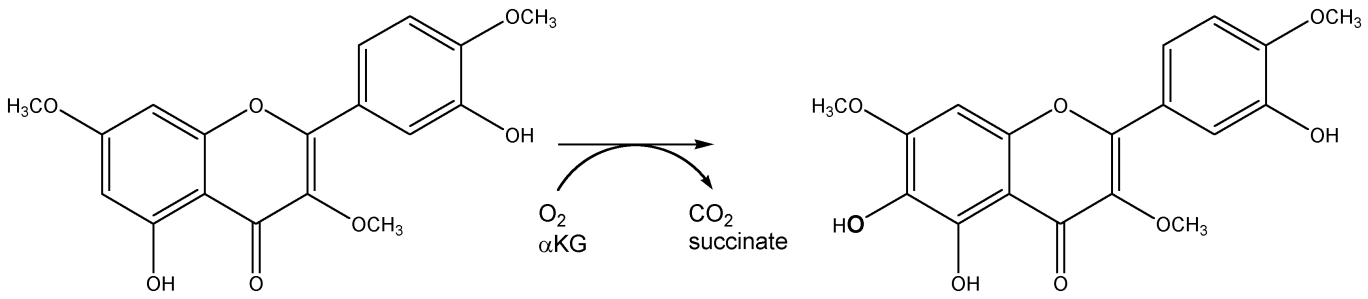

SCHEME 17.

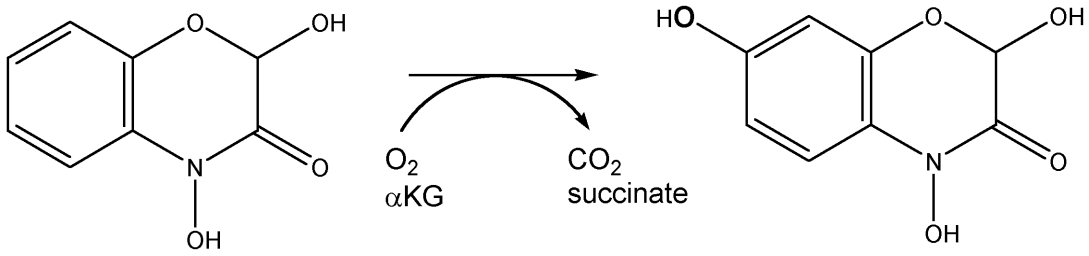

SCHEME 18.

shown in Scheme 18) converts 2,4-dihydroxy-2*H*-1,4-benzoxazin-3(4*H*)-one to 2,4,7-trihydroxyl-2*H*-1,4-benzoxazin-3(4*H*)-one, a natural pesticide produced in grasses (Frey *et al.*, 2003).

Within the complex network of gibberellin biosynthesis, the first Fe(II)/αKG-dependent step utilizes gibberellin 7-oxidase to catalyze aldehyde oxidation at the C-7 position, as illustrated in Scheme 19. This enzyme was shown to be Fe(II)/αKG-dependent and separated from two other Fe(II)/αKG-dependent dioxygenases in studies using cell-free extracts of developing pumpkin, *Cucurbita maxima* (Lange *et al.*, 1994b), but the activity appears to be cytochrome P450-dependent in other plant species (Hedden & Phillips, 2000). Subsequent cloning of the pumpkin gene allowed production of the recombinant enzyme, which was shown to catalyze the depicted reaction as well as several other less well-characterized activities (Lange, 1997). The protein sequence contains His 182, Asp 184, and His 238 as likely metal ligands along with Arg 248 and Ser 250 as potential αKG-binding residues (Table 1).

Gibberellin 20-oxidase catalyzes the sequential oxidation of the C-20 methyl group to form the alcohol, aldehyde, and (in some species) the carboxylate (Hedden, 1997, 1999), as shown in Scheme 20. Alternatively, the enzyme oxidatively transforms the aldehyde-containing species to a γ-lactone lacking C-20 (Scheme 21). Gibberellin 20-oxidase was first partially purified from seeds of pea (*Pisum sativum*) and shown to require αKG (Lange & Graebe, 1989). Studies of the isolated enzyme from *C. maxima* confirmed the capability of the enzyme to carry out all reactions shown in Schemes 20 and 21 (Lange, 1994). This same source was used for cloning the first gibberellin 20-oxidase gene (Lange *et al.*, 1994a), but many examples of the gene have since been cloned from other sources (including multiple copies for some plants) (Hedden & Phillips, 2000). Analysis of chimeric oxidases generated from fusions of portions of the gene from pumpkin (which makes primarily the carboxylate shown in Scheme 20) with that of the closely related species *Marah macrocarpus* (which favors γ-lactone production, shown

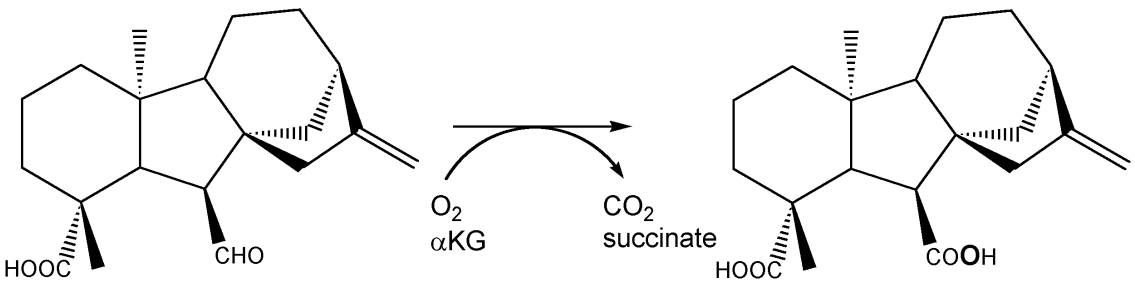

SCHEME 19.

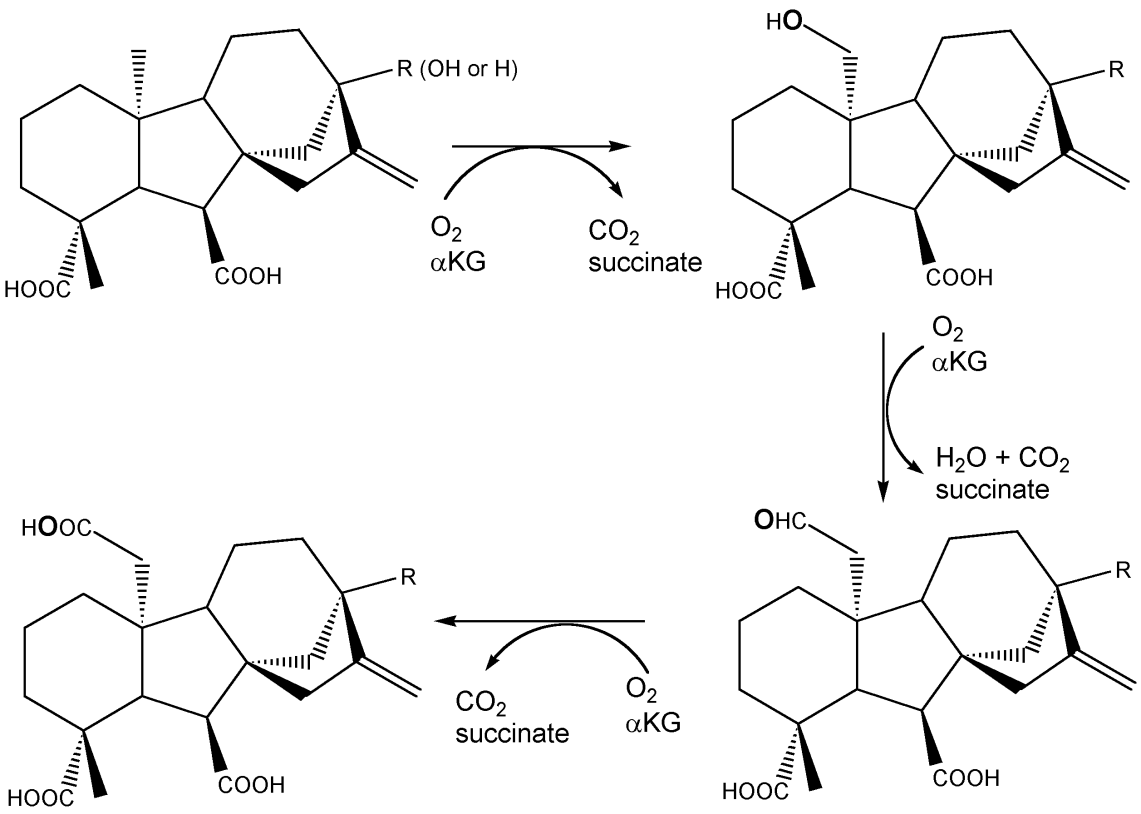

SCHEME 20.

in Scheme 21) highlights the importance of the carboxyl terminus of the protein as the major region controlling product specificity (Lange *et al.*, 1997a). The pumpkin protein sequence includes the likely metal liganding residues His243, Asp 245, and His 299 as well as the possible αKG-stabilizing residues Arg 309 and Ser 311 (Table 1).

Several other Fe(II)/αKG-dependent enzymes utilize the gibberellin γ-lactone as a substrate and catalyze reactions at C-2 and C-3 (indicated by arrows A and B in Scheme 21). Gibberellin 2-oxidase catalyzes initial hydroxylation and then oxidation to form the ketone at C-2, as shown by studies of recombinant enzymes from the runner bean (*Phaseolus coccineus*) (Thomas *et al.*, 1999) and pea (Lester *et al.*, 1999). Another related 2-hydroxylation activity acting on the non-γ–lactone substrate was identified and cloned from *Arabidopsis* (Schomburg *et al.*, 2003). Gibberellin 3β-hydroxylase activity was first demonstrated to be Fe(II)/αKG-dependent after enrichment from pumpkin (Lange *et al.*, 1994b). The gene encoding this activity was isolated initially from *Arabidopsis thaliana* (Chiang *et al.*, 1995), and has since been demonstrated to be associated with the pea stem-length gene (*Le*) studied by Gregor Mendel during his pioneering genetic investigations (Lester *et al.*, 1997; Martin *et al.*, 1997). Rice contains two genes encoding gibberellin 3-hydroxylase, one of which also exhibits 2,3-desaturation activity (Itoh *et al.*, 2001). A gene from pumpkin was shown to encode an enzyme with both 3β-hydroxylase and 2β-hydroxylase activities (Lange *et al.*, 1997b). Of biological significance, modification at C-2 leads to a less active gibberellin.

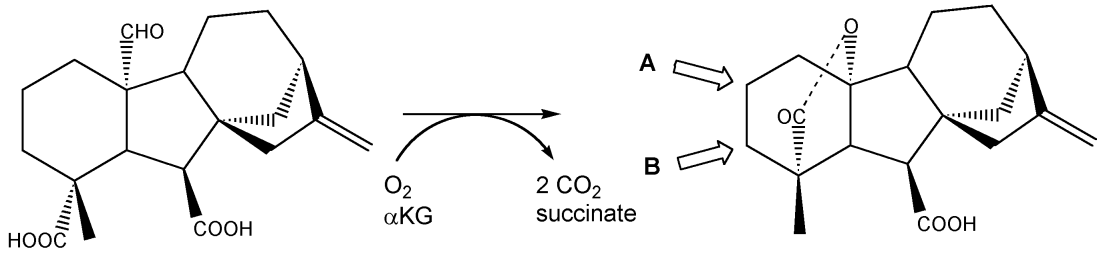

SCHEME 21.

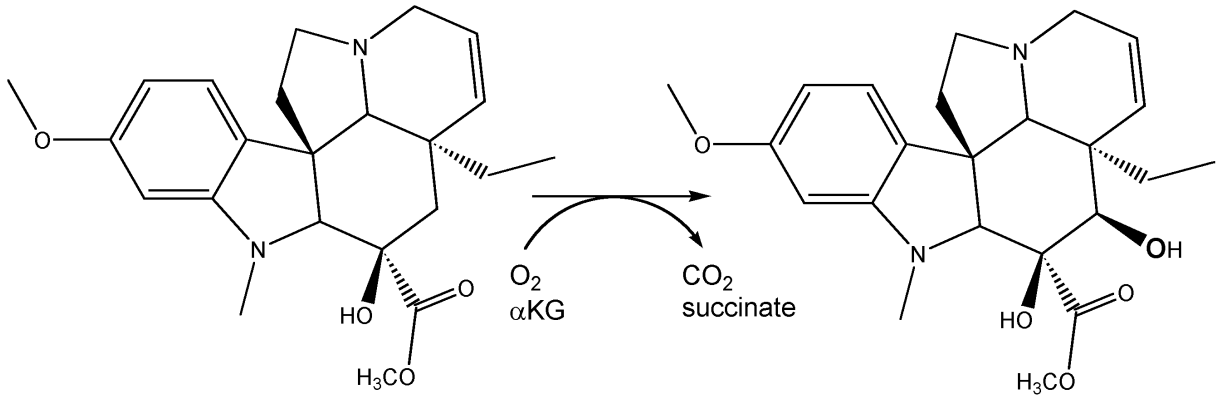

SCHEME 22.

At least two alkaloids require Fe(II)/αKG-dependent enzymes for their biosynthesis. The periwinkle plant, *Caranthus roseus*, synthesizes the vinca alkaloids vinblastine and vincristine that are used to treat Hodgkin's disease and leukemia, respectively. A critical component of these bis-indole alkaloids is vindoline, generated from tryptophan by a complex series of transformations. The second to last step in the vindoline biosynthetic pathway (Scheme 22) is catalyzed by an Fe(II)/αKG-dependent hydroxylase (De Carolis *et al.*, 1990). Similarly, an Fe(II)/αKG-dependent dioxygenase plays a key role in the synthesis of scopolamine, a hallucinogenic tropane alkaloid of henbane, *Hyoscyamus niger*. A single enzyme carries out both hydroxylation and epoxidation reactions (Scheme 23) as shown by using recombinant protein (Hashimoto *et al.*, 1993). Both of the alkaloid biosynthesis-related enzymes were purified (De Carolis & De Luca, 1993; Hashimoto & Yamada, 1987) and their genes cloned (Matsuda *et al.*, 1991; Vazquez-Flota *et al.*, 1997). In each case, metal-binding and αKG-interaction motifs are observed (His 308, Asp 310, His 366, Arg 376, and Ser 378 for deacetoxyvindoline 4-hydroxylase, and His 217, Asp 219, His 274, Arg 284, and Ser 286 of hyoscyamine 6β-hydroxylase; Table 1).

Another plant Fe(II)/αKG-dependent dioxygenase has been characterized from the seeds of fenugreek *Trigonella foenum-graecum* (Haefelè *et al.*, 1997). This enzyme forms 4-hydroxyisoleucine (Scheme 24), an insulinotropic compound that accounts for the use of this plant in traditional medicine for its antidiabetic properties (Sauvaire *et al.*, 1998). The role of this compound in the plant has not been reported.

E. Lipid Metabolism

Fe(II)/αKG-dependent hydroxylases play several important roles in lipid metabolism. Two of these enzymes are needed to synthesize carnitine, which transports activated fatty acids across the inner mitochondrial membrane to allow their degradation in the matrix by the β-oxidation

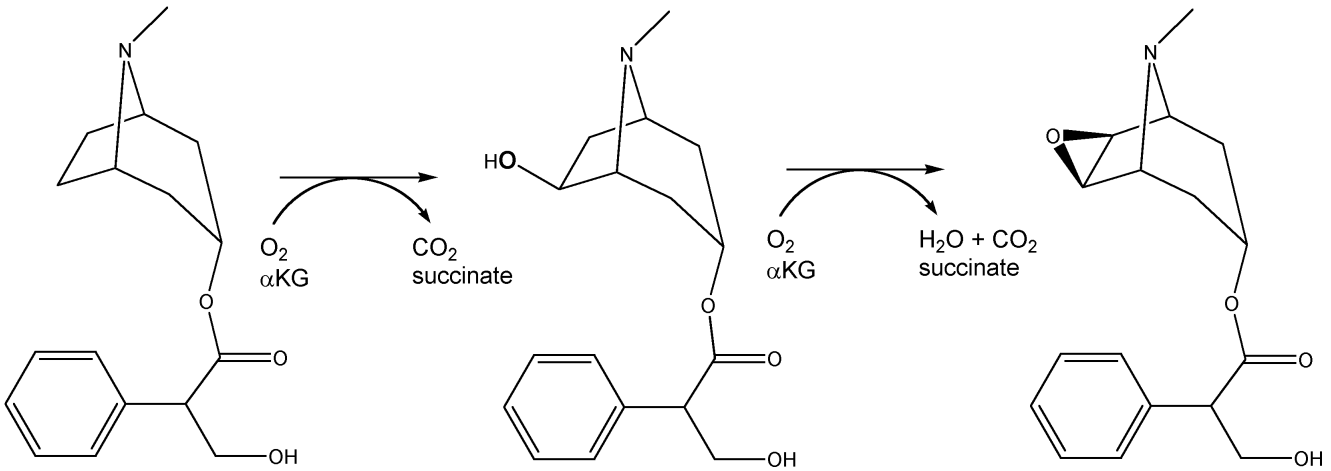

SCHEME 23.

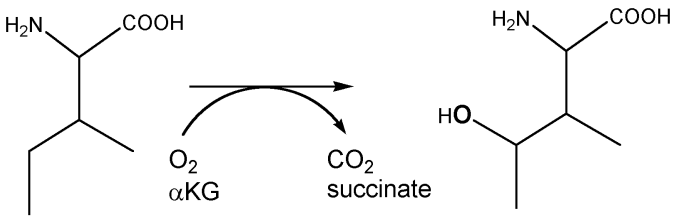

SCHEME 24.

pathway (Vaz & Wanders, 2002). A separate representative is required for degrading the plant lipid phytanic acid, and human deficiencies of this enzyme result in Refsum disease and other disorders (Wierzbicki *et al.*, 2002). Finally, on the basis of sequence results and physiological studies a family member appears to function in the synthesis of lipid A in several pathogenic bacteria (Gibbons *et al.*, 2000).

The synthesis of carnitine initiates with trimethyllysine, derived by hydrolysis of proteins that are modified through the action of an *S*-adenosylmethionine-dependent methyl transferase. As first illustrated for a rat liver mitochondrial sample (Hulse *et al.*, 1978), an Fe(II)/αKG-dependent hydroxylase converts ε-*N*-trimethyl-L-lysine to β-hydroxy-ε-*N*-trimethyl-L-lysine (Scheme 25). The dimeric rat enzyme has been purified and characterized, and the *Neurospora crassa* (Swiegers *et al.*, 2002), rat, mouse, and human (Vaz *et al.*, 2001) cDNAs were cloned and expressed in functional forms. The product of these enzymes is cleaved by an aldolase to produce glycine and γ-trimethylaminobutyraldehyde (γ-butyrobetaine aldehyde), with the latter compound being oxidized by a nicotinamide-dependent dehydrogenase to form γ-butyrobetaine. This product undergoes hydroxylation by a second Fe(II)/αKG-dependent hydroxylase to generate carnitine (Scheme 26). γ-Butyrobetaine hydroxylase was first purified from *Pseudomonas* sp. AK1 (Lindstedt *et al.*, 1977)

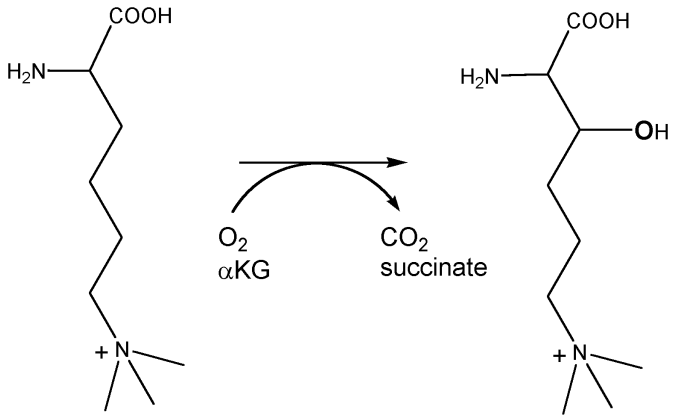

SCHEME 25.

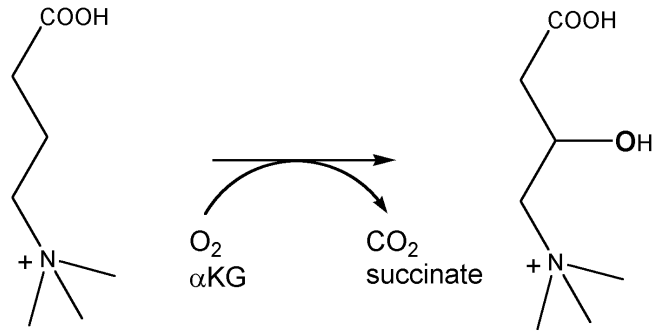

SCHEME 26.

and soon thereafter from calf liver (Kondo *et al.*, 1981). The bacterial protein sequence was determined by Edman degradation of the isolated peptides (Rüetschi *et al.*, 1993), whereas the sequences of animal enzymes were determined by translation of the cDNA sequences (Galland *et al.*, 1999; Vaz *et al.*, 1998). These γ-butyrobetaine hydroxylases are related to each other (Table 1), with the bacterial enzyme possessing His 209, Asp 211, and His 350 as likely metal-binding ligands and Arg 362 positioned for αKG binding. Furthermore, these enzymes are homologous to trimethyllysine hydroxylase, which appears to use glutamic acid rather than aspartic acid to bind the metal ion (Table 1).

Phytanoyl-CoA hydroxylase (Scheme 27) is required for the metabolism of phytanic acid (3,7,11,15-tetramethylhexadecanoic acid), a lipid derived from the phytol group of chlorophyll and found in dairy products, meat, and fish. The presence of the 3-methyl group precludes operation of the β-oxidation pathway; however, this oxidative degradation process can be utilized after removal of the C-1 carbon unit by action of a series of four enzymes (Mukherji *et al.*, 2003). A ligase is used to convert phytanic acid to phytanoyl-CoA (Watkins *et al.*, 1994). The CoA thioester is hydroxylated at the C-2 position by an αKG- and Fe(II)-dependent reaction (Scheme 27), as first demonstrated in rat liver peroxisomes in 1995 (Mihalik *et al.*, 1995) and later for human liver homogenates (Jansen *et al.*, 1996). Interestingly, GTP and ATP stimulate this reaction, although the role of the nucleotides is unclear (Croes *et al.*, 2000), and the participation of sterol carrier protein-2 in this reaction was suggested (Mukherji *et al.*, 2002). A thiamin pyrophosphate-dependent enzyme (Foulon *et al.*, 1999) catalyzes a lyase reaction of the hydroxylated intermediate to release formyl-CoA (Croes *et al.*, 1997b) and generate methylpentadecanal (pristanal) (Croes *et al.*, 1997a; Verhoeven *et al.*, 1997). After undergoing a nicotinamide-dependent oxidation to form pristanic acid, the ligase is used again to produce pristanoyl-CoA that is able to undergo β-oxidative degradation. Elevated levels of phytanic acid are observed in patients

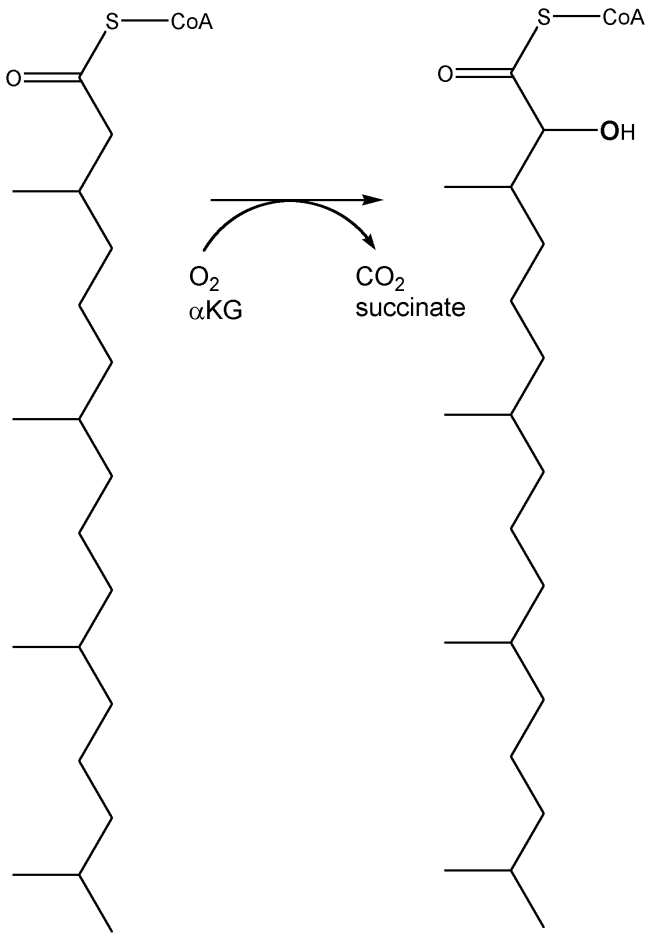

SCHEME 27.

suffering from Zellweger syndrome, rhizomelic chondrodysplasia punctata, and Refsum disease. These disorders are associated with a generalized defect in peroxisome assembly, a disturbance of a type of peroxisomal targeting signal, or a specific defect in phytanoyl-CoA hydroxylase activity, respectively.

Using the amino terminal sequence and an internal sequence of the rat liver enzyme, expressed sequence tag (EST) cDNAs were used to directly identify mouse and human clones of the phytanoyl-CoA hydroxylase gene, initially termed *PHYH* (Jansen *et al.*, 1997). The gene, renamed *PAHX*, was identified simultaneously by another group that searched for EST cDNAs encoding the required peroxisomal targeting signal, cloned the targeted sequence in an *E. coli* expression vector, and showed that affinity-purified sample exhibited Fe(II)/αKG-dependent phytanoyl-CoA hydroxylase activity (Mihalik *et al.*, 1997). Subsequently, the rat gene was cloned from its cDNA (Jansen *et al.*, 1999) and the complete ~21 kb human gene sequence was determined (Mukherji *et al.*, 2001a), revealing the presence of nine exons and eight introns. Refsum disease patients possess large (111 bp) or small (1 bp) deletions, insertions (3 bp), and a variety of single base changes (Jansen *et al.*, 1997; Mihalik *et al.*, 1997; Mukherji *et al.*, 2001a). Transfection of cDNA encoding the active form of the enzyme restored phytanoyl-CoA hydroxylase activity to fibroblasts isolated from two Refsum disease patients (Chahal *et al.*, 1998). On the basis of sequence comparisons (i.e., that of active human enzyme versus those of defective enzymes from Refsum disease patients), site-directed mutagenesis studies of the recombinant gene in various expression systems, and kinetic analysis of purified enzymes with αKG and alternative α-keto acids, the metal ligands of the human enzyme are likely to be His 175, Asp 177, and His 264, while Arg 275 assists in αKG binding (Table 1) (Mukherji *et al.*, 2001b).

Certain Gram-negative bacteria, including *Salmonella typhimurium* and *Pseudomonas aeruginosa*, appear to utilize an Fe(II)/αKG-dependent hydroxylase during the synthesis of lipid A (Gibbons *et al.*, 2000). When grown under aerobic conditions these pathogenic bacteria possess *S*-2 hydroxyacyl chains that are further decorated by acylation, whereas these modifications do not occur for anaerobically grown cells. Mass spectrometric studies confirm that the added oxygen atom is derived from O_2. Sequence analyses of the *S. typhimurium* genome were used to identify a possible homologue, denoted *lpxO*, to the mammalian gene for aspartyl/asparaginyl β-hydroxylase. This sequence includes His 155, Asp 157, His 202, and Arg 212 (Table 1), resembling the standard Fe(II)/αKG-dioxygenase motif. Curiously, however, these residues do not coincide with the likely metal- and αKG-binding residues of the mammalian hydroxylase used for sequence comparison (it does not contain this motif). Homologues to *lpxO* were noted in many other pathogenic bacteria that are known to make 2-hydroxyacyl-containing lipids. Expression of the *S. typhimurium* gene in *E. coli* leads to synthesis of 2-hydroxymyristate in this organism, thus confirming the function of the gene. Still unclear is whether the enzyme hydroxylates the acyl group after incorporation into the nascent lipid A (i.e., R in Scheme 28 is a glucosamine disaccharide) or whether hydroxylation of the acyl group occurs while bound to acyl carrier protein or CoA (e.g., R in Scheme 28 is a thiol). Notably, the latter situation would be highly reminiscent of the reaction carried out by phytanoyl-CoA hydroxylase (Scheme 27).

F. Other Fe(II)/αKG-Dependent Hydroxylases

This final grouping of Fe(II)/αKG-dependent hydroxylases describes an eclectic assembly of enzymes with diverse roles ranging from biodegradation (with examples that supply sulfur, phosphorus, or carbon to the cell) to nucleotide recycling to microbial biosynthesis of ethylene to still-unknown functions.

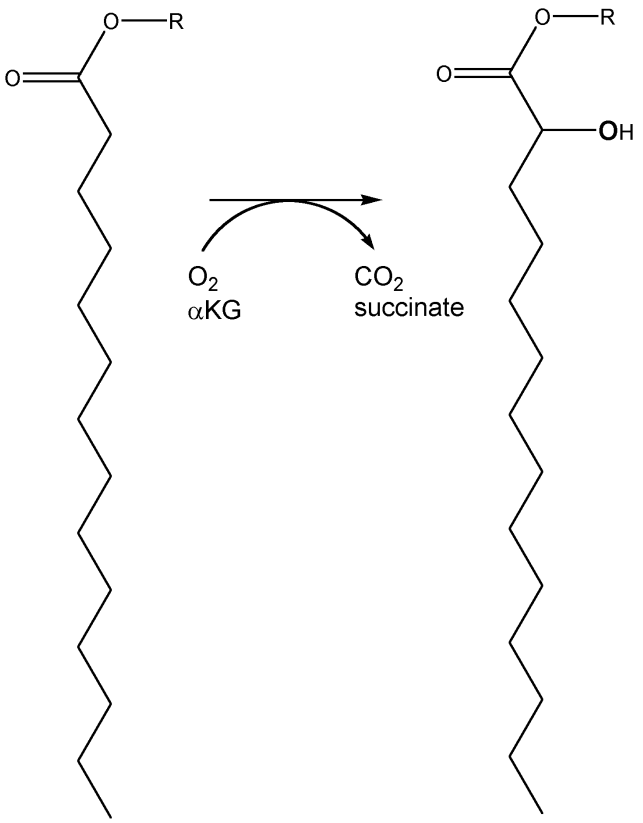

SCHEME 28.

Selected microorganisms decompose alkyl sulfonates or alkyl sulfates by using Fe(II)/αKG-dependent hydroxylases, thus providing sulfur for biosynthetic needs (Kertesz, 1999). For example, *E. coli* synthesizes taurine/αKG dioxygenase (TauD) during times of sulfur starvation (Eichhorn *et al.*, 1997). This enzyme hydroxylates taurine (2-aminoethanesulfonate) to create an unstable intermediate that decomposes to aminoacetaldehyde and sulfite (Scheme 29), which is subsequently utilized as a sulfur source. Structural studies (Elkins *et al.*, 2002; O'Brien *et al.*, 2003) demonstrate that His 99, Asp 101, and His 255 bind Fe(II), while Arg 266 and Thr 126 stabilize the C-5 carboxylate of αKG (Tables 1 and 2). An open reading frame in *Saccharomyces cerevisiae* (YLL057c) encodes a protein with 31.5% identity to TauD. The recombinant yeast protein was purified from *E. coli* and shown to possess weak taurine/αKG dioxygenase activity, but it

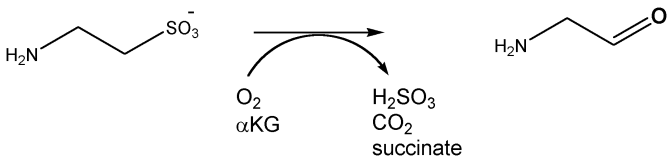

SCHEME 29.

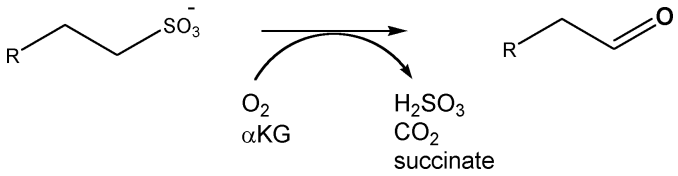

SCHEME 30.

exhibited 50- to 150-fold greater catalytic efficiency when using the bile salt taurocholate, hydroxyethanesulfonate (isethionate), *N*-phenyltaurine, and MOPS or MOPSO buffers as alternative substrates (Hogan *et al.*, 1999). Thus, the yeast enzyme appears to be a broad specificity sulfonate/αKG dioxygenase (Scheme 30). Alkyl sulfates, rather than sulfonates, are the substrates of an enzyme encoded by the *atsK* gene in *Pseudomonas putida* S-313 (Kahnert & Kertesz, 2000). The isolated alkylsulfatase hydroxylates alkyl sulfate esters (C_4 to C_{12} in length) at the C-1 position to create unstable intermediates that release sulfate and form the corresponding aldehydes (Scheme 31). AtsK is closely related to TauD (38% identity) and, as shown by structural studies (Table 2) (Müller *et al.*, 2004), contains the expected key residues (His 108, Asp 110, His 264, and Arg 275; Table 1).

A particularly interesting Fe(II)/αKG-dependent hydroxylase participates in a pathway that provides phosphorus for cellular needs. *Pseudomonas stutzeri* WM88 exemplifies an expanding group of microorganisms that are capable of growth using reduced forms of phosphorus, including hypophosphite (H_3PO_2) and phosphite (H_3PO_3). Molecular genetic analyses of this bacterium identified the *htxA* and *ptxD* genes that encode an Fe(II)/αKG-dependent hydroxylase and a NAD-dependent enzyme, respectively (Metcalf & Wolfe, 1998). Overexpression of *htxA* in *E. coli* allowed the isolation of an enzyme shown to hydroxylate hypophosphite (White & Metcalf, 2002), as illustrated in Scheme 32. PtxD then oxidizes phosphite, with concomitant reduction of NAD, to generate phosphate (Garcia Costas *et al.*, 2001). The sequence of HtxA resembles those of proline 4-hydroxylase, phytanoyl-CoA hydroxylase, and selected other family members, and includes the metal-binding residues His 116, Asp 118, and His 206, along with Arg 217, which likely facilitates αKG

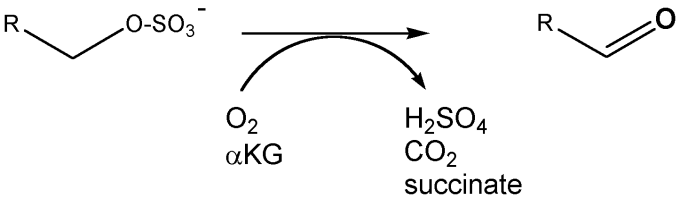

SCHEME 31.

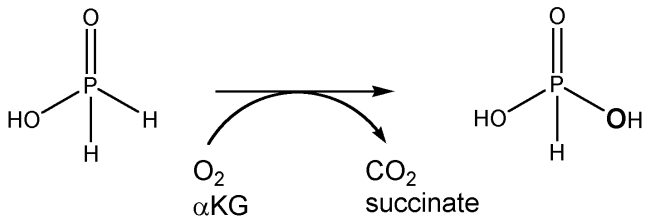

SCHEME 32.

binding (Table 1). Although it seems reasonable to suggest that Fe(II)/αKG-dependent hydroxylases might participate in the degradation of alkyl phosphonates and alkyl phosphates, in parallel to the alkyl sulfonate- and alkyl sulfate-degrading systems, these activities have not been reported.

A herbicide-degrading Fe(II)/αKG-dependent hydroxylase is found in bacteria that metabolize 2,4-dichlorophenoxyacetic acid (2,4-D), including microbes that are capable of using this molecule as their sole carbon source (Hausinger *et al.*, 1997). Catabolism of 2,4-D has long been known to initiate with ether bond cleavage (Tiedje & Alexander, 1969), but the gene encoding the corresponding enzyme (*tfdA*) is unlike other known ether cleavage systems (Streber *et al.*, 1987). By examining the overproduced *Ralstonia eutropha* enzyme in *E. coli*, 2,4-D/αKG dioxygenase (TfdA) was shown to catalyze the reaction shown in Scheme 33 (Fukumori & Hausinger, 1993b); i.e., the oxidative cleavage of αKG to CO_2 plus succinate is coupled to the hydroxylation of 2,4-D with subsequent decomposition of the hydroxy-intermediate to yield glyoxylate and 2,4-dichlorophenol. The purified enzyme decomposes a variety of other phenoxyacetic acid derivatives (Fukumori & Hausinger, 1993a), thiophenoxyacetic acids (Saari & Hausinger, 1998), naphthoxyacetic acids, benzofuran-2-carboxylate, and various cinnamic acids (Dunning Hotopp & Hausinger, 2001), with release of the corresponding substituted phenols, thiophenols, and, for the benzofuran-2-carboxylate and cinnamic acids, the epoxide products. Whereas some ethene-containing cinnamic acids are substrates, the acetylenic compound phenylpropiolic acid is a

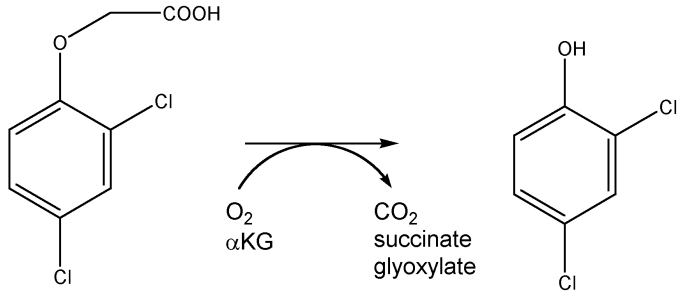

SCHEME 33.

mechanism-based inactivator that forms a covalent bond to the protein (Dunning Hotopp & Hausinger, 2002). In addition, TfdA transforms the *S* enantiomer of the 2-phenoxypropionate, dichloroprop, to the substituted phenol plus pyruvate (Saari *et al.*, 1999). Interestingly, *Alcaligenes denitrificans* possesses an enzyme that utilizes the opposite enantiomer of a related phenoxypropionate (mecoprop) (Tett *et al.*, 1997) and both *Sphingomonas herbicidovorans* MG and *Delftia acidovorans* MC1 have two Fe(II)/αKG-dependent phenoxypropionate-degrading hydroxylases—one specific to each enantiomer (Nickel *et al.*, 1997; Westendorf *et al.*, 2003). Analyses of Fe(II)-bound TfdA and Cu(II)-substituted protein by X-ray absorption spectroscopy (XAS) suggested the presence of two imidazole ligands (Cosper *et al.*, 1999). Electron paramagnetic resonance (EPR) and electron spin-echo envelop modulation (ESEEM) spectroscopic analyses of the Cu-substituted protein similarly provided evidence for His ligation, and showed that binding of αKG and 2,4-D perturbs the metal site (Whiting *et al.*, 1997). The results of site-directed mutagenesis studies of *tfdA* (Dunning Hotopp & Hausinger, 2002; Hogan *et al.*, 2000) are consistent with His 114, Asp 116, and His 263 serving to bind the metal and Arg 274 assisting in binding αKG (Table 1). The modeled structure of the enzyme, generated by comparison to structures of other known family members, is consistent with these interactions (Elkins *et al.*, 2002).

Thymine hydroxylase catalyzes three sequential Fe(II)/αKG-dependent hydroxylations of the methyl group of thymine (Scheme 34). The activity was first studied in *Neurospora crassa* (Abbott *et al.*, 1967; Holme, 1975; Holme *et al.*, 1971) and has been noted in *Aspergillus nidulans* (Shaffer *et al.*, 1984), but recent investigations have focused on the enzyme from *Rhodotorula glutinis*. For example, additional reactivities were uncovered, including epoxidation of 5-vinyluracil, sulfur oxidation of 5-(methylthio)uracil, and conversion of an amine to an aldehyde using 1-methylthymine (Thornburg *et al.*, 1993). Mechanism-based inactivation was observed using the acetylenic analogue of thymine, allowing characterization of the covalently modified peptides (Thornburg & Stubbe, 1989, 1993; Thornburg *et al.*, 1993; Warn-Cramer *et al.*, 1983). On the other hand, the complete sequence is unknown and no structure has been reported for this enzyme.

At least two Fe(II)/αKG-dependent hydroxylases utilize nucleosides as their substrates and catalyze transformations involving the sugar moiety. *N. crassa, A. nidulans*, and *R. glutinis* possess pyrimidine deoxyribonucleoside 2′-hydroxylases that convert thymidine or uridine to the ribosides, as shown in Scheme 35 (where X is a methyl group or hydrogen atom, respectively) (Bankel *et al.*, 1972; Shaffer *et al.*, 1968, 1984; Warn-Cramer *et al.*, 1983). In addition, *R. glutinis* contains a deoxyuridine (uridine)

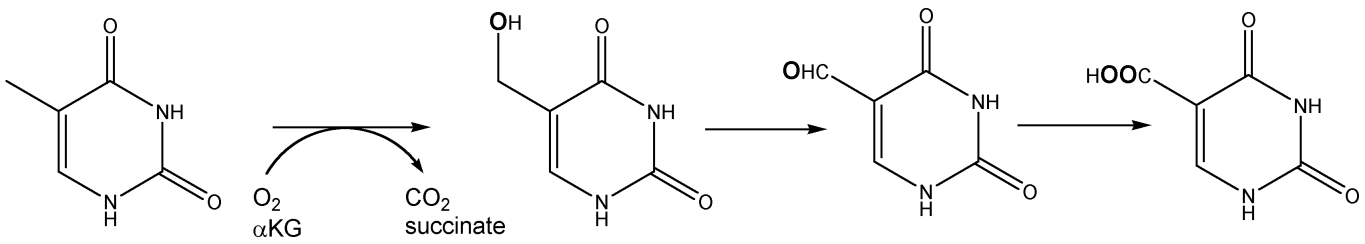

SCHEME 34.

1′-hydroxylase that replaces the hydrogen atom indicated by the arrow with a hydroxyl group for the case where X = H (Stubbe, 1985). No genes have been sequenced or proteins structurally characterized for these enzymes.

Penicillium digitalum and *Pseudomonas syringae* pv. *phaseolicola* PK2 synthesize the plant hormone ethylene by action of an enzyme that is distinct from the ethylene-forming system found in plants (described further in Section II part G). The fungal activity was described in 1986 and shown to require αKG, Fe(II), and L-arginine (Fukuda *et al.*, 1986). Although this enzyme has been purified (Fukuda *et al.*, 1989), little is known about its properties compared to the corresponding bacterial enzyme. A cell-free extract of *P. syringae* initially was suggested to generate ethylene from αKG with no stimulation by arginine (Goto & Hyodo, 1987); however subsequent studies demonstrated that the amino acid and oxygen are essential components of catalysis (Nagahama *et al.*, 1991a). The monomeric enzyme was purified (Nagahama *et al.*, 1991b) and the corresponding gene cloned and expressed in *E. coli* (Fukuda *et al.*, 1992a). The sequence displays the likely metal-binding residues His 189 and Asp 191, along with histidines at positions 268, 284, 305, 309, or 335 and arginines at positions 275, 277, 316, 321, 332, and 346. Site-directed mutagenesis studies revealed that the H189Q variant is inactive, and the H268Q, H305Q, and H335Q variants possess 1.8%, 40%, and 60% of wild-type activity, respectively (Nagahama *et al.*, 1998). On the basis of these results and comparison to sequences of other family members, His 268 and Arg 277 are likely to participate in metal- and αKG-binding (Table 1). The bacterial enzyme appears to catalyze two reactions in a 2:1 stoichiometry (Fukuda *et al.*, 1992b). The minor reaction is more straightforward and involves the Fe(II)/αKG-dependent hydroxylation of arginine with subsequent decomposition of this intermediate and formation of guanidine plus L-Δ^1-pyrroline-5-carboxylate (Scheme 36). The major reaction involves the remarkable oxidative transformation of αKG to three molecules of CO_2 plus one molecule each of H_2O and ethylene (Scheme 37). An intriguing "dual-circuit mechanism" has been proposed in order to account for the two reactions (Fukuda *et al.*, 1992b). In this proposal, αKG forms a Schiff's base with arginine, the coligand binds Fe(II) in a tridentate complex (with only two enzyme side chains binding the metal), and an intermediate formed after reaction with oxygen partitions in such a manner as to give rise to the observed products. Other than the appropriate product stoichiometries, no experimental evidence has been reported to support this biochemically suspect mechanism.

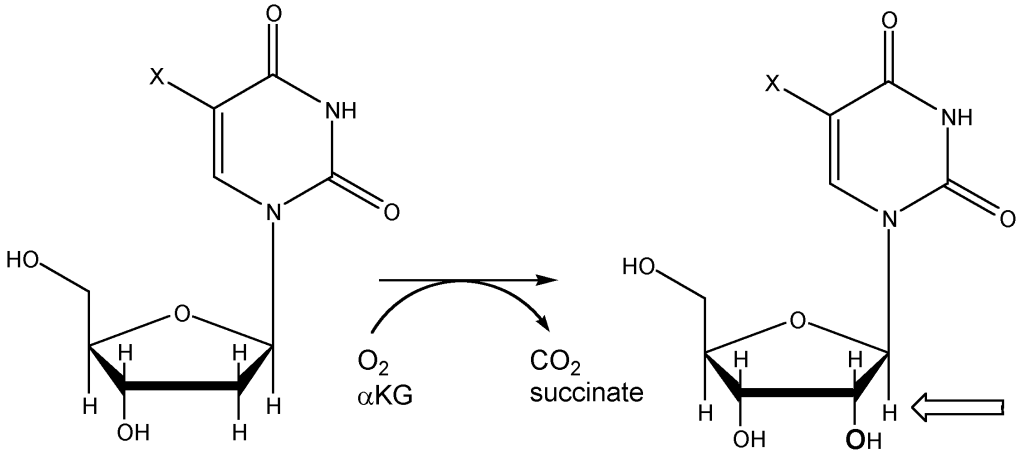

SCHEME 35.

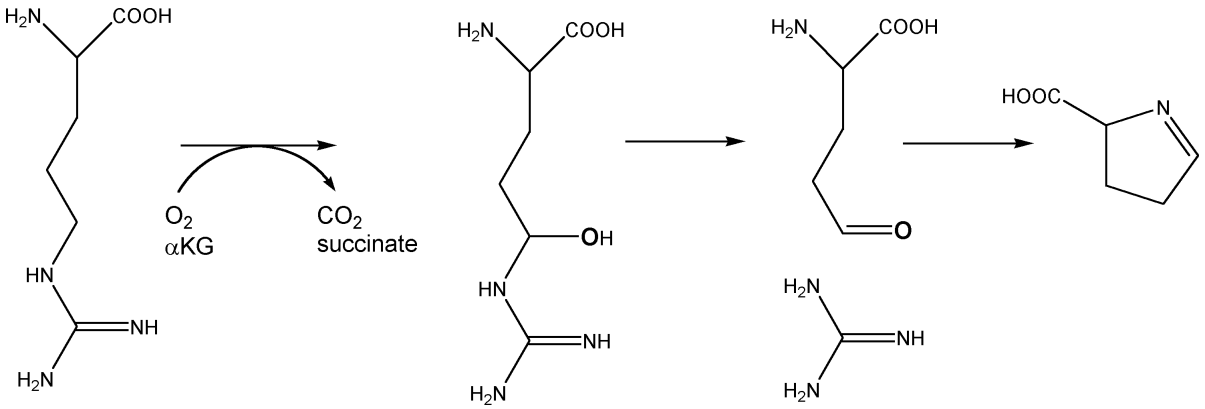

SCHEME 36.

The final putative Fe(II)/αKG-dependent hydroxylase to be discussed is the *E. coli* Gab protein, whose function is still unknown. The structure of this protein was solved as part of a structural genomics effort (Chance *et al.*, 2002). It revealed a fold that, despite the lack of sequence similarity, resembles CAS, DAOCS, and other members of the Fe(II)/αKG-dioxygenase superfamily. The crystallographically observed metal ion, possibly Fe(III) since the protein was crystallized aerobically, is bound to His 160, Asp 162, and His 292. Nearby and appropriately positioned to interact with αKG is Arg 305; however, no electron density for αKG was observed when this molecule was added to the protein. Additional electron density was observed at the position likely to be occupied by substrate, but the identity of this species could not be discerned. The authors speculate that the protein plays a role related to γ-aminobutyrate metabolism since the gene is located in the γ-aminobutyrate operon.

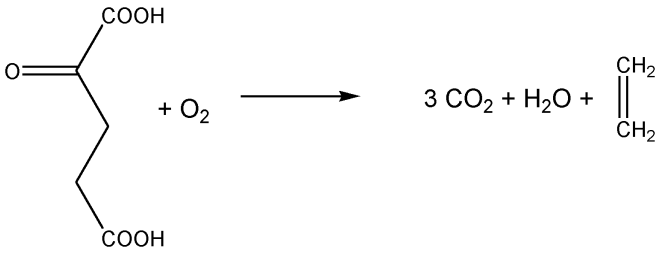

SCHEME 37.

G. Related Enzymes

Isopenicillin *N* synthase (IPNS) is structurally related to the Fe(II)/αKG-dependent dioxygenases, but it does not utilize αKG as a cosubstrate. Rather, this enzyme catalyzes the remarkable reaction illustrated in Scheme 38 in which a linear tripeptide (δ-(L-α-aminoadipoyl)-L-cysteinyl-D-valine) is transformed to a bicyclic structure while carrying out the four-electron reduction of oxygen (Kreisberg-Zakarin *et al.*, 1999; Schofield *et al.*, 1997). The gene encoding this enzyme was first cloned and sequenced from *Cephalosporium acremonium* (Samson *et al.*, 1985), and spectroscopic studies have focused on this recombinant enzyme. The Mössbauer spectrum associated with the high-spin mononuclear Fe(II) site is perturbed by substrate binding, consistent with direct substrate interaction with the metallocenter (Chen *et al.*, 1989). The same study examined the nitric oxide (NO) complex of the enzyme and showed optical spectral changes indicative of substrate thiol binding to the metal. ESEEM studies of Cu(II)-substituted protein (Jiang *et al.*, 1991) were interpreted in terms of two His ligands, whereas ^{1}H nuclear magnetic resonance spectra of Fe(II) and Co(II) derivatives indicated the likely presence of three His ligands (Ming *et al.*,

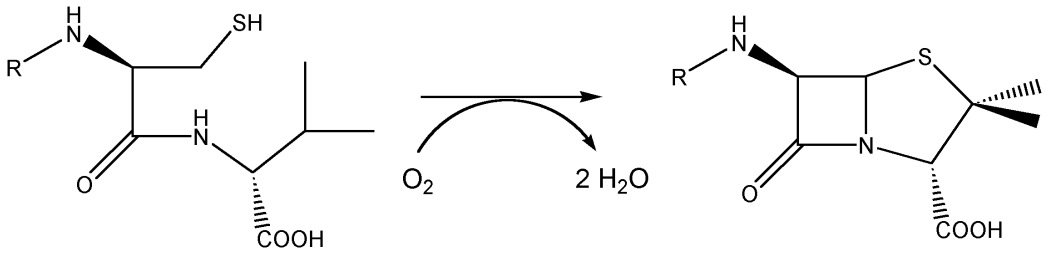

SCHEME 38.

1990, 1991). Results from XAS studies were consistent with 2–3 imidazole ligands along with substrate thiol interaction with the metal (Randall *et al.*, 1993; Scott *et al.*, 1992). Site-directed mutagenesis studies of the genes from *C. acremonium* and *Streptomyces jumonjinensis* identified the likely His^1-X-Asp-X_n-His^2 metal-binding ligands (Borovok *et al.*, 1996; Kreisberg-Zakarin *et al.*, 2000; Tan & Sim, 1996; Tiow-Suan & Tan, 1994) (Table 1), and these assignments were confirmed by crystal structure determination of the *Aspergillus (Emericella) nidulans* enzyme (Table 2) (Roach *et al.*, 1995). An intriguing feature revealed by the structure is that a fourth amino acid side chain, the carboxyl terminal Gln residue, coordinates the metal in the absence of substrate. Additional mutagenesis studies have shown this residue is not important to catalysis (Landman *et al.*, 1997; Sami *et al.*, 1997), a result in accord with additional structural studies showing that substrate displaces the Gln residue (Roach *et al.*, 1997). In addition, crystallographic investigations confirm that substrate thiol binds the metal.

Like IPNS, 1-aminocyclopropane-1-carboxylate (ACC) oxidase (also known as ethylene-forming enzyme) is related by sequence to the Fe(II)/αKG-dependent hydroxylases, yet this enzyme does not utilize αKG as a cosubstrate. ACC is an intermediate in formation of the plant-ripening hormone ethylene from methionine (Adams and Yang, 1979), and ACC oxidase catalyzes the reaction shown in Scheme 39 (Dong *et al.*, 1992). Since the initial cloning and sequencing of the gene encoding tomato ACC oxidase (Hamilton *et al.*, 1991) homologues have been characterized from many plants, and all reveal the typical Fe(II)/αKG dioxygenase superfamily sequence motif (Table 1). Numerous site-directed mutagenesis studies have been carried out (e.g., Lay *et al.*, 1996; Shaw *et al.*, 1996) to support the metal ligand assignments; however, no crystal structure has yet been reported. On the basis of EPR and electron nuclear double resonance (ENDOR) spectroscopic investigations of NO-bound enzyme, alanine (a structural analogue of ACC) was shown to bind the metal ion through both its α-amino and α-carboxylate groups (Rocklin *et al.*, 1999). Such a binding mode for ACC would be reminiscent of the chelate binding observed for αKG in the Fe(II)/αKG-dependent hydroxylases, as described in Sections III and IV. Significantly, the spectroscopic studies of ACC oxidase were interpreted to suggest that ACC and oxygen simultaneously bind to the metal to promote catalysis, whereas the data are incompatible with previously proposed mechanisms involving simultaneous metal binding of ascorbate and oxygen. Kinetic studies of the avocado (Brunhuber *et al.*, 2000) and tomato (Thrower *et al.*, 2001) ACC oxidases are inconsistent in terms of the order of substrate binding to the enzyme, but both suggest the need to bind ascorbate, ACC, and oxygen for multiple rounds of catalysis. An especially intriguing aspect of ACC oxidase is its activation by carbon dioxide (Dong *et al.*, 1992; Pirrung *et al.*, 1993; Poneleit & Dilley, 1993; Smith & John, 1993). On the basis of near-infrared circular dichroism (CD) and magnetic circular dichroism (MCD) spectroscopic studies, the role of CO_2 is now understood in terms of preventing an aberrant reaction that results in enzyme inactivation (Zhou *et al.*, 2002). Thus, binding of ACC to the CO_2-free resting enzyme converts the six-coordinate metal site into a five-coordinate site that reacts with oxygen in an uncoupled reaction, leading to loss of enzyme activity. In contrast, CO_2 stabilizes a six-coordinate ACC-bound state (perhaps by reacting with a metal-bound water molecule to create a metal-bound bicarbonate ligand) until ascorbate is present, at which time the sixth ligand is lost to create a productive oxygen-binding site. Of interest, inactivation of ACC oxidase is accompanied by protein fragmentation due to metal-catalyzed oxidative reactions that cleave the peptide backbone (Barlow *et al.*, 1997; Zhang *et al.*, 1997). It is possible that this aberrant chemistry is catalyzed by an activated oxygen species related to one that normally participates in catalysis.

4-Hydroxyphenylpyruvate dioxygenase (HPPD) is not related in sequence to the Fe(II)/αKG-dependent hydroxylases, but it exhibits close chemical parallels to this enzyme family. As shown in Scheme 40, HPPD catalyzes the oxidative cleavage of an α-keto acid while hydroxylating a substrate, but in this case the α-keto acid group is part of the substrate and the hydroxylation is associated with an "NIH shift" involving acetyl group migration to a different position on the aromatic ring. The enzyme functions in tyrosine catabolism, and inhibitors of HPPD are

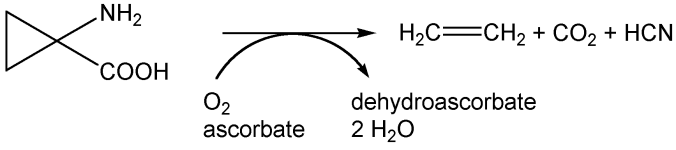

SCHEME 39.

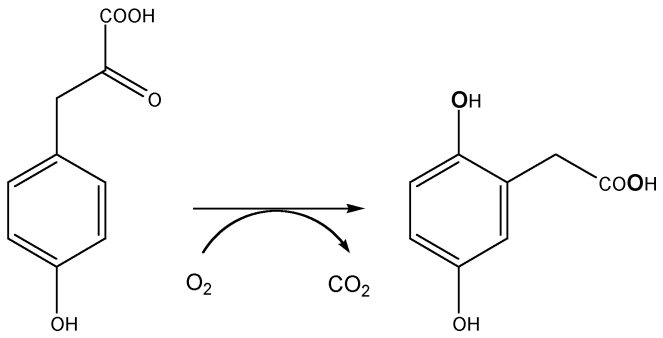

SCHEME 40.

useful as herbicides (preventing the production of plastoquinone) and for human patients with type 1 tyrosinemia (lacking fumarylacetoacetase, the enzyme catalyzing the final step in tyrosine degradation, so that a toxic intermediate accumulates). HPPD was purified from human liver, shown to be a dimer of M_r 87,000, and found to require ferrous ions (Lindblad *et al.*, 1977). Aerobically purified enzyme from *Pseudomonas* sp. strain P.J.874 is inactive and possesses a blue color ($\lambda_{max} \sim 595$ nm, $\varepsilon_{595} = 2.6\ mM^{-1}\ cm^{-1}$) associated with its metal site (0.95 Fe per subunit) (Lindstedt & Rundgren, 1982). Reduction of this enzyme led to the loss of color and gain of activity. On the basis of resonance Raman (rR) spectroscopic investigations, the blue color of oxidized bacterial HPPD was suggested to arise from tyrosinate coordination to Fe(III) (Bradley *et al.*, 1986). Surprisingly, however, the crystal structure of the closely related HPPD from *Pseudomonas fluorescens* reveals a mononuclear iron site with the metal coordinated by His 161, His 240, and Glu 322, and lacking any Tyr residue in its vicinity (Serre *et al.*, 1999). This finding prompted speculation that the enzyme might catalyze a self-hydroxylation reaction to create one or more hydroxy-phenylalanine residues that bind to the oxidized metal ion (Ryle & Hausinger, 2002). Kinetic and spectroscopic studies with recombinant *Streptomyces avermitilis* HPPD apoprotein show an ordered binding of Fe(II), then substrate and oxygen (with a 3600-fold increase in oxygen reactivity if substrate binds first) (Johnson-Winters *et al.*, 2003). These investigations further indicate that substrate binds to the metal in a chelating mode (i.e., via the side chain carboxylate and keto groups) and reveal the presence of an intermediate during its reaction with oxygen (Johnson-Winters *et al.*, 2003). The identity and properties of this intermediate are currently unknown, but are likely to be related to intermediates in the Fe(II)/αKG-dependent hydroxylases (see Section IV).

A reaction closely analogous to that catalyzed by HPPD is carried out by 4-hydroxymandelate synthase (Scheme 41) (Choroba *et al.*, 2000; Hubbard *et al.*, 2000). This enzyme is related in sequence to HPPD and unrelated to the Fe(II)/αKG-dependent hydroxylases. Like HPPD, 4-hydroxymandelate synthase uses 4-hydroxyphenylpyruvate as substrate and decomposes the substrate-associated α-keto acid; however, it hydroxylates the alkyl side chain rather than the aromatic ring. The gene encoding this enzyme is part of the chloroeremomycin gene cluster that also encodes 4-hydroxymandelate oxidase and 4-hydroxyphenylglycine transaminase that provide the 4-hydroxyphenylglycine used for synthesis of the antibiotic. Like HPPD, 4-hydroxymandelate synthase requires ferrous ions for activity. A mutagenesis approach was used to obtain clues about specific protein features responsible for the distinct chemistries of 4-hydroxymandelate synthase and HPPD. Specifically, the *S. avermitilis* HPPD gene was

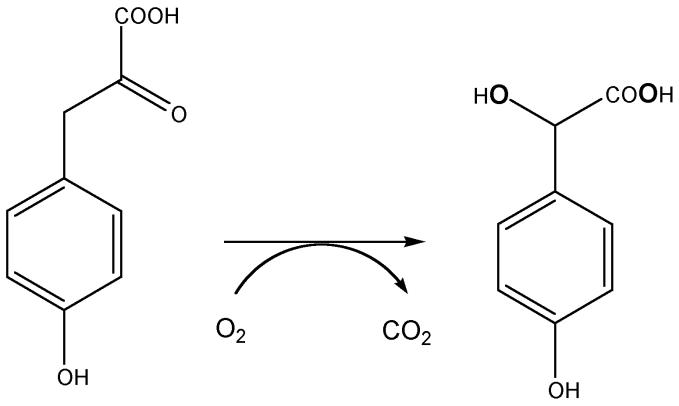

SCHEME 41.

engineered to create a variant enzyme (F337I) that produced 4-hydroxymandelate along with its normal product (Gunsior *et al.*, 2004).

Until recently α-ketoisocaproate dioxygenase also was thought to catalyze a reaction involving hydroxylation of a substrate that provides its own α-keto acid (Scheme 42). Proteins possessing this activity have been purified and characterized from several sources (e.g., Han & Pascal, 1990; Sabourin & Bieber, 1982); however, the rat liver enzyme was shown to be identical to rat liver HPPD (Crouch *et al.*, 1997). Thus, *a separate α-ketoisocaproate dioxygenase may not exist*.

III. STRUCTURAL STUDIES

Structurally characterized Fe(II)/αKG-dependent hydroxylases and related proteins are listed in Table 2 along with their bound metal and substrates, crystallographic resolution, and PDB accession numbers. The structures of the Fe(II)/αKG-dependent proteins are unified by possession of a "jellyroll" structural fold comprised of eight β-strands forming two, four-stranded sides (Figure 1, left). Surrounding this protein core, and likely contributing to its stability, are additional α-helices, β-strands, and protein loops as illustrated for the first representative of this protein family, the non-αKG-dependent enzyme IPNS (Figure 1,

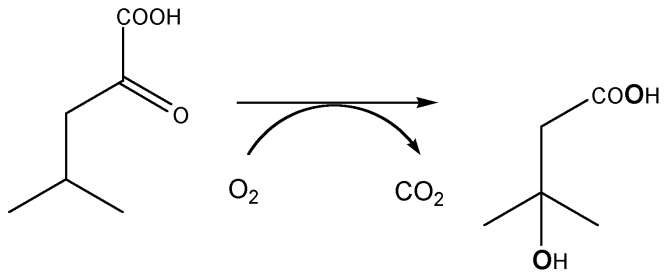

SCHEME 42.

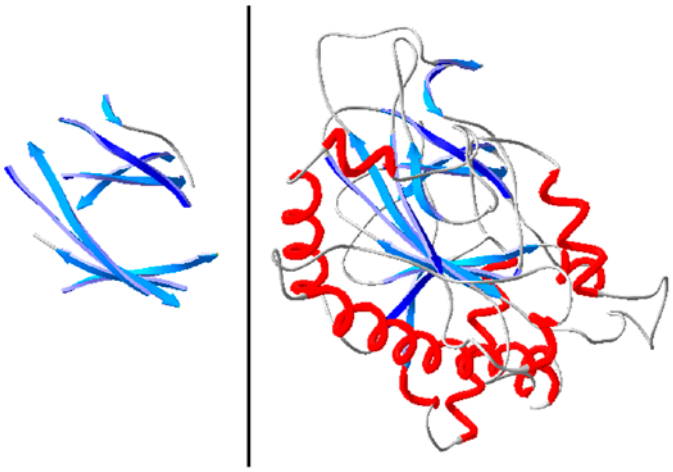

FIG. 1. Jellyroll fold found in all Fe(II)/αKG-dependent dioxygenases. On the left are the eight β-strands that combine to form the core of all Fe(II)/αKG dioxygenases, as first identified in the related enzyme IPNS (Roach *et al.*, 1995). Additional β-strands and α-helices are present at the amino terminus, and inserted into the jellyroll fold and at the carboxyl terminus, as illustrated for the complete IPNS structure shown on the right. These additional features stabilize the core structure, participate in interprotein contacts, and modify the substrate-binding site. The IPNS structure contains a total of 10 α-helices and 16 β-strands, with the jellyroll motif incorporating the β^5 and β^{8-14} secondary structure features.

right). The insertions and extensions to this jellyroll fold differ for each protein and help to define the substrate-binding sites and establish protein–protein contact surfaces. IPNS (Roach *et al.*, 1995), CAS (Zhang *et al.*, 2000), and ANS (Wilmouth *et al.*, 2002) are monomeric proteins, and DAOCS equilibrates between monomeric and trimeric species in solution, but crystallizes as a trimeric protein (Lloyd *et al.*, 1999a). In contrast, FIH (Dann *et al.*, 2002; Elkins *et al.*, 2003; Lee *et al.*, 2003), proline 3-hydroxylase (Clifton *et al.*, 2001), and TauD (Elkins *et al.*, 2002; O'Brien *et al.*, 2003) are dimeric proteins, AtsK (Müller *et al.*, 2004) and the Gab protein (Chance *et al.*, 2002) are tetrameric, and CarC is hexameric (a dimer of trimers) (Clifton *et al.*, 2003).

The active site structures of the Fe(II)/αKG dioxygenases exhibit nearly identical arrangements of the three amino acid side chains (associated with the His^1-X-Asp/Glu-X_n-His^2 motif) that bind one face of the metal. On the basis of the αKG binding mode, the active site structures are resolved into two distinct categories (Figures 2 and 3). In both classes, the C-1 carboxylate and C-2 keto group chelate the metal and the C-5 carboxylate is stabilized by a salt bridge to an Arg residue or by ionic interaction with a Lys side chain. Additional hydrogen-bond interactions are found to participate in C-5 carboxylate binding, and critically positioned Arg residues often help orient the C-1 carboxylate (not shown). One category of enzymes is represented by CAS (Zhang *et al.*, 2000), TauD (Elkins *et al.*, 2002), and FIH (Dann *et al.*, 2002; Elkins *et al.*, 2003; Figure 2), along with AtsK (Müller *et al.*, 2004). In these enzymes, His^1 and the carboxylate ligand are located approximately in plane with αKG (C-1 carboxylate opposite His^1 and C-2 ketone opposite the acidic residue). The primary substrate does not bind to the metal, but rather binds nearby and above this plane. An open metal coordination site exists near the primary substrate and opposite His^2 in this "in line" binding mode. In the second category of enzymes, represented by CarC (Clifton *et al.*, 2003) and ANS (Wilmouth *et al.*, 2002; Figure 3), the C-1 carboxylate of αKG binds opposite His^2, and the keto group again is located opposite the acidic residue. Thus, the open coordination site is located opposite His^1 and oriented away from the substrate in this "off line" binding mode. The two αKG binding modes may simply represent conformational flexibility in binding this cosubstrate, with different protein structures tending to stabilize one mode over the other. For example, the αKG binding mode reverses for CAS (with a different substrate bound) in the presence of the oxygen analogue NO (Figure 4). Furthermore, the C-1 carboxylate of αKG flips from the "in line" to the "off line" mode when Fe(II) is replaced by sodium ion in AtsK (Müller *et al.*, 2004). Thus, it is reasonable to posit that αKG conformational flexibility in ANS and/or CarC may allow oxygen to bind opposite His^2 and near the substrate for productive catalysis. As described below, these chelate binding modes cannot account for the chemistry observed with DAOCS.

Multiple structures of DAOCS and its variants have revealed a series of intriguing features related to this active site. Figure 5 (left) depicts the αKG-bound holoprotein in which the cosubstrate C-1 carboxylate binds opposite His^2 and the keto group coordinates opposite the Asp (Valegård *et al.*, 1998), analogous to the situation in the "off line" enzymes ANS and CarC shown in Figure 3. In contrast to the latter enzymes, however, the substrate-binding site of DAOCS overlaps the binding site of the cosubstrate; thus, simultaneous binding cannot occur (Valegård *et al.*, 2004). To illustrate, in Fe(II)DAOCS/penicillin G the substrate overlaps both the keto group and C-5 carboxylate positions of the αKG (structure not shown). For DAOCS apoprotein crystals soaked with Fe(II), αKG, and penicillin G (or ampicillin), the structures reveal a mixture of two species containing either the cosubstrate or the substrate. Notably, the substrate-binding mode differs for these samples compared to the case where crystals are soaked with only Fe(II) and substrate; i.e., the presence of αKG somehow causes the penicillin G (or ampicillin) to orient so that its ring sulfur atom binds Fe(II) (Valegård

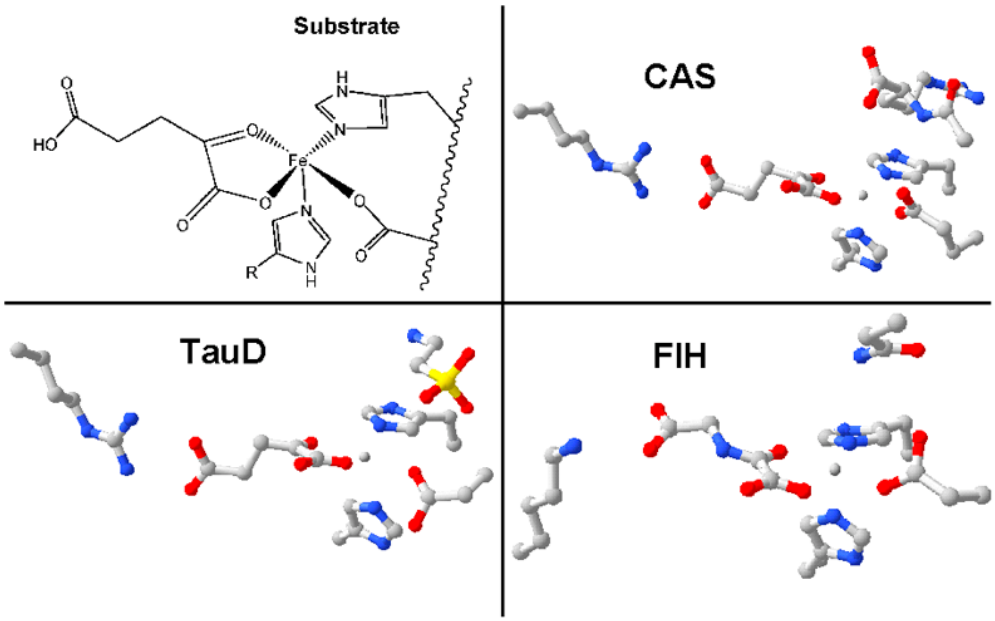

FIG. 2. "In-line" active site structure. Some Fe(II)/αKG-dependent dioxygenases bind their substrates as depicted in this model. The αKG chelates the metal approximately in the same plane as His^1 and the carboxylate ligand of the His^1-X-Asp/Glu-X_n-His^2 motif (with the C-1 carboxylate opposite His^1 and the keto group opposite the acidic residue). The His^2 ligand lies below this plane, leaving an open coordination site above the plane and directed toward the primary substrate. Examples of structures illustrating this substrate-binding mode include CAS (with bound *N*-acetyl-L-arginine) (Zhang *et al.*, 2000), TauD (with bound taurine) (Elkins *et al.*, 2002; O'Brien *et al.*, 2003), FIH (with a bound peptide that includes the Asn residue shown) (Elkins *et al.*, 2003), and AtsK (with bound 2-ethylhexyl-1-sulfate, not shown) (Müller *et al.*, 2004). The αKG C-5 carboxylate forms a salt bridge to Arg residues in CAS, TauD, and AtsK, whereas a Lys residue is used to stabilize this group in FIH. Other residues form hydrogen-bonds to the C-5 carboxylate, and additional Arg residues orient the C-1 carboxylate of αKG (not shown). The FIH structure was obtained by using *N*-oxaloylglycine as a substitute for αKG.

et al., 2004). This binding mode is remarkably similar to that observed for product (isopenicillin N) binding to IPNS (Figure 5, right) (Burzlaff *et al.*, 1999). A product-bound structure of DAOCS reveals similar binding interactions (Valegård *et al.*, 2004). The enzyme was also structurally characterized with another product of the reaction, succinate (Valegård *et al.*, 2004). One carboxylate of this molecule binds Fe(II) opposite the Asp ligand, and the other forms a salt bridge to Arg, a pattern expected to arise upon decarboxylation of αKG. A similar structure was observed for the succinate-bound form of Δ307A DAOCS (with the last four residues replaced by Ala), but the salt bridge is absent and a linear, unhydrated CO_2 molecule (derived from bicarbonate added to buffer) binds opposite His^2 (Lee *et al.*, 2001a).

IPNS is not an Fe(II)/αKG dioxygenase, but it is related in sequence and structure to this enzyme family. The initial IPNS structure, obtained for the Mn-substituted form of this enzyme in the absence of substrate, indicated that the metal is bound via His 214, Asp 216, Gln 330, and His 270 within an eight β strand jellyroll structural motif (Roach *et al.*, 1995). Followup studies showed the Gln residue is displaced by substrate (δ-(L-α-aminoadipoyl)-L-cysteinyl-D-valine) that binds via its thiol directly to the mononuclear Fe(II) active site (Roach *et al.*, 1997). Exposure of these crystals to the oxygen analogue NO identified a likely site of oxygen binding, illustrated in Figure 6. Alternatively, direct exposure of these crystals to high pressures of oxygen afforded the bicyclic product-bound structure, i.e., the IPNS complex with bound isopenicillin N (Burzlaff *et al.*, 1999). Similar treatment with high-pressure oxygen for short time periods was used with crystals containing either of two substrate analogues, δ-(L-α-aminoadipoyl)-L-cysteinyl-L-*S*-methylcysteine and δ-(L-α-aminoadipoyl)-L-cysteinyl-D-α-hydroxyvaleryl ester, leading to structures containing bound monocyclic compound (Burzlaff *et al.*, 1999) or bound thiocarboxylate (Ogle *et al.*, 2001), respectively. The in-crystal formation of the monocyclic product is consistent with the generation of a postulated reaction pathway intermediate, while formation of the thiocarboxylate suggests attack of a thioaldehyde by a hydroperoxide intermediate. These and

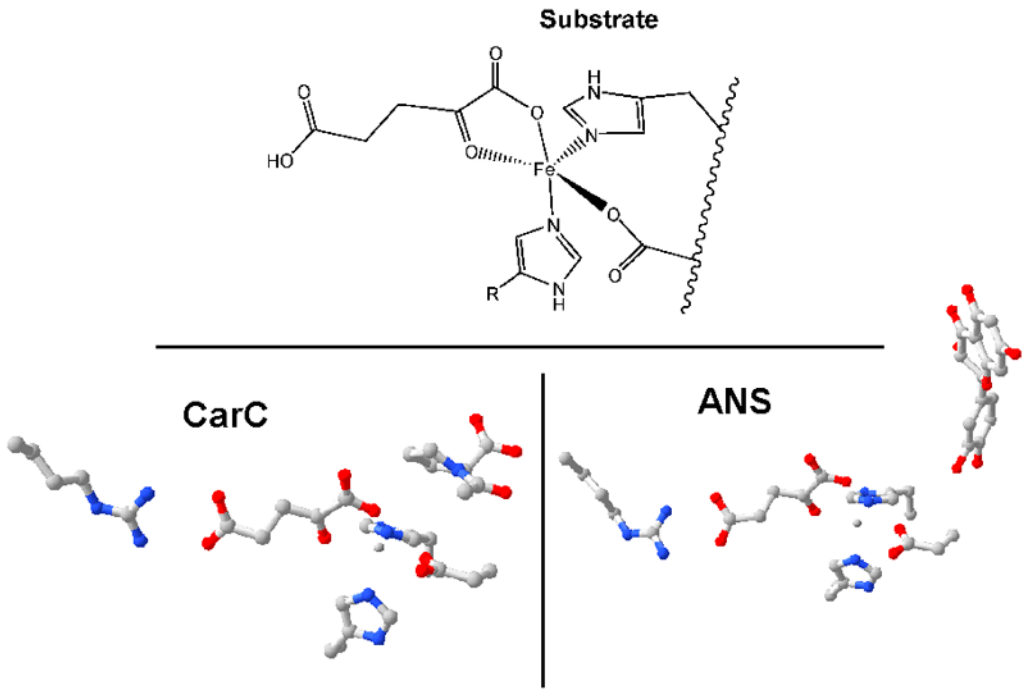

FIG. 3. "Off-line" active site structure. Some Fe(II)/αKG-dependent dioxygenases bind their substrates as depicted in this alternative model. While the αKG keto group is similarly positioned opposite the acidic ligand, the αKG C-1 carboxylate is shifted so as to bind opposite His^2. The open coordination site is thus located opposite His^1, a site that is not directed toward the substrate. Examples of structures illustrating this arrangement include ANS (with bound dihydroquercetin) (Wilmouth *et al.*, 2002) and CarC (with bound L-*N*-acetylproline) (Clifton *et al.*, 2003).

additional structural studies (Long *et al.*, 2003) are providing important insights that will help to define how IPNS carries out its remarkable chemistry.

HPPD is thought to catalyze chemistry similar to the Fe(II)/αKG-dependent hydroxylases, but this protein possesses a clearly distinct structure (Serre *et al.*, 1999) related to the extradiol cleavage enzymes 2,3-dihydroxybiphenyl dioxygenase (Han *et al.*, 1995; Senda *et al.*, 1996) and catechol 2,3-dioxygenase (Kita *et al.*, 1999). Rather than possessing a jellyroll fold, two barrel-like domains are found, with Fe(II) bound to His 161, His 240, and Glu 322 in the second domain. Although the 2 His-1 carboxylate ligand set is similar to the Fe(II)/αKG dioxygenases, the architecture of this site is clearly different. No structure is available for substrate-bound enzyme, but the α-keto acid-containing substrate is likely to chelate the metal ion on the basis of spectroscopic studies (Johnson-Winters *et al.*, 2003).

IV. MECHANISTIC STUDIES

This section examines several proposals for the enzymatic mechanisms of Fe(II)/αKG-dependent hydroxylases and related enzymes while reviewing the associated experimental evidence derived from crystallographic, spectroscopic, and isotope incorporation studies.

A. In-Line Hydroxylation Mechanisms

As a starting point for discussion, I describe the intermediates of the representative hydroxylation mechanism illustrated in Scheme 43. This mechanism has evolved from a model first postulated for prolyl hydroxylase over 20 years ago (Hanauske-Abel & Günzler, 1982).

Intermediate **A** depicts resting enzyme with Fe(II) bound to the three protein side chains found in the His^1-X-Asp/Glu-X_n-His^2 sequence. All Fe(II)/αKG-dependent hydroxylases, with the exception of aspartyl (asparaginyl) β-hydroxylase, contain this signature motif (Table 1). Furthermore, all protein structures available for this class of enzymes disclose this metal-binding mode, with the side chains found in the same orientation on one face of the metal (Table 2). The crystal structure of Fe(II)-bound but substrate- and αKG-free DAOCS (not a hydroxylase, but found in the same superfamily of enzymes) clearly reveals three additional water molecules in the metal coordination sphere (Valegård *et al.*, 1998). Crystal structures also are reported for Fe(II)-bound proline 3-hydroxylase (Clifton *et al.*, 2001) and FIH (Dann *et al.*, 2002). Metal-bound

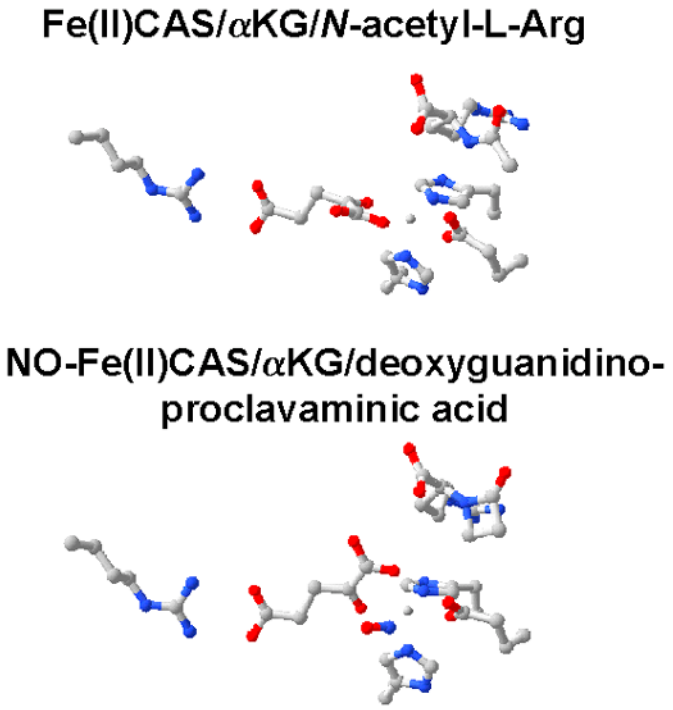

FIG. 4. Conformational flexibility of cosubstrate binding. CAS active site structures are compared for Fe(II)- and αKG-bound forms of the enzyme containing *N*-acetyl-arginine versus deoxyguanidinoproclavaminic acid (Zhang *et al.*, 2000). Significantly, the oxygen analogue NO is bound to the metal ion in the latter structure and the αKG binding mode has shifted.

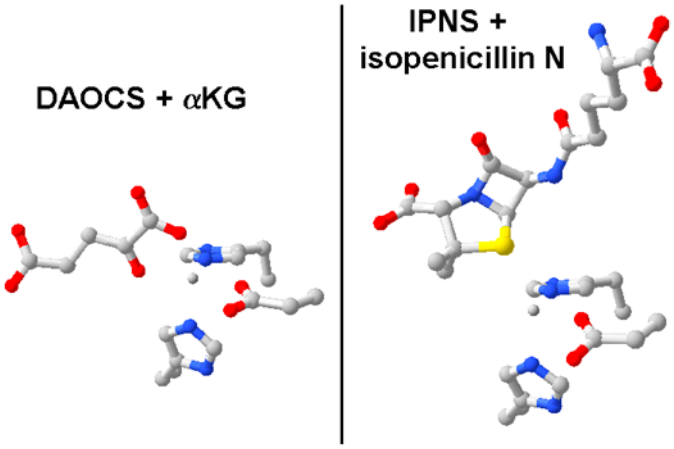

FIG. 5. Active site structures of αKG-bound DAOCS and product-bound IPNS. The cosubstrate- and substrate- (αKG and penicillin) binding sites of DAOCS overlap, precluding simultaneous binding of both molecules (Valegård *et al.*, 2004). The αKG/Fe(II)DAOCS active site structure (Valegård *et al.*, 1998) is illustrated on the left, whereas the substrate-bound DAOCS active site is represented on the right by the very similar structure reported for product (isopenicillin N)-bound IPNS (Burzlaff *et al.*, 1999).

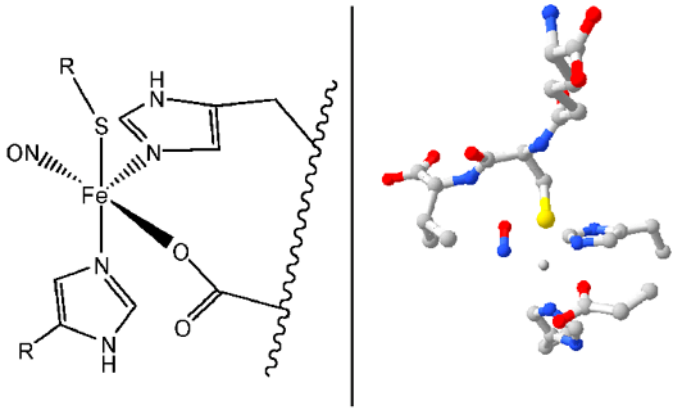

FIG. 6. Substrate-bound IPNS in the presence of the oxygen analogue NO. The active site of IPNS is depicted for enzyme-containing bound δ-(L-α-aminoadipoyl)-L-cysteinyl-D-valine and NO (Roach *et al.*, 1997).

solvent molecules were not observed in these lower resolution structures; although a tartrate molecule (from the crystallization buffer) was found to chelate Fe(II) in the case of FIH. The metal site displays no UV/visible spectral features; however, other types of spectroscopy have been used to characterize the metallocenter. Near-infrared magnetic circular dichroism (MCD) spectroscopy of CAS identified the two d → d transitions (~8,500 cm^{-1} and ~10,000 cm^{-1} at 278 K) expected of a six-coordinate distorted octahedral center (Pavel *et al.*, 1998; Zhou *et al.*, 1998; Zhou *et al.*, 2001). On the basis of Fe(II)-dependent quenching of the intrinsic tryptophan fluorescence of TfdA, a metal ion K_d of 7.45 ± 0.61 μM was estimated (Dunning Hotopp *et al.*, 2003). Kinetic studies show similar μM Fe(II) affinities of related enzymes. By exploiting the weak metal binding affinity of this site, ^{57}Fe was substituted into TauD, allowing analysis by Mössbauer spectroscopy (Price *et al.*, 2003b). The observed isomer shift and quadrupole splitting (δ and ΔE_Q, 1.27 ± 0.05 mm/s and 3.06 ± 0.05 mm/s, respectively) are consistent with high-spin Fe(II) in this holoprotein.

Intermediate **B** corresponds to enzyme with bound Fe(II) and chelated αKG. As summarized in Table 2, structures of this species are available for FIH, CAS, DAOCS, CarC, and AtsK. The five-membered ring formed by αKG chelation of the metal is associated with metal-to-ligand charge-transfer (MLCT) transitions (17,820, 20,820, and 24,070 cm^{-1}), as revealed by UV/visible, CD, and MCD spectroscopy of CAS (Pavel *et al.*, 1998). These CAS studies also reveal the d → d transitions expected of a six-coordinate complex (Zhou *et al.*, 2001). The lilac-colored chromophore exhibits a λ_{max} at 530 nm for both αKG/Fe(II)TauD (Ryle *et al.*, 1999) and αKG/Fe(II)TfdA (Hegg *et al.*, 1999b) (ε_{530} of 140 M^{-1} cm^{-1}

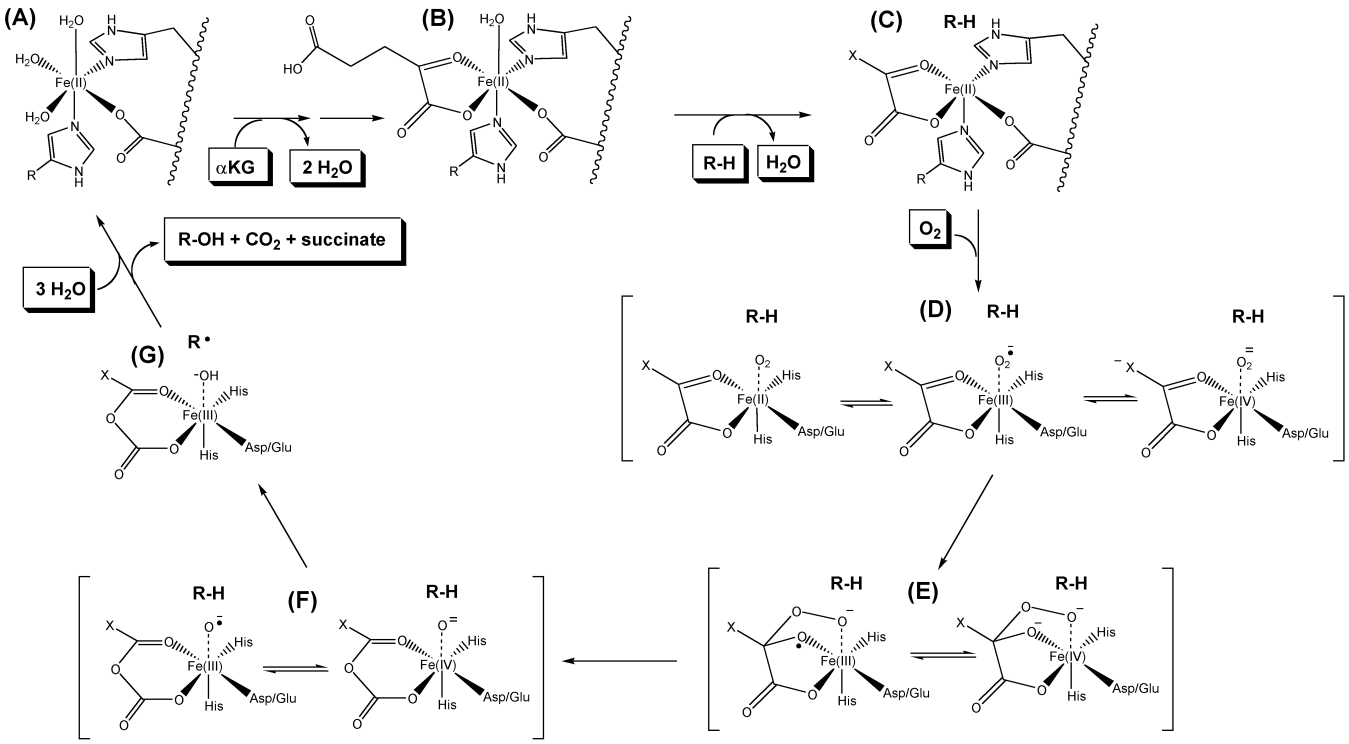

SCHEME 43.

and 180 M^{-1} cm^{-1}, respectively), whereas the feature is observed at 500 nm in αKG/Fe(II)AlkB (Trewick *et al.*, 2002). Stopped-flow UV/visible spectroscopic methods were used to monitor the rate of chromophore formation in the case of TauD (Ryle *et al.*, 1999), and the absorption changes were found to be independent of αKG concentration. These findings were interpreted to indicate that αKG binds in two steps, with initial binding of cosubstrate to the metal ion (e.g., by the αKG carboxylate) followed by a rate-determining conformational change (accompanied by metal chelation) to create the chromophore. Excitation into this TauD absorption band gives rise to two resonance Raman (rR) features at 460 cm^{-1} and 1686 cm^{-1}, both of which are sensitive to ^{18}O labeling of the carbonyl group (i.e., analysis in $H_2{}^{18}O$ leads to shifts of these vibrations to 451 cm^{-1} and 1648 cm^{-1}) (Ho *et al.*, 2001).

Intermediate **C** represents an enzyme with cosubstrate coordinated directly to the metal and the primary substrate bound nearby in the active site. Protein structures are available for FIH, CAS, CarC, ANS, TauD, and AtsK with both the cosubstrate and substrate bound (see Table 2); however, Scheme 43 focuses on the "in line" enzymes (described in Section III and shown in Figure 2), where the open coordination site is directed towards the substrate. This situation is found in FIH, CAS, TauD, and AtsK. The crystal structures of FIH (Elkins *et al.*, 2003), TauD (Elkins *et al.*, 2002; O'Brien *et al.*, 2003), and AtsK (Müller *et al.*, 2004) reveal a five-coordinate metal site indicating the loss of a water molecule as substrate binds. The CAS metallocenter, by contrast, remains 6-coordinate in the crystal, but the metal-to-water bond distance increases from 2.2 to 2.35 Å (Zhang *et al.*, 2000). Substrate-induced changes to the metallocenters of Fe(II)/αKG-dependent hydroxylases also are apparent when using various spectroscopic methods. For example, perturbations to the UV/visible spectra of αKG/Fe(II)TauD and αKG/Fe(II)TfdA are observed when the appropriate substrates bind to these enzymes (Hegg *et al.*, 1999b; Ryle *et al.*, 1999). In both cases, the MLCT features increase slightly in intensity, sharpen so as to reveal three overlapping transitions, and undergo a blue shift (resulting in 520 nm (TauD) and 515 nm (TfdA) as λ_{max} of the major transitions). Stopped-flow UV/visible spectroscopic methods demonstrate that substrate binds to αKG/Fe(II)TauD within the dead time of the instrument (7 ms) (Ryle *et al.*, 1999). The binding of taurine to αKG/Fe(II)TauD also leads to upshifts in the rR vibrations (to 470 cm^{-1} and 1688 cm^{-1} in H_2O, or 460 cm^{-1} and 1653 cm^{-1} in $H_2{}^{18}O$) associated with the chelated metal site (Ho *et al.*, 2001). On the basis of comparisons to similar rR changes in model compounds, this result is attributed to the conversion of a six-coordinate site to a five-coordinate metal center. The Mössbauer parameters of this site also shift ($\delta = 1.16 \pm 0.05$ mm/s and $\Delta E_Q = 2.76 \pm 0.05$ mm/s) in accord with a reduction in coordination number (Price *et al.*, 2003b). Convincing

evidence for a substrate-induced conversion was obtained for αKG/Fe(II)CAS by using UV/visible, near-infrared CD/MCD, and variable-temperature variable-field MCD approaches (Zhou *et al.*, 1998, 2001). The d → d transitions in the near infrared at ~5,200 cm^{-1} and ~8,700 cm^{-1} indicate a five-coordinate site, and the observed MLCT transitions (350 and 500 nm) confirm metal ion chelation by αKG. Substrate-induced creation of an open coordination site on the metal center to allow for oxygen binding is an appealing mechanism for minimizing oxygen reactivity with Fe(II) until substrate is present.

The reaction of oxygen with intermediate **C** and subsequent chemistry leading to substrate hydroxylation are the least well characterized aspects of the mechanism of Fe(II)/αKG-dependent hydroxylases. Oxygen addition initially yields the isoelectronic Fe(II)-O_2, Fe(III)-superoxo, or Fe(IV)-peroxo species (intermediates **D**). Nucleophilic attack on the keto group of αKG results in an Fe(III) or Fe(IV) peroxyhemiketal bicyclic complex (intermediates **E**). By inserting an oxygen atom into the C1-C2 carbon–carbon bond of αKG, the cosubstrate is transformed to a carbonate-succinate mixed anhydride bound to an Fe(III)-hydroxyl radical or Fe(IV)-oxo species (intermediates **F**). Finally, the activated oxygen species positioned near the substrate abstracts a hydrogen atom and forms a substrate radical plus an Fe(III)-hydroxide species (intermediate **G**). Subsequent recombination (joining the hydroxyl group and the substrate radical) results in hydroxylated substrate and restores the Fe(II) form of the enzyme. These last steps in the reaction are comparable to the radical rebound reaction observed in heme-containing oxygenases (Sono *et al.*, 1996). Experimental evidence for an Fe(IV)-oxo intermediate has been obtained for TauD and will be described in Section IV part B.

It is important to note that the carbonate-succinate mixed-anhydride species shown in Scheme 43 (and later) could reasonably transform to yield the separately bound succinate and CO_2 products. Alternatively, αKG may decompose directly to these products without the intermediacy of the anhydride. In either case, the resulting intermediates would be expected to exhibit facile loss of CO_2 to expose an extra metal coordination site as illustrated in Scheme 44.

B. Evidence for an Fe(IV)-oxo Intermediate in TauD

As stated earlier, the least well-understood steps of the hydroxylase mechanism occur after oxygen addition. TauD is the only Fe(II)/αKG-dependent hydroxylase for which an intermediate has been directly detected at this stage of the reaction. UV/visible stopped-flow spectroscopy was used to reveal the existence of a species exhibiting an absorption maximum near 318 nm that forms 20–25 ms after mixing taurine/αKG/Fe(II)TauD with oxygen at 5°C (Price *et al.*, 2003b). This intermediate was trapped by a rapid freeze-quench approach, and the novel species was characterized by Mössbauer and EPR spectroscopies. On the basis of its well-resolved quadrupole doublet ($\delta = 0.31 \pm 0.03$ mm/s and $\Delta E_Q = 0.88 \pm 0.03$ mm/s, assigned to an integer spin species with $S \geq 2$) and the observation of an Fe(III) EPR signal after cryoreduction, the intermediate was identified as some type of Fe(IV)-containing species. Significantly, the rate of decay of the intermediate exhibits a 37-fold decrease when using deuterated taurine. This substantial kinetic isotope effect indicates that the Fe(IV) intermediate is directly responsible for hydrogen atom abstraction from the substrate (Price *et al.*, 2003a). Continuous-flow rR difference spectra (i.e., the rR spectrum of sample mixed with $^{16}O_2$ minus that of sample mixed with $^{18}O_2$) acquired at −38°C after a 0.22 s delay reveals isotope-sensitive vibrations assigned to an Fe(IV)-oxo species (787 cm^{-1} for ^{18}O and 821 cm^{-1} for ^{16}O) as well as additional vibrations (555 cm^{-1} for ^{18}O and 583 cm^{-1} for ^{16}O) that are not yet assigned but may be associated with an Fe(III)-superoxo species (Proshlyakov *et al.*, 2004). Analysis of TauD active site variants provides evidence that Fe(IV)-oxo intermediate is stabilized by a more hydrophobic environment (Ryle *et al.*, unpublished data). Because clear evidence for an Fe(IV)-oxo intermediate is available for TauD, putative mechanistic pathways for other enzymes also will emphasize this species.

C. Off-Line Hydroxylation Mechanisms

For αKG-dependent dioxygenases classified in the "off line" αKG binding mode (Figure 3), such as CarC (Clifton *et al.*, 2003) and ANS (Wilmouth *et al.*, 2002), two

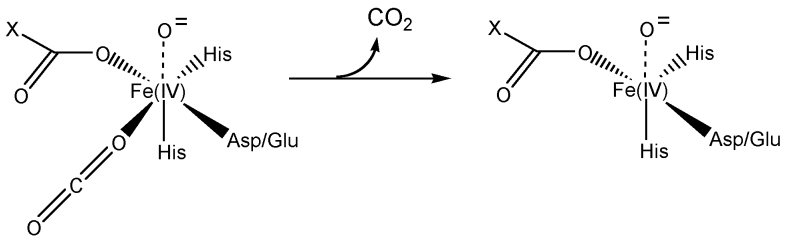

SCHEME 44.

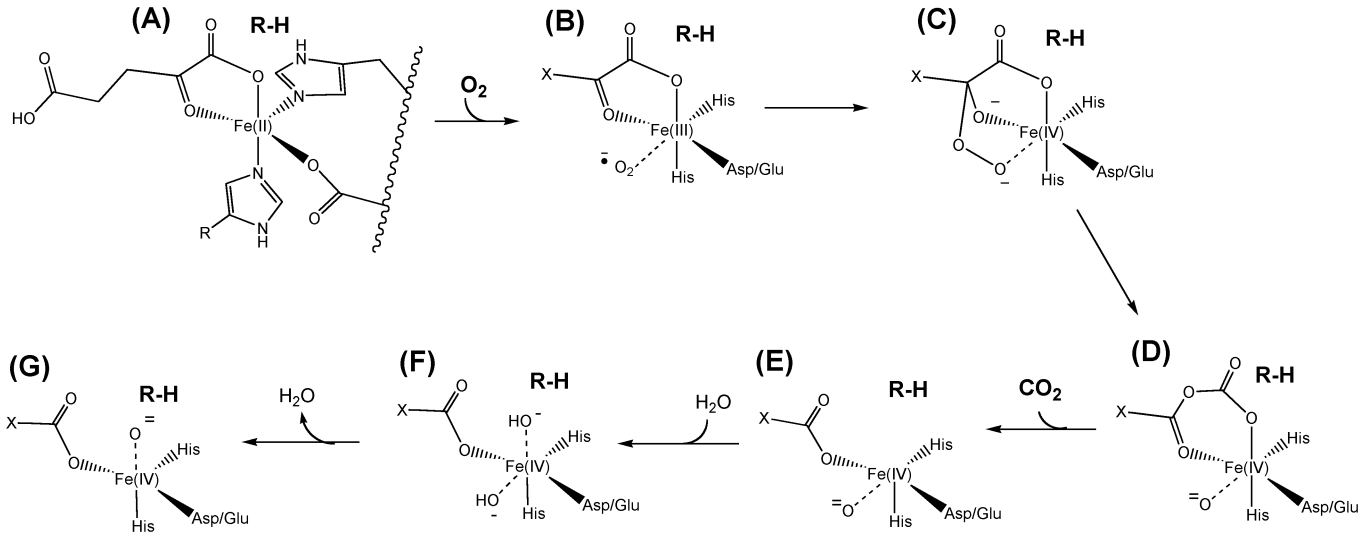

SCHEME 45.

reasonable options can explain how an activated oxygen atom becomes appropriately positioned near the substrate. One possibility is that conformational flexibility of αKG allows it to reorient to adopt an "in line" geometry, so that subsequent steps are equivalent to those in Scheme 43. Alternatively, the "off line" enzymes may undergo a series of steps analogous to those of Scheme 43, but resulting in an Fe(IV)-oxo (or Fe(III)-hydroxyl radical) species positioned away from the substrate (Scheme 45, species **A** to **D**; note that only one possible species is shown here for each intermediate). Loss of CO_2 provides an open coordination site to which water can bind (**D** to **F**). Subsequent loss of water from the dihydroxylated metal site (**F** to **G**) results in a "ferryl flip" (Zhang *et al.*, 2002) to position the activated oxygen near the substrate. Hydrogen atom abstraction and radical recombination can then proceed as described earlier to achieve substrate hydroxylation.

D. Desaturation Mechanisms

The mechanism of αKG-dependent desaturases is likely to be closely related to that of the αKG-dependent hydroxylases. As described in Section II, these enzymes include CarC, flavone synthase, flavonol synthase, and ANS, as well as one reaction catalyzed by CAS. One reasonable mechanism to explain this chemistry invokes an Fe(IV)-oxo abstraction of a hydrogen atom, radical recombination to give the hydroxylated product, followed by a dehydration reaction to form the double bond. Arguing against this mechanism, the hydroxylated intermediate generally is not observed as a side product of these enzymes, nor can it be used as a substrate for dehydration reactions. An alternative mechanism also begins with formation of the Fe(IV)-oxo species, but it is followed by two hydrogen atom transfers from the substrate to directly produce the product as illustrated in Scheme 46.

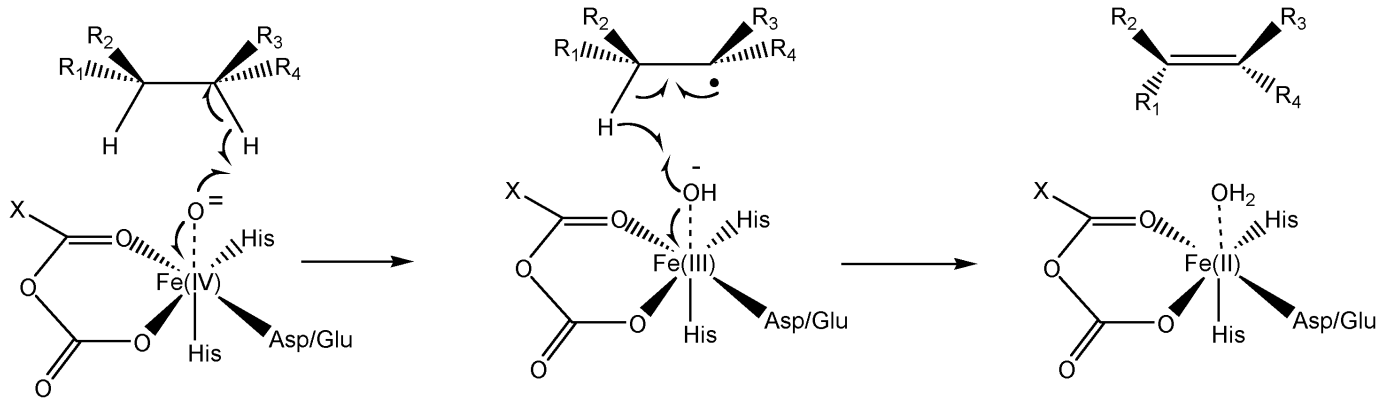

SCHEME 46.

E. Ring-Expansion Mechanisms

DAOCS most probably utilizes an Fe(IV)-oxo (or Fe(III)-hydroxyl radical) intermediate to catalyze an αKG-dependent ring expansion reaction. Structural and kinetic studies suggest that αKG and the substrate penicillin N cannot simultaneously bind to the active site (Valegård *et al.*, 2004), hence this enzyme does not fall into the "in line" or "off line" categories. Rather, it appears that oxygen reacts with αKG/Fe(II)DAOCS (depicted in Figure 5, left panel) to produce an activated oxygen intermediate in the absence of substrate; CO_2 and succinate then dissociate and penicillin N later binds to allow further chemistry. Assuming that the DAOCS protein environment is capable of adequately stabilizing the standard activated oxygen species, the first portion of the DAOCS reaction is able to be accommodated by the chemistry shown in steps **A** through **E** of Scheme 45. Alternatively, the Fe(IV)-oxo species has been proposed to derive from a mechanism involving a persuccinic acid intermediate (Scheme 47) (Valegård *et al.*, 2004). *Ab initio* quantum molecular dynamics and simulated annealing calculations indicate that the planar peracid is less reactive than a ferryl species and should be a more stable intermediate. Arguing against a more general mechanism involving a peracid for this family of enzymes is the lack of observed activity when synthetic persuccinic acid (in place of αKG plus oxygen) is added to prolyl hydroxylase or pyrimidine deoxyribonucleoside 2′-hydroxylase (Abbott & Udenfriend, 1974). It is possible that the peracid behaves differently when added to the enzyme than when generated *in situ*, or it may be that different Fe(II)/αKG-dependent dioxygenases use distinct pathways to generate the terminal oxygenating intermediate.

Once DAOCS has generated a reactive oxygen species, the second half of the reaction takes place. One possible mechanism to account for the ring-expansion reaction is illustrated in Scheme 48 (Valegård *et al.*, 2004). This sequence suggests that CO_2 and succinate dissociate (**A** to **B**), penicillin N binds (**B** to **C**, yielding a structure analogous to that shown in Figure 5, right panel), hydrogen atom abstraction yields a substrate radical and Fe(III)-OH species (**C** to **D**), the radical rearranges (**D** to **F**), and a second hydrogen atom transfer (**F** to **G**) yields product plus Fe(II)-OH_2. Note that the latter step is analogous to that proposed for desaturases and shown in Scheme 46.

F. IPNS Mechanism

IPNS also is likely to use an Fe(IV)-oxo intermediate during its remarkable bicyclization reaction to form the antibiotic β-lactam unit. In this case, the critical intermediate is generated without use of αKG. Extensive studies over the years, primarily carried out by the Oxford group (Baldwin & Abraham, 1988; Schofield *et al.*, 1997), have led to the proposed mechanism shown in Scheme 49. An end-on Fe(IV)-peroxo species is suggested to deprotonate the methylene position of the cysteinyl residue (**C**). The O─O bond of the Fe(II)-hydroperoxide is heterolytically cleaved as the amide proton is removed and the four-membered ring forms (**D**). The resulting Fe(IV)-oxo species carries out hydrogen atom abstraction, leading to formation of the five-membered ring (**E** to **G**) (Burzlaff *et al.*, 1999; Ogle *et al.*, 2001; Roach *et al.*, 1995, 1997). As noted in Section III, structures are available depicting several "snapshots" of this reaction including bound substrate, bound substrate in the presence of NO as an O_2 analogue (Figure 6), a structure representing the monocyclic intermediate, and bound product (Figure 5, right).

G. ACC Oxidase Mechanism

The ethylene-forming enzyme of plants, ACC oxidase, utilizes ascorbic acid rather than αKG as the two-electron reductant. Several potential mechanisms have been proposed for this extraordinary reaction (e.g., Barlow *et al.*, 1997; Pirrung *et al.*, 1998; Rocklin *et al.*, 1999), but a single hypothesis that most closely parallels the other reactions of this enzyme family is discussed here (Scheme 50). CO_2 plays a critical role in maximizing activity of the enzyme by minimizing the extent of autoinactivation,

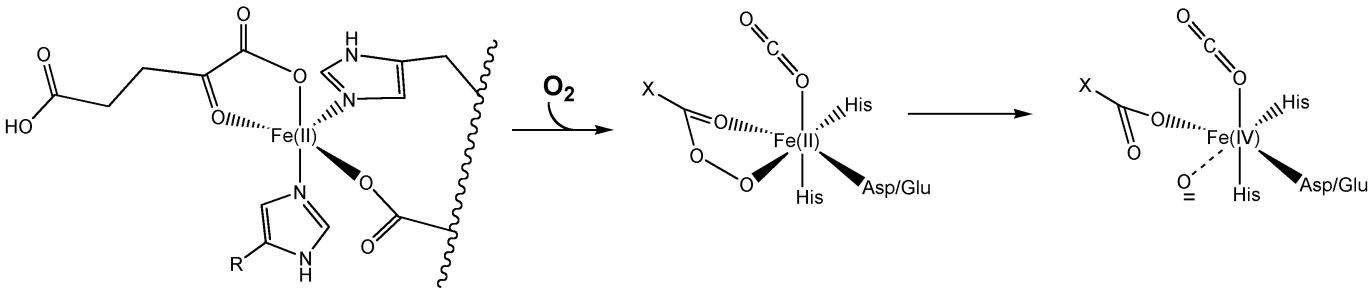

SCHEME 47.

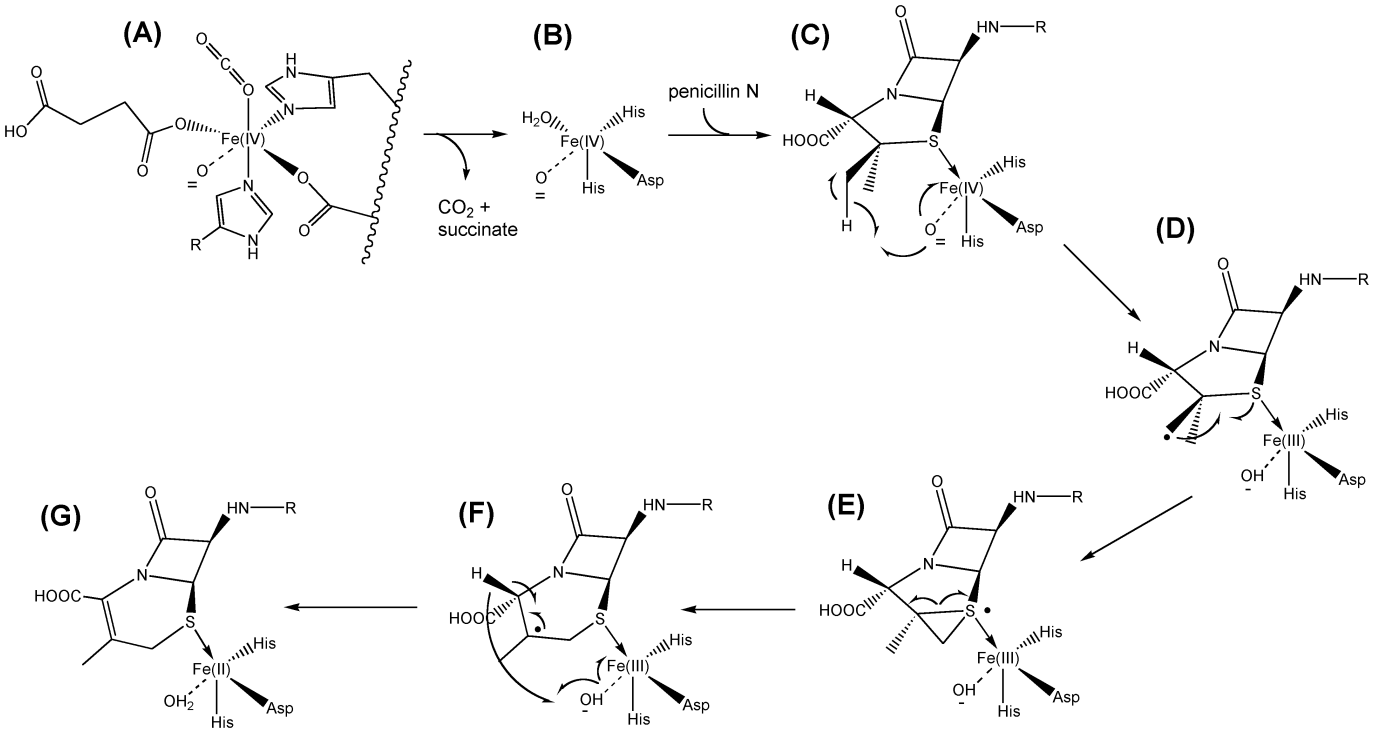

SCHEME 48.

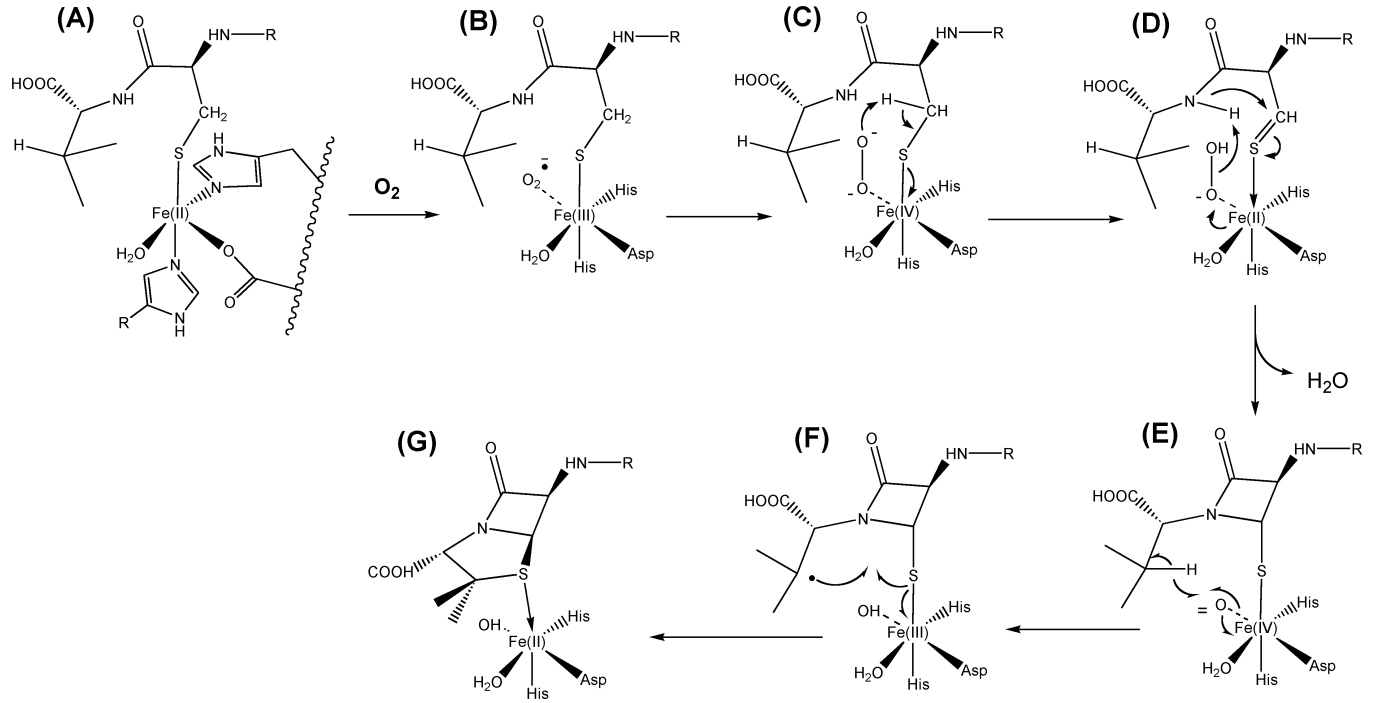

SCHEME 49.

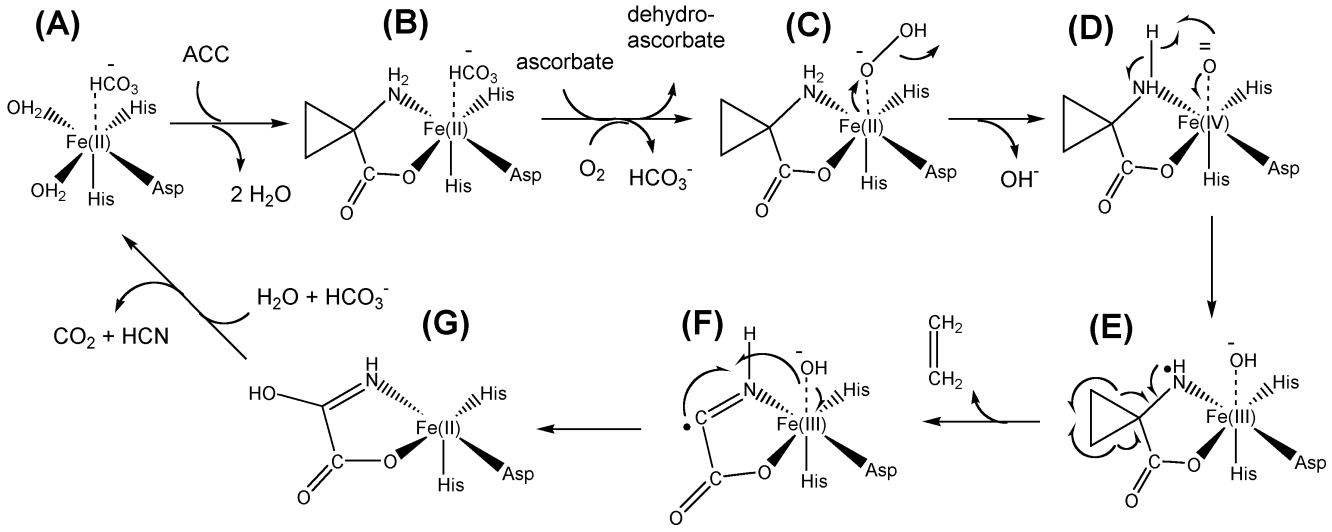

SCHEME 50.

presumably by reacting with a metal-bound solvent molecule to generate the bicarbonate-bound species (**A**) (Zhou *et al.*, 2002). ACC is suggested to chelate the metal ion (**B**) on the basis of ENDOR studies of NO-bound enzyme in the presence of isotopically labeled substrate analogues (Rocklin *et al.*, 1999). Binding of ascorbic acid stimulates loss of the bound bicarbonate and enhances reactivity with oxygen. As oxygen binds, ascorbate donates two electrons by an outer sphere mechanism to generate an Fe(II)-hydroperoxo species (**C**). Heterolytic O-O cleavage (analogous to that just described for IPNS) results in loss of hydroxide and formation of the Fe(IV)-oxo species (**D**). Hydrogen atom abstraction, radical rearrangement, and hydroxyl radical transfer yields a metal-bound intermediate (**G**) that decomposes to the observed products.

H. HPPD Mechanism

Although unrelated to the αKG-dependent dioxygenases in sequence or structure, HPPD catalyzes a chemically similar mechanism and is likely to utilize analogous intermediates. A reasonable mechanism of HPPD is illustrated in Scheme 51. Resting enzyme contains Fe(II) bound to a 2 His-1 carboxylate motif (**A**). The α-keto acid is proposed to chelate the metal (**B**), thus greatly enhancing oxygen reactivity (Johnson-Winters *et al.*, 2003). Oxygen binds to form an Fe(III)-superoxo or analogous species (**C**) followed by nucleophilic attack to form a bicyclic species (**D**). Still analogous to the αKG-dependent enzymes, O─O bond cleavage provides an Fe(IV)-oxo intermediate and the 4-hydroxyphenylacetate-bicarbonate anhydride (**E**, or its decarboxylation products CO_2 and 4-hydroxyphenylacetate). The activated oxygen inserts into the aromatic ring to form the arene oxide (**F**). This species can rearrange to form oxepinone (Gunsior *et al.*, 2004), providing support for the epoxide, or undergoes an "NIH shift" and rearranges further to yield the known products.

I. Nonproductive Reactions with Oxygen

Further complicating analyses of the Fe(II)/αKG-dependent dioxygenase mechanisms are nonproductive reactions that take place with oxygen. For example, the metal sites of substrate-free forms of these enzymes are oxidized by oxygen, resulting in inactive Fe(III)-containing enzymes. Alternatively, αKG-bound enzymes may exhibit "uncoupled turnover" in which αKG decomposes to CO_2 and succinate (with no corresponding substrate transformation) as the enzyme becomes inactivated. This situation has long been known to occur in prolyl hydroxylase (e.g., Counts *et al.*, 1978; Rao & Adams, 1978; Tuderman *et al.*, 1977), where the uncoupling reaction was shown to result in the metal becoming oxidized (Jong & Kemp, 1984) in an ascorbic acid-reversible manner (Myllylä *et al.*, 1978, 1984). Similar ascorbate-reversible uncoupling reactions occur in several other representatives of this enzyme family, especially if inhibitors or poor substrates are included (e.g., lysyl hydroxylase (Puistola *et al.*, 1980), thymine hydroxylase (Hsu *et al.*, 1981), γ-butyrobetaine hydroxylase (Holme *et al.*, 1984), TfdA (Saari & Hausinger, 1998), and AlkB (Trewick *et al.*, 2002; Welford *et al.*, 2003)). The ability of ascorbic acid to reverse metal oxidation accounts for its widespread use in buffers for assaying these enzymes. Whereas the rates of product formation often decrease rapidly over time for these enzymes, inclusion of ascorbate yields more linear progress curves (e.g., Fukumori & Hausinger, 1993). Significantly, the rates of

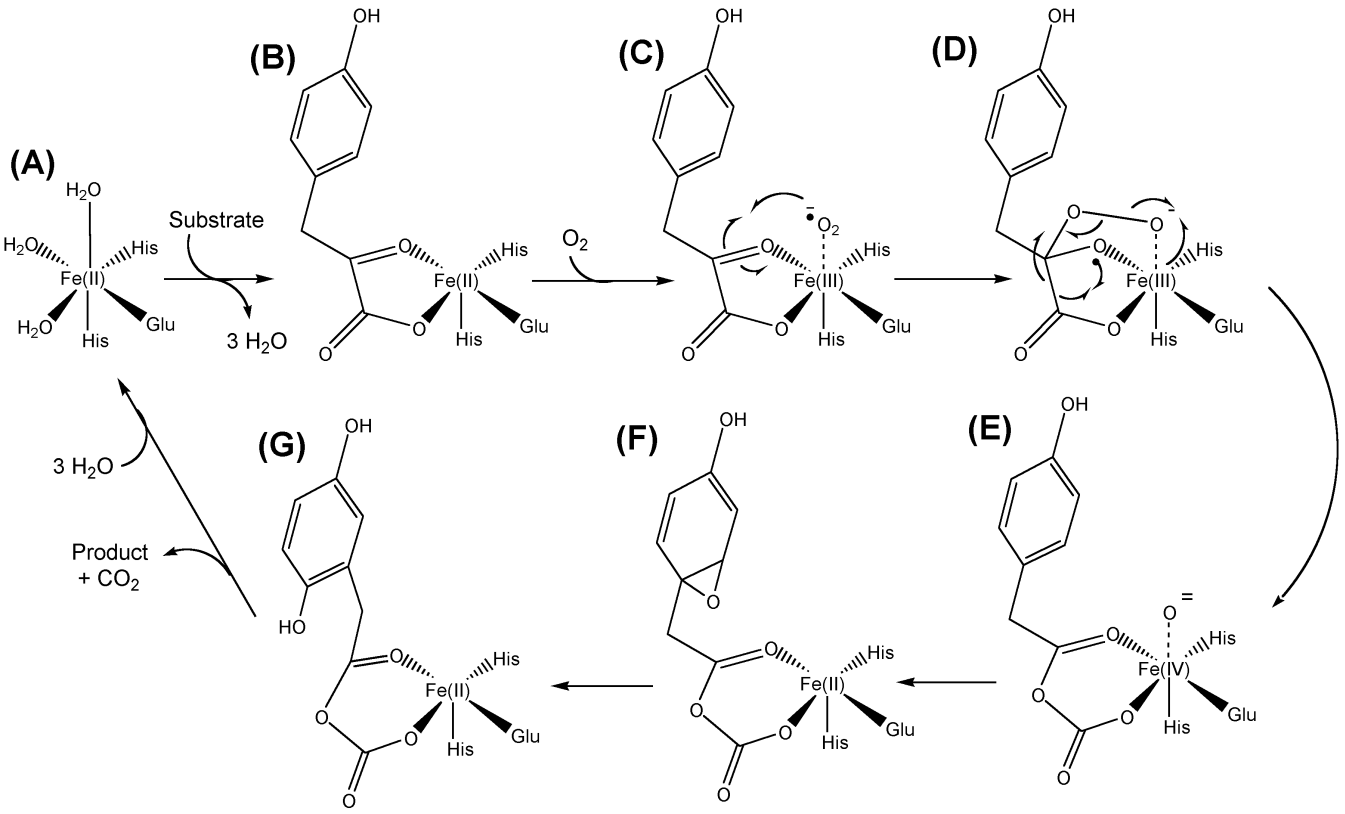

SCHEME 51.

metal center oxidation by direct or uncoupled reaction pathways are generally much slower than the rates of substrate transformation.

In addition to the ascorbate-reversible inactivating reactions associated with uncoupled turnover, uncoupling reactions leading to irreversible protein modifications have been noted in TfdA, AlkB, and TauD. Exposure to oxygen of αKG/Fe(II)TfdA and αKG/Fe(II)AlkB converts the samples with pink chromophores (due to MLCT transitions of the Fe(II)/αKG chelates) to blue species (λ_{max} of 580 nm and 595 nm with $\varepsilon_{580–590}$ of ~1000 M^{-1} cm^{-1} and 960 M^{-1} cm^{-1}, respectively) (Henshaw *et al.*, 2004; Liu *et al.*, 2001). Several lines of evidence were used to assign the new chromophores to ligand-to-metal charge-transfer (LMCT) transitions arising from hydroxy-tryptophan (OH-Trp) coordination to Fe(III). The metal-oxidation state of TfdA was identified as Fe(III) by EPR identification. In addition, specific rR vibrations (corresponding to hydroxyindole-Fe(III) features observed in model compounds) were observed for TfdA. Finally, OH-Trp residues were identified in each protein on the basis of mass spectrometric evidence. The modified residue in TfdA (Trp 113) lies adjacent to the His^1 metal ligand (His 114) (Liu *et al.*, 2001), whereas the target for self hydroxylation of AlkB (Trp 178) is located nine residues before His^2 in the sequence (His 187). Despite these differences, a predicted structure of AlkB positions Trp 178 in the active site environment and only 4.7 Å from the metal (Henshaw *et al.*, 2004). TauD exhibits a distinct form of protein modification in which a tyrosine side chain is transformed into a catechol (Ryle *et al.*, 2003a, 2003b). Stopped-flow UV/visible spectroscopy revealed that αKG/Fe(II)TauD reacts with oxygen to generate an intermediate species (λ_{max} at 408 nm) followed by a final protein product (λ_{max} of 550 nm). The 408 nm species was assigned to a tyrosyl radical species on the basis of EPR characterization, and the 550 nm species was identified as a catecholate-Fe(III) LMCT transition by using rR spectroscopy (Ryle *et al.*, 2003b). Both the tyrosyl radical and the modified tyrosine were shown to derive from Tyr 73, a residue located 6.5 Å from the metal ion. A distinct type of catecholate-Fe(III) species (λ_{max} at ~700 nm) also involving Tyr 73 was identified in hydrogen peroxide-treated enzyme sample (Ryle *et al.*, 2003a). The spectroscopically distinct samples were interconverted depending on whether bicarbonate was bound to the metal, leading to the suggestion that αKG-derived CO_2/bicarbonate remains associated with the oxidized metallocenter. As illustrated in Scheme 52, formation of the tyrosyl radical and catechol species are readily accommodated in mechanisms that

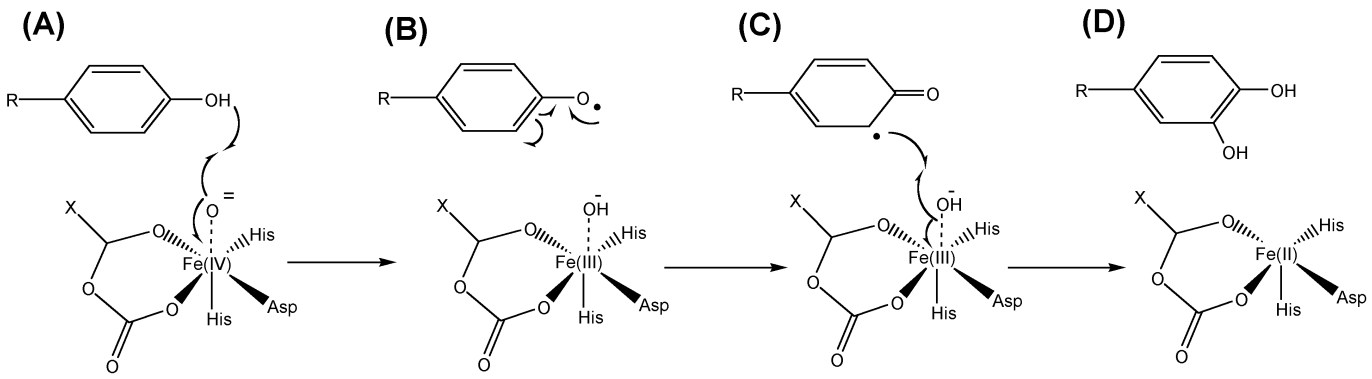

SCHEME 52.

utilize Fe(IV)-oxo intermediates. An analogous reaction is plausible for generating the OH-Trp residues in TfdA and AlkB. Notably, the uncoupling reactions leading to aberrant self-hydroxylation chemistry occur at rates that are much slower than the catalytic reactions involving substrate.

J. Insights from ^{18}O Isotope Labeling Studies

Experimental evidence from $^{18}O_2$ and $H_2{}^{18}O$ isotope studies has been used to identify the sources of the oxygen atoms incorporated into succinate and the hydroxylated substrate of various representatives of this enzyme class and to provide additional insight into the possible intermediacy of an Fe(IV)-oxo species. For all cases examined, O_2 supplies the majority of the oxygen incorporated into succinate (e.g., studies of γ-butyrobetaine hydroxylase (Lindblad *et al.*, 1969), DAOCS (Baldwin *et al.*, 1989), thymine hydroxylase (Holme *et al.*, 1971; Thornburg *et al.*, 1993), HPPD (Lindblad *et al.*, 1970), and α-ketoisocaproate dioxygenase (Sabourin & Bieber, 1982); note that the latter two activities were later shown to be associated with the same enzyme (Crouch *et al.*, 1997)). Oxygen gas also is the predominant source of oxygen incorporated into the products (or, in some cases, the side products) of several αKG-dependent dioxygenases; e.g., collagen-specific prolyl hydroxylase (Kikuchi *et al.*, 1983; Min *et al.*, 2000), HIF-specific prolyl hydroxylase (McNeill *et al.*, 2002b), FIH (Hewitson *et al.*, 2002), CAS (Lloyd *et al.*, 1999b), DAOCS (Baldwin *et al.*, 1993), thymine hydroxylase (Holme *et al.*, 1971), anthocyanidin synthase, flavonol synthase, and flavanone 3β-hydroxylase (Turnbull *et al.*, 2004). Significantly, many of these reactions were shown to be less than 100% efficient, with the remainder of the oxygen presumed to derive from water. Furthermore, only a small percentage of the incorporated oxygen is supplied from O_2 for lysyl hydroxylase (Kikuchi *et al.*, 1983), HPPD (Lindblad *et al.*, 1970), and α-ketocaproate dioxygenase (where this activity is associated with HPPD (Crouch *et al.*, 1997)) (Sabourin & Bieber, 1982). Moreover, the slow self-hydroxylation reactions noted earlier for TfdA and TauD (Liu *et al.*, 2001; Ryle *et al.*, 2003a) were shown by rR spectroscopy of the resulting chromophores to incorporate oxygen primarily from water. (The source of oxygen incorporated into the normal products of these enzymes has not yet been elucidated). Clearly, the latter hydroxylation reactions must utilize an intermediate that exchanges with solvent.

A reasonable hypothesis to explain the divergence in solvent exchange rates of αKG-dependent dioxygenases is that a critical intermediate differs in lifetime and solvent accessibility among these proteins. For example, the postulated succinate-bicarbonate anhydride intermediates may decompose with different kinetics, allowing a range of rates associated with CO_2 loss and solvent access. Alternatively, one must consider that different enzymes utilize distinct activated oxygen species to hydroxylate their substrates. For example, some enzymes may utilize Fe(IV)-oxo (capable of solvent exchange) as their activated oxygen species, others may exploit the Fe(III)-hydroxyl radical species (likely to be less capable of exchanging with solvent), or equilibration may occur between these species in selected enzymes. Potential support for a nonexchangeable intermediate is offered by ANS, an "off line" enzyme according to structural studies (Wilmouth *et al.*, 2002), that shows no exchange with solvent despite a possible requirement for a ferryl flip to orient the reactive oxygen species towards the substrate. It is also possible, however, that αKG reorients in the ANS active site to allow proper positioning of the reactive oxygen, which rapidly reacts with substrate before significant levels of solvent exchange can occur.

K. Biomimetic Studies

Additional evidence for the proposed Fe(IV)-oxo intermediate in the enzymatic reaction has been obtained by studies of high-valent Fe compounds containing nonporphyrin

ligands. Two such Fe(IV)-oxo compounds have been described, including one which was sufficiently stable to allow crystallographic characterization (Lim *et al.*, 2003; Rohde *et al.*, 2003). Other chemical models containing α-keto acids exhibit chemical reactivity similar to the Fe(II)/αKG-dependent hydroxylases, including catalysis of ligand hydroxylation (much like the enzyme self-hydroxylation reactions (Henshaw *et al.*, 2004; Liu *et al.*, 2001; Ryle *et al.*, 2003a)) and are thought to generate Fe(IV)-oxo intermediates (Hegg *et al.*, 1999a; Jensen *et al.*, 2003; Mehn *et al.*, 2003). Activated oxygen intermediates other than the Fe(IV)-oxo species also must still be considered, and Fe(III)-oxo (MacBeth *et al.*, 2000), Fe(III)-peroxide (e.g., Chen & Que, 1999; Hazell *et al.*, 2002; Ho *et al.*, 1999a, 1999b; Jensen *et al.*, 1999; Roelfes *et al.*, 1999, 2000; Simaan *et al.*, 1999; Wada *et al.*, 1999), and other species have been characterized as summarized in an excellent review on this topic (Solomon *et al.*, 2000).

V. CONCLUDING REMARKS

The Fe(II)/αKG-dependent hydroxylases and related enzymes participate in a vast array of biologically important reactions. Ongoing genomic and proteomic studies, followed up by appropriate biochemical analyses, are certain to uncover additional reactions catalyzed by this superfamily of enzymes. Structural studies have advanced very rapidly for this group of proteins, but further structural investigations (buttressed by site-directed mutagenesis analyses) are needed to better define the features important for substrate recognition and choice of reaction pathway, and to identify critical intermediates of these enzymes. An Fe(IV)-oxo species is likely to be the key reactive intermediate in at least some of these enzymes and has been characterized by pre-steady–state techniques, but further spectroscopic and other efforts are needed to elucidate additional or alternative intermediates in the various family members.

ACKNOWLEDGMENTS

I thank Michael Kertesz and Inger Andersson for communication of unpublished information. Studies related to Fe(II)/αKG-dependent hydroxylases carried out in the Hausinger laboratory were supported by National Institutes of Health Grant GM063584.

REFERENCES

Aas, P.A., Otterlei, M., Falnes, P.O., Vagbe, C.B., Skorpen, F., Akbari, M., Sundheim, O., Bjoras, M., Slupphaug, G., Seeberg, E., and Krokan, H.E. 2003. Human and bacterial oxidative demethylases repair alkylation damage in both RNA and DNA. *Nature* **421:**859–863.

Abbott, M.T., Schandl, E.K., Lee, R.F., Parker, T.S., and Midgett, R.J. 1967. Cofactor requirements of thymine hydroxylase. *Biochim Biophys Acta* **132:**525–528.

Abbott, M.T. and Udenfriend, S. 1974. α-Ketoglutarate-coupled dioxygenases, In: *Molecular Mechanisms of Oxygen Activation*. pp. 167–214, O. Hayaishi, Ed., Academic Press, New York.

Abbruzzese, A., Hanauske-Able, H.M., Park, M.H., Henke, S., and Folk, J.E. 1991. The active site of deoxyhypusyl hydroxylase: use of catecholpeptides and their component chelator and peptide moieties as molecular probes. *Biochim Biophys Acta* **1077:**159–166.

Abbruzzese, A., Park, M.H., and Folk, J.E. 1986. Deoxyhypusine hydroxylase from rat testis. Partial purification and characterization. *J Biol Chem* **261:**3085–3089.

Adams, D.O. and Yang, S.F. 1979. Ethylene biosynthesis: identification of 1-aminopropane-1-carboxylic acid as an intermediate in the conversion of methionine to ethylene. *Proc Natl Acad Sci USA* **76:**170–174.

Annunem, P., Koivunen, P., and Kivirikko, K.I. 1999. Cloning of the α-subunit of prolyl 4-hydroxylase from *Drosophila* and expression and characterization of the corresponding enzyme tetramer with some unique properties. *J Biol Chem* **274:**6790–6796.

Anzellotti, D. and Ibrahim, R.K. 2000. Novel flavonol 2-oxoglutarate dependent dioxygenase: affinity purification, characterization, and kinetic properties. *Arch Biochem Biophys* **382:**161–172.

Aravind, L. and Koonin, E.V. 2001. The DNA-repair protein AlkB, EGL-9, and leprecan define new families of 2-oxoglutarate-dependent- and iron-dependent dioxygenases. *Genomebiology.com* **2:**7.1–7.8.

Baker, B.J., Dotzlaf, J.E., and Yeh, W.-K. 1991. Deacetoxycephalosporin C hydroxylase of *Streptomyces clavuligerus*. Purification, characterization, bifunctionality, and evolutionary implication. *J Biol Chem* **266:**5087–5093.

Baldwin, J.E. and Abraham, E. 1988. The biosynthesis of penicillins and cephalosporins. *Nat Prod Rep* **5:**129–145.

Baldwin, J.E., Adlington, R.M., Coates, J.B., Crabbe, M.J.C., Crouch, N.P., Keeping, J.W., Knight, G.C., Schofield, C.J., Ting, H.-H., Vallejo, C.A., Thorniley, M., and Abraham, E.P. 1987. Purification and initial characterization of an enzyme with deacetoxycephalosporin C synthetase and hydroxylase activities. *Biochem J* **245:**831–841.

Baldwin, J.E., Adlington, R.M., Crouch, N.P., and Pereira, I.A.C. 1993. Incorporation of ^{18}O-labelled water into oxygenated products produced by the enzyme deacetoxy/deacetylcephalosporin C synthase. *Tetrahedron* **49:**7499–7518.

Baldwin, J.E., Adlington, R.M., Schofield, C.J., Sobey, W.J., and Wood, M.E. 1989. The role of α-ketoglutarate in cephalosporin biosynthesis. *Chem Commun* 1012–1015.

Bankel, L., Lindstedt, G., and Lindstedt, S. 1972. Thymidine 2′-hydroxylation in *Neurospora crassa*. *J Biol Chem* **247:**6128–6134.

Barlow, J.N., Zhang, Z., John, P., Baldwin, J.E., and Schofield, C.J. 1997. Inactivation of 1-aminocyclopropane-1-carboxylate oxidase involves oxidative modification. *Biochemistry* **36:**3563–3569.

Bohm, B.A. 1998. *Introduction to Flavonoids*. Harwood Academic Publishers, Amsterdam, The Netherlands.

Borovok, I., Landman, O., Kreisberg-Zakarin, R., Aharonowitz, Y., and Cohen, G. 1996. Ferrous active site of isopenicillin N synthase: genetic and sequence analysis of the endogenous ligands. *Biochemistry* **35:**1981–1987.

Bradley, F.C., Lindstedt, S., Lipscomb, J.D., Que, L., Jr., Roe, A.L., and Rundgren, M. 1986. 4-Hydroxyphenylpyruvate dioxygenase is an iron-tyrosinate protein. *J Biol Chem* **261:**11693–11696.

Britsch, L. 1990. Purification and characterization of flavone synthase I, a 2-oxoglutarate-dependent desaturase. *Arch Biochem Biophys* **282:**152–160.

Britsch, L., Dedio, J., Saedler, H., and Forkmann, G. 1993. Molecular characterization of flavanone 3ß-hydroxylases. Consensus sequence, comparison with related enzymes and the role of conserved histidine residues. *Eur J Biochem* **217:**745–754.

Britsch, L. and Grisebach, H. 1986. Purification and characterization of (2*S*)-flavanone 3-hydroxylase from *Petunia hybrida*. *Eur J Biochem* **156:**569–577.

Britsch, L., Ruhnau-Brich, B., and Forkmann, G. 1992. Molecular cloning, sequence analysis, and in vitro expression of flavanone 3β-hydroxylase from *Petunia hybrida*. *J Biol Chem* **267:**5380–5387.

Bruick, R.K. and McKnight, S.L. 2001. A conserved family of prolyl-4-hydroxylases that modify HIF. *Science* **294:**1337–1340.

Brunhuber, N.M.W., Mort, J.L., Christoffersen, R.E., and Reich, N.O. 2000. Steady-state kinetic mechanism of recombinant avocado ACC oxidase: initial velocity and inhibitor studies. *Biochemistry* **39:**10730–10738.

Burzlaff, N.I., Rutledge, P.J., Clifton, I.J., Hensgens, C.M.H., Pickford, M., Adlington, R.M., Roach, P.L., and Baldwin, J.E. 1999. The reaction cycle of isopenicillin *N* synthase observed by X-ray diffraction. *Nature* **401:**721–724.

Busby, R.W., Chang, M.D.-T., Busby, R.C., Wimp, J., and Townsend, C.A. 1995. Expression and purification of two isozymes of clavaminate synthase and initial characterization of the iron binding site. General error analysis in polymerase chain reaction amplification. *J Biol Chem* **270:**4262–4269.

Calcutt, M.J. and Schmidt, F.J. 1994. Gene organization in the bleomycin-resistance region of the producer organism. *Streptomycin verticillus*. *Gene* **151:**17–21.

Chahal, A., Khan, M., Pai, S.G., Barbosa, E., and Singh, I. 1998. Restoration of phytanic acid oxidation in Refsum disease fibroblasts from patients with mutations in the phytanoyl-CoA hydroxylase gene. *FEBS Lett* **429:**119–122.

Chance, M.R., Bresnick, A.R., Burley, S.K., Jiang, J.-S., Lima, C.D., Sali, A., Almo, S.C., Bonanno, J.B., Buglino, J.A., Boulton, S., Chen, H., Eswar, N., He, G., Huang, R., Iiyin, V., McMahan, L., Pieper, U., Ray, S., Vidal, M., and Wang, L.K. 2002. Structural genomics: a pipeline for providing structures for the biochemist. *Prot Science* **11:**723–738.

Charrier, B., Coronado, C., Kondorosi, A., and Ratet, P. 1995. Molecular characterization and expression of alfalfa (*Medicago sativa* L.) flavanone 3-hydroxylase and dihydroflavonol-4-reductase encoding genes. *Plant Molec Biol* **29:**773–786.

Chen, B.J., Carroll, P., and Samson, L. 1994. The *Escherichia coli* AlkB protein protects human cells against alkylation-induced toxicity. *J Bacteriol* **176:**6255–6261.

Chen, H., Thomas, M.G., O'Conner, S.E., Hubbard, B.K., Burkart, M.D., and Walsh, C.T. 2001. Aminoacyl-*S*-enzyme intermediates in β-hydroxylations and α,β-desaturations of amino acids in peptide antibiotics. *Biochemistry* **40:**1651–11659.

Chen, K. and Que, L., Jr. 1999. Evidence for the participation of a high-valent iron-oxo species in stereospecific alkane hydroxylation by a non-heme iron catalyst. *Chem Commun* 1375–1376.

Chen, V.J., Orville, A.M., Harpel, M.R., Frolik, C.A., Surerus, K.K., Münck, E., and Lipscomb, J.D. 1989. Spectroscopic studies of isopenicillin N synthase. A mononuclear nonheme Fe^{2+} oxidase with metal coordination sites for small molecules and substrate. *J Biol Chem* **264:**21677–21681.

Chen, W., Zeng, H., and Tan, H. 2000. Cloning, sequencing, and function of *sanF*: a gene involved in nikkomycin biosythesis of *Streptomyces ansochromogenes*. *Curr Microbiol* **41:**312–316.

Chiang, H.H., Hwang, I., and Goodman, H.M. 1995. Isolation of the *Arabidopsis GA4* locus. *Plant Cell* **7:**195–201.

Choroba, O.W., Williams, D.H., and Spencer, J.B. 2000. Biosynthesis of the vancomycin group of antibiotics: involvement of an unusual dioxygenase in the pathway to (*S*)-4-hydroxyphenylglycine. *J Am Chem Soc* **122:**5389–5390.

Clement, P.M., Hanauske-Abel, H.M., Wolff, E.C., Kleinman, H.K., and Park, M.H. 2002. The antifungal drug ciclopirox inhibits deoxyhypusine and proline hydroxylation, endothelial cell growth and angiogenesis in vitro. *Int J Cancer* **100:**491–498.

Clifton, I.J., Doan, L.X., Sleeman, M.C., Topf, M., Suzuki, H., Wilmouth, R.C., and Schofield, C.J. 2003. Crystal structure of carbapenem synthase (CarC). *J Biol Chem* **278:**20843–20850.

Clifton, I.J., Hsueh, L.-C., Baldwin, J.E., Harlos, K., and Schofield, C.J. 2001. Structure of proline 3-hydroxylase. Evolution of the family of 2-oxoglutarate dependent dioxygenases. *Eur J Biochem* **268:**6625–6636.

Cosper, N.J., Stälhandske, C.M.V., Saari, R.E., Hausinger, R.P., and Scott, R.A. 1999. X-ray absorption spectroscopic analysis of Fe(II) and Cu(II) forms of an herbicide-degrading α-ketoglutarate dioxygenase. *J Biol Inorg Chem* **4:**122–129.

Counts, D.F., Cardinale, G.J., and Udenfriend, S. 1978. Prolyl hydroxylase half reaction: peptidyl prolyl-independent decarboxylation of α-ketoglutarate. *Proc Natl Acad Sci USA* **75:**2145–2149.

Croes, K., Casteels, M., Asselberghs, S., Herdewijn, P., Mannaerts, G.P., and Van Veldhoven, P.P. 1997a. Formation of 2-methyl-branched fatty aldehyde during peroxisomal α-oxidation. *FEBS Lett* **412:**643–645.

Croes, K., Van Veldhoven, P.P., Mannaerts, G.P., and Casteels, M. 1997b. Production of formyl-CoA during peroxisomal α-oxidation of 3-methyl-branched fatty acids. *FEBS Lett* **407:**197–200.

Croes, K., Foulon, V., Casteels, M., Van Veldhoven, P.P., and Mannaerts, G.P. 2000. Phytanoyl-CoA hydroxylase: recognition of 3-methyl-branched acyl-CoAs and requirement for GTP or ATP and Mg^{2+} in addition to its known hydroxylation cofactors. *J Lipid Res* **41:**629–636.

Crouch, N.P., Adlington, R.M., Baldwin, J.E., Lee, M.-H., and MacKinnon, C.H. 1997. A mechanistic rationalization for the substrate specificity of recombinant mammalian 4-hydroxyphenylpyruvate dioxygenase (HPPD). *Tetrahedron* **53:**6993–7010.

Cundliffe, E., Bate, N., Butler, A., Fish, S., Gandecha, A., and Merson-Davies, L. 2001. The tylosin-biosynthetic genes of *Streptomyces fradiae*. *Antonie van Leeuwenhoek* **79:**229–234.

Dames, S.A., Martinez-Yamout, M., De Guzman, R.N., Dyson, H.J., and Wright, P.E. 2002. Structural basis for HIF-1α/CBP recognition in the cellular hypoxic response. *Proc Natl Acad Sci USA* **99:**5271–5276.

Dann, C.E., III, Bruick, R.K., and Deisenhofer, J. 2002. Structure of a factor-inhibiting hypoxia-inducible factor 1: an essential asparaginyl hydroxylase involved in the hypoxic response pathway. *Proc Natl Acad Sci USA* **99:**15351–15356.

De Carolis, E., Chan, F., Balsevich, J., and De Luca, V. 1990. Isolation and characterization of a 2-oxoglutarate dependent dioxygenase involved in the second-to-last step in vindoline biosynthesis. *Plant Physiol* **94:**1323–1329.

De Carolis, E. and De Luca, V. 1993. Purification, characterization, and kinetic analysis of a 2-oxoglutarate-dependent dioxygenase involved in vindoline biosynthesis from *Catharanthus roseus*. *J Biol Chem* **268:**5504–5511.

De Carolis, E. and De Luca, V. 1994. 2-Oxoglutarate-dependent dioxygenases and related enzymes: biochemical characterization. *Phytochem* **36:**1093–1107.

Dinglay, S., Trewick, S.C., Lindahl, T., and Sedgwick, B. 2000. Defective processing of methylated single-stranded DNA by *E. coli alkB* mutants. *Genes Develop* **14:**2097–2105.

Dong, J.G., Fernàndez-Maculet, J.C., and Yang, S.F. 1992. Purification and characterization of 1-aminoacyclopropane-1-carboxylate oxidase from apple fruit. *Proc Natl Acad Sci USA* **89:**9789–9793.

Dotzlaf, J.E. and Yeh, W.-K. 1987. Copurification and characterization of deacetoxycephalosporin C synthetase/hydroxylase from *Cephalosporium acremonium*. *J Bacteriol* **169:**1611–1618.

Dotzlaf, J.E. and Yeh, W.-K. 1989. Purification and properties of deacetoxycephalosporin C synthase from recombinant *Escherichia coli* and its comparison to the native enzyme purified from *Streptomyces clavuligerus*. *J Biol Chem* **264:**10219–10227.

Duncan, T., Trewick, S.C., Koivisto, P., Bates, P.A., Lindahl, T., and Sedgwick, B. 2002. Reversal of DNA alkylation damage by two human dioxygenases. *Proc Natl Acad Sci USA* **99:**16660–16665.

Dunning Hotopp, J.C., Auchtung, T.A., Hogan, D.A., and Hausinger, R.P. 2003. Intrinsic tryptophan fluorescence as a probe of metal and α-ketoglutarate binding to TfdA, a mononuclear non-heme iron dioxygenase. *J Inorg Biochem* **93:**66–70.

Dunning Hotopp, J.C. and Hausinger, R.P. 2001. Alternative substrates for 2,4-dichlorophenoxyacetate/α-ketoglutarate dioxygenase. *J Molec Catalysis B* **15:**155–162.

Dunning Hotopp, J.C. and Hausinger, R.P. 2002. Probing the 2,4-dichlorophenoxyacetate/α-ketoglutarate dioxygenase substrate binding site by site-directed mutagenesis and mechanism-based inactivation. *Biochemistry* **41:**9787–9794.

Eichhorn, E., van der Ploeg, J.R., Kertesz, M.A., and Leisinger, T. 1997. Characterization of α-ketoglutarate-dependent taurine dioxygenase from *Escherichia coli*. *J Biol Chem* **272:**23031–23036.

Elkins, J.M., Hewitson, K.S., McNeill, L.A., Seibel, J.F., Schlemminger, I., Pugh, C.W., Ratcliffe, P.J., and Schofield, C.J. 2003. Structure of factor-inhibiting hypoxia-inducible factor (HIF) reveals mechanism of oxidative modification of HIF-1α. *J Biol Chem* **278:**1802–1806.

Elkins, J.M., Ryle, M.J., Clifton, I.J., Dunning Hotopp, J.C., Lloyd, J.S., Burzlaff, N.I., Baldwin, J.E., Hausinger, R.P., and Roach, P.L. 2002. X-ray crystal structure of *Escherichia coli* taurine/α-ketoglutarate dioxygenase complexed to ferrous iron and substrates. *Biochemistry* **41:**5185–5192.

Epstein, A.C.R., Gleadle, J.M., McNeill, L.A., Hewitson, K.S., O'Rourke, J., Mole, D.R., Mukherji, M., Metzen, E., Wilson, M.I., Dhanda, A., Tian, Y.-M., Masson, N., Hamilton, D.L., Jaakkola, P., Barstead, R., Hodgkin, J., Maxwell, P.H., Pugh, C.W., Schofield, C.J., and Ratcliffe, P.J. 2001. *C. elegans* EGL-9 and mammalian homologs define a family of dioxygenases that regulate HIF by prolyl hydroxylation. *Cell* **107:**43–54.

Ericksson, M., Myllyharju, J., Tu, H., Hellman, M., and Kivirikko, K.I. 1999. Evidence for 4-hydroxyproline in viral proteins. Characterization of a viral prolyl 4-hydroxylase and its peptide substrates. *J Biol Chem* **274:**22131–22134.

Falnes, P.O., Johansen, R.F., and Seeberg, E. 2002. AlkB-mediated oxidative demethylation reverses DNA damage in *Escherichia coli*. *Nature* **419:**178–182.

Foulon, V., Antonenkov, V.D., Croes, K., Waelkens, E., Mannaerts, G.P., Van Veldhoven, P.P., and Casteels, M. 1999. Purification, molecular cloning, and expression of 2-hydroxyphytanoyl-CoA lyase, a peroxisomal thiamin pyrophosphate-dependent enzyme that catalyzes the carbon-carbon cleavage during α-oxidation of 3-methyl-branched fatty acids. *Proc Natl Acad Sci USA* **96:**10039–10044.

Freedman, S.J., Sun, Z.-Y.J., Poy, F., Kung, A.L., Livingston, D.M., Wagner, G., and Eck, M.J. 2002. Structural basis for recruitment of CBP/p300 by hypoxia-inducible factor-1α. *Proc Natl Acad Sci USA* **99:**5367–5372.

Frey, M., Huber, K., Park, W.J., Sicker, D., Lindberg, P., Meeley, R.B., Simmons, C.R., Yalpani, N., and Gierl, A. 2003. A 2-oxoglutarate-dependent dioxygenase is integrated in the DIMBOA-biosynthesis. *Phytochem* **62:**371–376.

Fukuda, H., Fujii, T., and Ogawa, T. 1986. Preparation of a cell-free ethylene-forming system from *Penicillium digitatum*. *Agric Biol Chem* **50:**977–981.

Fukuda, H., Kitajima, H., Fujii, T., Tazaki, M., and Ogawa, T. 1989. Purification and some properties of a novel ethylene-forming enzyme produced by *Penicillium digitatum*. *FEMS Microbiol Lett* **59:**1–6.

Fukuda, H., Ogawa, T., Ishihara, K., Fujii, T., Nagahama, K., Omata, T., Inoue, Y., Tanase, S., and Morino, Y. 1992a. Molecular cloning in *Escherichia coli*, expression, and nucleotide sequence of the gene for the ethylene-forming enzyme of *Pseudomonas syringae* pv. *phaseolicola* PK2. *Biochem Biophys Res Commun* **188:**826–832.

Fukuda, H., Ogawa, T., Tazaki, M., Nagahama, K., Fujii, T., Tanase, S., and Morino, Y. 1992b. Two reactions are simultaneously catalyzed by a single enzyme: the arginine-dependent simultaneous formation of two products, ethylene and succinate, from 2-oxoglutarate by an enzyme from *Pseudomonas syringae*. *Biochem Biophys Res Commun* **188:**483–489.

Fukumori, F. and Hausinger, R.P. 1993a. Purification and characterization of 2,4-dichlorophenoxyacetate/α-ketoglutarate dioxygenase. *J Biol Chem* **268:**24311–24317.

Fukumori, F. and Hausinger, R.P. 1993b. *Alcaligenes eutrophus* JMP134 "2,4-dichlorophenoxyacetate monooxygenase" is an α-ketoglutarate-dependent dioxygenase. *J Bacteriol* **175:**2083–2086.

Galland, S., Le Borgne, F., Bouchard, F., Georges, B., Clouet, P., Grand-Jean, F., and Demarquoy, J. 1999. Molecular cloning and characterization of the cDNA encoding rat liver γ-butyrobetaine hydroxylase. *Biochim Biophys Acta* **1441:**85–92.

Garcia Costas, A.M., White, A.K., and Metcalf, W.W. 2001. Purification and characterization of a novel phosphorus-oxidizing enzyme from *Pseudomonas stutzeri* WM88. *J Biol Chem* **276:**17429–17436.

Gibbons, H.S., Lin, S., Cotter, R.J., and Raetz, C.R.H. 2000. Oxygen requirement for the biosynthesis of the *S*-2-hydroxymyristate moiety in *Salmonella typhimurium* lipid A. Function of LpxO, a new Fe^{2+}/α-ketoglutarate-dependent dioxygenase homologue. *J Biol Chem* **275:**32940–32949.

Goto, M. and Hyodo, H. 1987. Ethylene production by cell-free extract of the kudzu strain of *Pseudomonas syringae* pv. *phaseolicola*. *Plant Cell Physiol* **28:**405–414.

Gronke, R.S., VanDusen, W.J., Garsky, V.M., Jacobs, J.W., Sardana, M.K., Stern, A.M., and Friedman, P.A. 1989. Aspartyl β-hydroxylase: *in vitro* hydroxylation of a synthetic peptide based on the structure of the first growth factor-like domain of human factor IX. *Proc Natl Acad Sci USA* **86:**3609–3613.

Gunsior, M., Ravel, J., Challis, G.L., and Townsend, C.A. 2004. Engineering *p*-hydroxyphenylpyruvate dioxygenase to a *p*-hydroxymandelate synthase and evidence for the proposed benzene oxide intermediate in homogentisate formation. *Biochemistry* **43:**663–674.

Haefelè, C., Bonfils, C., and Sauvaire, Y. 1997. Characterization of a dioxygenase from *Trigonella foenum-graecum* involved in 4-hydroxyisoleucine biosythesis. *Phytochem* **44:**563–566.

Hamilton, A.J., Bouzayen, M., and Grierson, D. 1991. Identification of a tomato gene for the ethylene-forming enzyme by expression in yeast. *Proc Natl Acad Sci USA* **88:**7434–7437.

Han, H. and Pascal, R.A., Jr. 1990. α-Ketoisocaproate dioxygenase: the stereochemical course of the hydroxylation reaction. *J Org Chem* **55:**5173–5176.

Han, S., Eltis, L.D., Timmis, K.N., Muchmore, S.W., and Bolin, J.T. 1995. Crystal structure of the biphenyl-cleaving extradiol dioxygenase from a PCB-degrading pseudomonad. *Science* **270:**976–980.

Hanauske-Abel, H.M. and Günzler, V. 1982. A stereochemical concept for the catalytic mechanism of prolylhydroxylase. Applicability to classification and design of inhibitors. *J Theor Biol* **94:**421–455.

Hashimoto, T., Matsuda, J., and Yamada, Y. 1993. Two-step epoxidation of hyoscyamine to scopolamine is catalyzed by bifunctional hyoscyamine 6ß-hydroxylase. *FEBS Lett* **329:**35–39.

Hashimoto, T. and Yamada, Y. 1987. Purification and characterization of hyoscyamine 6β-hydroxylase from root cultures of *Hyoscyamus niger* L. Hydroxylase and epoxidase activities of enzyme preparations. *Eur J Biochem* **164:**277–285.

Hausinger, R.P., Fukumori, F., Hogan, D.A., Sassanella, T.M., Kamagata, Y., Takami, H., and Saari, R.E. 1997. Biochemistry of 2,4-D degradation: evolutionary implications, In *Microbial Diversity and Genetics of Biodegradation*, pp. 35–51, K. Horikoshi, M. Fukuda, and T. Kudo, Eds., Japan Scientific Press, Tokyo.

Hautala, T., Byers, M.G., Eddy, R.L., Shows, T.B., Kivirikko, K.I., and Myllylä, R. 1992. Cloning of human lysyl hydroxylase: complete cDNA-derived amino acid sequence and assignment of the gene (*PLOD*) to chromosome 1p36.1–p36.2. *Genomics* **13:**62–69.

Hazell, A., McKensie, C.J., Nielsen, L.P., Schindler, S., and Weitzer, M. 2002. Mononuclear non-heme iron(III) peroxide complexes: syntheses, characterization, mass spectrometric and kinetic studies. *J Chem Soc Dalton Trans* 310–317.

Hedden, P. 1997. The oxidases of gibberellin biosynthesis: their function and mechanism. *Physiol Plant* **101:**709–719.

Hedden, P. 1999. Recent advances in gibberellin biosynthesis. *J Exper Bot* **50:**553–563.

Hedden, P. and Kamiya, Y. 1997. Gibberellin biosynthesis: enzymes, genes and their regulation. *Annu Rev Plant Physiol Plant Molec Biol* **48:**431–460.

Hedden, P. and Phillips, A.L. 2000. Gibberellin metabolism: new insights revealed by the genes. *Trend Plant Sci* **5:**523–528.

Hegg, E.L., Ho, R.Y.N., and Que, L., Jr. 1999a. Oxygen activation and arene hydroxylation by functional mimics of α-keto acid-dependent iron(II) dioxygenases. *J Am Chem Soc* **121:**1972–1973.

Hegg, E.L., Whiting, A.K., Saari, R.E., McCracken, J., Hausinger, R.P., and Que, L., Jr. 1999b. Herbicide-degrading α-keto acid-dependent enzyme TfdA: metal coordination environment and mechanistic insights. *Biochemistry* **38:**16714–16726.

Helaakoski, T., Vuori, K., Myllylä, R., Kivirikko, K.I., and Pihlajaniemi, T. 1989. Molecular cloning of the α-subunit of human prolyl 4-hydroxylase: the complete cDNA-derived amino acid sequence and evidence for alternative splicing of RNA transcripts. *Proc Natl Acad Sci USA* **86:**4392–4396.

Henshaw, T.F., Feig, M., and Hausinger, R.P. 2004. Aberrant activity of the DNA repair enzyme AlkB. *J Inorg Biochem* in press:

Hewitson, K.S., McNeill, L.A., Elkins, J.M., and Schofield, C.J. 2003. The role of iron and 2-oxoglutarate oxygenases in signalling. *Biochem Soc Trans* **31:**510–515.

Hewitson, K.S., McNeill, L.A., Riordan, M.V., Tian, Y.-M., Bullock, A.N., Welford, R.W., Elkins, J.M., Oldham, N.J., Bhattacharya, S., Gleadle, J.M., Ratcliffe, P.J., Pugh, C.W., and Schofield, C.J. 2002. Hypoxia-inducible factor (HIF) asparagine hydroxylase is identical to factor inhibiting HIF (FIH) and is related to the cupin structural familly. *J Biol Chem* **277:**26351–26355.

Hieta, R. and Myllyharju, J. 2002. Cloning and characterization of a low molecular weight prolyl 4-hydroxylase from *Arabidopsis thaliana*. Effective hydroxylation of proline-rich, collagen-like, and hypoxia-inducible transcription factor α-like peptides. *J Biol Chem* **277:**23965–23971.

Ho, R.Y.H., Roelfe, G., Hermant, R., Hage, R., Feringa, B.L., and Que, L., Jr. 1999a. Resonance Raman evidence for the interconversion between an $[Fe^{III}\text{-}n^{I}\text{-}O_2]^+$ species and mechanistic implications thereof. *Chem Commun* 2161–2162.

Ho, R.Y.N., Mehn, M.P., Hegg, E.L., Liu, A., Ryle, M.A., Hausinger, R.P., and Que, L., Jr. 2001. Resonance Raman studies of the iron(II)-α-keto acid chromophore in model and enzyme complexes. *J Am Chem Soc* **123:**5022–5029.

Ho, R.Y.N., Roelfes, G., Feringa, B.L., and Que, L., Jr. 1999b. Raman evidence for a weakened O—O bond in mononuclear low-spin iron(III)-hydroperoxides. *J Am Chem Soc* **121:**264–265.

Hogan, D.A., Auchtung, T.A., and Hausinger, R.P. 1999. Cloning and characterization of a sulfonate/α-ketoglutarate dioxygenase from *Saccharomyces cerevisiae*. *J Bacteriol* **181:**5876–5879.

Hogan, D.A., Smith, S.R., Saari, E.A., McCracken, J., and Hausinger, R.P. 2000. Site-directed mutagenesis of 2,4-dichlorophenoxyacetic acid/α-ketoglutarate dioxygenase. Identification of residues involved in metallocenter formation and substrate binding. *J Biol Chem* **275:**12400–12409.

Holme, E. 1975. A kinetic study of thymine 7-hydroxylase from *Neurospora crassa*. *Biochemistry* **14:**4999–5003.

Holme, E., Lindstedt, G., Lindstedt, S., and Tofft, M. 1971. ^{18}O studies of the 2-ketoglutarate-dependent sequential oxygenation of thymine to 5-carboxyuracil. *J Biol Chem* **246:**3314–3319.

Holme, E., Lindstedt, S., and Nordin, I. 1984. Uncoupling and isotope effects in γ-butyrobetaine hydroxylation. *Biosci Rep* **4:**433–440.

Holton, T.A., Brugliera, F., and Tanaka, Y. 1993. Cloning and expression of flavonol synthase from *Petunia hybrida*. *Plant J* **4:**1003–1010.

Hon, W.-C., Wilson, M.I., Harlos, K., Claridge, T.D.W., Schofield, C.J., Pugh, C.W., Maxwell, P.H., Ratcliffe, P.J., Stuart, D.I., and Jones, E.Y. 2002. Structural basis for the recognition of hydroxyproline in HIF-1α by pVHL. *Nature* **417:**975–978.

Hsu, C.-A., Saewert, M.D., Polsinelli, L.F., Jr., and Abbott, M.T. 1981. Uracil's uncoupling of the decarboxylation of α-ketoglutarate in the

thymine 7-hydroxylase reaction of *Neurospora crassa*. *J Biol Chem* **256:**6098–6101.

Hubbard, B.K., Thomas, M.G., and Walsh, C.T. 2000. Biosynthesis of L-*p*-hydroxyphenylglycine, a non-proteinogenic amino acid constituent of peptide antibiotics. *Chem Biol* **7:**931–942.

Hulse, J.D., Ellis, S.R., and Henderson, L.M. 1978. Carnitine biosynthesis. β-Hydroxylation of trimethyllysine by an α-ketoglutarate-dependent mitochondrial dioxygenase. *J Biol Chem* **253:**1654–1659.

Hutton, J.J., Jr., Trappel, A.L., and Udenfriend, S. 1966. Requirement for α-ketoglutarate, ferrous ion and ascorbate for collagen proline hydroxylase. *Biochem Biophys Res Commun* **24:**179–184.

Ince, N., de la Monte, S.M., and Wands, J.R. 2000. Overexpression of human aspartyl (asparaginyl) β-hydroxylase is associated with malignant transformation. *Cancer Res* **60:**1261–1266.

Itoh, H., Ueguchi-Tanaka, M., Sentoku, N., Kitano, H., Matsuoka, M., and Kobayashi, M. 2001. Cloning and functional analysis of two gibberellin 3β-hydroxylase genes that are differently expressed during growth of rice. *Proc Natl Acad Sci USA* **98:**8909–8914.

Ivan, M., Kondo, K., Yang, H., Kim, W., Valiando, J., Ohh, M., Salic, A., Asara, J.M., Lane, W.S., and Kaelin, W.G., Jr. 2001. HIFα targeted for VHL-mediated destruction by proline hydroxylation: implications for O_2 sensing. *Science* **292:**464–467.

Jaakkola, P., Mole, D.R., Tian, Y.-M., Wilson, M.I., Gielbert, J., Gaskell, S.J., von Kriegsheim, A., Hebestreit, H.F., Mukherji, M., Schofield, C.J., Maxwell, P.H., Pugh, C.W., and Ratcliffe, P.J. 2001. Targeting of HIF-α to the von Hippel-Lindau ubiquitylation complex by O_2-regulated prolyl hydroxylation. *Science* **292:**468–472.

Janc, J.W., Egan, L.A., and Townsend, C.A. 1995. Purification and characterization of clavaminate synthase from *Streptomyces antibioticus*. A multifunctional enzyme of clavam biosynthesis. *J Biol Chem* **270:**5399–5404.

Jansen, G.A., Mihalik, S.J., Watkins, P.A., Moser, H.W., Jakobs, C., Denis, S., and Wanders, R.J.A. 1996. Phytanoyl-CoA hydroxylase is present in human liver, located in peroxisomes, and deficient in Zellweger syndrome: direct, unequivocal evidence for the new, revised pathway of phytanic acid α-oxidation in humans. *Biochem Biophys Res Commun* **229:**205–210.

Jansen, G.A., Ofman, R., Denis, S., Ferdinandusse, S., Hogenhout, E.M., Jakobs, C., and Wanders, R.J.A. 1999. Phytanoyl-CoA hydroxylase from rat liver: protein purification and cDNA cloning with implications for the subcellular localization of phytanic acid α-oxidation. *J Lipid Res* **40:**2244–2254.

Jansen, G.A., Ofman, R., Ferdinandusse, S., Ijlst, L., Muijsers, A.O., Skjeldal, O.H., Stokke, O., Jakobs, C., Besley, G.T., Wraith, J.E., and Wanders, R.J.A. 1997. Refsum disease is caused by mutations in the phytanoyl-CoA hydroxylase gene. *Nature Genet* **17:**190–193.

Jensen, K.B., McKensie, C.J., Nielsen, L.P., Pedersen, J.Z., and Svendsen, H.M. 1999. Deprotonation of low-spin mononuclear iron(III)-hydroperoxide complexes give transient blue species assigned to high-spin iron(III)-peroxide complexes. *Chem Commun* 1313–1314.

Jensen, M.P., Lange, S.J., Mehn, M.P., Que, E.L., and Que, L., Jr. 2003. Biomimetic aryl hydroxylation derived from alkyl hydroperoxide at a nonheme iron center. Evidence for an $Fe^{IV} = O$ oxidant. *J Am Chem Soc* **125:**2113–2128.

Jia, S., McGinnis, K., VanDusen, W.J., Burke, C.J., Kuo, A., Griffin, P.R., Sardana, M.K., Elliston, K.O., Stern, A.M., and Friedman, P.A. 1994. A fully active catalytic domain of bovine aspartyl (asparginyl) ß-hydroxylase expressed in *Escherichia coli*: characterization and evidence for the identification of an active-site region in vertebrate α-ketoglutarate-dependent dioxygenases. *Proc Natl Acad Sci USA* **91:**7227–7231.

Jia, S., VanDusen, W.J., Diehl, R.E., Kohl, N.E., Dixon, R.A.F., Elliston, K.O., Stern, A.M., and Friedman, P.A. 1992. cDNA cloning and expression of bovine aspartyl (asparginyl) β-hydroxylase. *J Biol Chem* **267:**14322–14327.

Jiang, F., Peisach, J., Ming, L.-J., Que, L., Jr., and Chen, V.J. 1991. Electron spin echo envelope modulation studies of the Cu(I)-substituted derivative of isopenicillin N synthase: a structural and spectroscopic model. *Biochemistry* **30:**11437–11445.

Johnson-Winters, K., Purpero, V.M., Kavana, M., Nelson, T., and Moran, G.R. 2003. (4-Hydroxyphenyl)pyruvate dioxygenase from *Streptomyces avermitilis*: the basis for ordered substrate addition. *Biochemistry* **42:**2072–2080.

Jong, E. and Kemp, A. 1984. Stoichiometry and kinetics of the prolyl 4-hydroxylase partial reaction. *Biochim Biophys Acta* **787:** 105–111.

Kahnert, A. and Kertesz, M.A. 2000. Characterization of a sulfur-regulated oxygenative alkylsulfatase from *Pseudomonas putida* S-313. *J Biol Chem* **275:**31661–31667.

Kaska, D.D., Myllylä, R., Günzler, V., Gibor, A., and Kivirikko, K.I. 1988. Prolyl 4-hydroxylase from *Volvox carteri*. A low-M_r enzyme antigenically related to the α subunit of the invertebrate enzyme. *Biochem J* **256:**257–263.

Kataoka, H. and Sekiguchi, M. 1985. Molecular cloning and characterization of the *alkB* gene of *Escherichia coli*. *Molec Gen Genet* **198:**263–269.

Kataoka, H., Yamamoto, Y., and Sekiguchi, M. 1983. A new gene (*alkB*) of *Escherichia coli* that controls sensitivity to methyl methane sulfonate. *J Bacteriol* **153:**1301–1307.

Kawauchi, H., Tohno, M., Tsuchiya, Y., Hayashida, M., Adachi, Y., Mukai, T., Hayashi, I., Kimura, S., and Kondo, S. 1983. Studies on the structure of a novel peptide antibiotic, K-582. *Int J Pept Prot Res* **21:**546–554.

Kertesz, M.A. 1999. Riding the sulfur cycle-metabolism of sulfonates and sulfate esters in Gram-negative bacteria. *FEMS Microbiol Rev* **24:**135–175.

Khaleeli, N., Busby, R.W., and Townsend, C.A. 2000. Site-directed mutagenesis and biochemical analysis of the endogenous ligands in the ferrous active site of clavaminate synthase. The His-3 variant of the 2-His-1-carboxylase model. *Biochemistry* **39:**8666–8673.

Kieliszewski, M.J. and Lamport, D.T. 1994. Extensin: repetitive motifs, functional sites, post-translational codes, and phylogeny. *Plant J* **5:**157–172.

Kikuchi, Y., Suzuki, Y., and Tamiya, N. 1983. The source of oxygen in the reaction catalyzed by collagen lysyl hydroxylase. *Biochem J* **213:**507–512.

Kita, A., Kita, S.-I., Fujisawa, I., Inaka, K., Ishida, T., Horiike, K., Nozaki, M., and Miki, K. 1999. An archetypical extradiol-cleaving catecholic dioxygenase: the crystal structure of catechol 2,3-dioxygenase (metapyrocatechase) from *Pseudomonas putida* mt-2. *Structure* **7:**25–34.

Kivirikko, K.I. and Pihlajaniemi, T. 1998. Collagen hydroxylases and the protein disulfide isomerase subunit of prolyl 4-hydroxylase. *Adv Enzymol Rel Areas Mol Biol* **72:**325–398.

Koivisto, P., Duncan, T., Lindahl, T., and Sedgwick, B. 2003. Minimal methylated substrate and extended substrate range of *Escherichia*

coli AlkB protein, a 1-methyladenine-DNA dioxygenase. *J Biol Chem* **278:**44348–44354.

Kondo, A., Blanchard, J.S., and Englard, S. 1981. Purification and properties of calf liver γ-butyrobetaine hydroxylase. *Arch Biochem Biophys* **212:**338–346.

Kondo, H., Nakabeppu, Y., Kataoka, H., Kuhara, S., Kawabata, S., and Sekiguchi, M. 1986. Structure and expression of the *alkB* gene of *Escherichia coli* related to the repair of alkylated DNA. *J Biol Chem* **261:**15772–15777.

Korioth, F., Gieffers, C., and Frey, J. 1994. Cloning and characterization of the human gene encoding aspartyl β-hydroxylase. *Gene* **150:**395–399.

Kovacevic, S., Weigel, B.J., Tobin, M.B., Ingolia, T.D., and Miller, J.R. 1989. Cloning, characterization, and expression in *Escherichia coli* of the *Streptomyces clavuligerus* gene encoding deacetoxycephalosporin C synthetase. *J Bacteriol* **171:**754–760.

Kreisberg-Zakarin, R., Borovok, I., Yanko, M., Aharonowitz, Y., and Cohen, G. 1999. Recent advances in the structure and function of isopenicillin N synthase. *Antonie van Leeuwenhoek* **75:** 33–39.

Kreisberg-Zakarin, R., Borovok, I., Yanko, M., Frolow, F., Aharonowitz, Y., and Cohen, G. 2000. Structure-function studies of non-heme iron active site of isopenicillin N synthase: some implications for catalysis. *Biophys Chem* **86:**109–118.

Kurowski, M.A., Bhagwat, A.S., Papaj, G., and Bujnicki, J.M. 2003. Phylogenomic identification of five new human homologues of the DNA repair enzyme AlkB. *BMC Genomics* **4:**48.

Lamberg, A., Pihlajaniemi, T., and Kivirikko, K.I. 1995. Site-directed mutagenesis of the α subunit of human prolyl 4-hydroxylase. Identification of three histidine residues critical for catalytic activity. *J Biol Chem* **270:**9926–9931.

Landman, O., Borovok, I., Aharonowitz, Y., and Cohen, G. 1997. The glutamine ligand in the ferrous iron active site of isopenicillin N synthase of *Streptomyces jumonjinensis* is not essential for catalysis. *FEBS Lett* **405:**172–174.

Lando, D., Peet, D.J., Whelan, D.A., Gorman, J.J., and Whitelaw, M.L. 2002. Asparagine hydroxylation of the HIF transactivation domain: a hypoxic switch. *Science* **295:**858–861.

Lange, T. 1994. Purification and partial amino-acid sequence of gibberellin 20-oxidase from *Cucurbita maxima* L. endosperm. *Planta* **195:**108–115.

Lange, T. 1997. Cloning gibberellin dioxygenase genes from pumpkin endosperm by heterologous expression of enzyme activities in *Escherichia coli*. *Proc Natl Acad Sci USA* **94:**6553–6558.

Lange, T. and Graebe, J. E. 1989. The partial purification and characterization of a gibberellin C-20 hydroxylase from immature *Pisum sativum* L. seeds. *Planta* **179:**211–221.

Lange, T., Hedden, P., and Graebe, J.E. 1994a. Expression cloning of a gibberellin 20-oxidase, a multifunctional enzyme involved in gibberellin synthesis. *Proc Natl Acad Sci USA* **91:**8552–8556.

Lange, T., Kegler, C., Hedden, P., Phillips, A.L., and Graebe, J.E. 1997a. Molecular characterization of gibberellin 20-oxidases. Structure-function studies on recombinant enzymes and chimaeric proteins. *Physiol Plant* **100:**543–549.

Lange, T., Robatzek, S., and Frisse, A. 1997b. Cloning and expression of a gibberellin 2β,3β-hydroxylase cDNA from pumpkin endosperm. *The Plant Cell* **9:**1459–1467.

Lange, T., Schweimer, A., Ward, D.A., Hedden, P., and Graebe, J.E. 1994b. Separation and characterization of three 2-oxoglutarate-dependent dioxygenases from *Cucurbita maxima* L. endosperm involved in gibberellin biosynthesis. *Planta* **195:**98–107.

Lawrence, C.C., Sobey, W.J., Field, R.A., Baldwin, J.E., and Schofield, C.J. 1996. Purification and initial characterization of proline 4-hydroxylase from *Streptomyces griseoviridus* P8648: a 2-oxoacid, ferrous-dependent dioxygenase involved in etamycin biosynthesis. *Biochem J* **313:**185–191.

Lay, V.J., Prescott, A.G., Thomas, P.G., and John, P. 1996. Heterologous expression and site-directed mutagenesis of the 1-aminocyclopropane-1-carboxylate oxidase from kiwi fruit. *Eur J Biochem* **242:**228–234.

Le Marchand, L. 2002. Cancer prevention effects of flavonoids–a review. *Biomed Pharmacother* **56:**296–301.

Lee, C., Kim, S.J., Jeong, D.G., Lee, S.M., and Ryu, S.E. 2003. Structure of human FIH-1 reveals a unique active site pocket and interaction sites for HIF-1 and von Hipple-Lindau. *J Biol Chem* **278:**7558–7563.

Lee, H.J., Lloyde, M.D., Clifton, I.J., Baldwin, J.E., and Schofield, C.J. 2001a. Kinetic and crystallographic studies on deacetoxycephalosporin C synthase (DAOCS). *J Mol Biol* **308:**937–948.

Lee, H.-J., Lloyd, M.D., Clifton, I.J., Harlos, K., Dubus, A., Baldwin, J.E., Frere, J.-M., and Schofield, C.J. 2001b. Alteration of the co-substrate selectivity of deacetoxycephalosporin C synthase. The role of arginine 258. *J Biol Chem* **276:**18290–18295.

Lee, H.J., Schofield, C.J., and Lloyde, M.D. 2002. Active site mutations of recombinant deacetoxycephalosporin C synthase. *Biochem Biophys Res Commun* **292:**66–70.

Lester, D.R., Ross, J.J., Davies, P.J., and Reid, J.B. 1997. Mendel's stem length gene (*Le*) encodes a gibberellin 3β-hydroxylase. *The Plant Cell* **9:**1435–1443.

Lester, D.R., Ross, J.J., Smith, J.J., Elliott, R.C., and Reid, J.B. 1999. Gibberellin 2-oxidation and the *SLN* gene of *Pisum sativum*. *Plant J* **19:**65–73.

Lim, M.H., Rohde, J.-U., Stubna, A., Bukowski, M.R., Costas, M., Ho, R.Y.N., Münck, E., Nam, W., and Que, L., Jr. 2003. An $Fe^{IV} = O$ complex of a tetradentate tripodal nonheme ligand. *Proc Natl Acad Sci USA* **100:**3665–3670.

Lindblad, B., Lindstedt, G., and Lindstedt, S. 1970. The mechanism of enzymic formation of homogentisate from *p*-hydroxyphenylpyruvate. *J Am Chem Soc* **92:**7446–7449.

Lindblad, B., Lindstedt, G., Lindstedt, S., and Rundgren, M. 1977. Purification and some properties of human 4-hydroxyphenylpyruvate dioxygenase. *J Biol Chem* **252:**5073–5084.

Lindblad, B.G.L., Tofft, M., and Lindstedt, S. 1969. The mechanism of α-ketoglutarate oxidation in coupled enzymatic oxygenations. *J Am Chem Soc* **91:**4604–4606.

Lindstedt, G., Lindstedt, S., and Nordin, I. 1977. Purification and properties of γ-butyrobetaine hydroxylase from *Pseudomonas* sp. AK1. *Biochemistry* **16:**2181–2188.

Lindstedt, S. and Rundgren, M. 1982. Blue color, metal content, and substrate binding in 4-hydroxyphenylpyruvate dioxygenase from *Pseudomonas* sp. strain P. J. 874. *J Biol Chem* **257:**11922–11931.

Lipscomb, S.J., Lee, H.-J., Mukherji, M., Baldwin, J.E., Schofield, C.J., and Lloyd, M.D. 2002. The role of arginine residues in substrate binding and catalysis by deacetoxycephalosporin C synthase. *Eur J Biochem* **269:**2735–2739.

Liu, A., Ho, R.Y.N., Que, L., Jr., Ryle, M.J., Phinney, B.S., and Hausinger, R.P. 2001. Alternative reactivity of an α-ketoglutarate-dependent iron(II) oxygenase: enzyme self-hydroxylation. *J Am Chem Soc* **123:**5126–5127.

Lloyd, M.D., Lee, H.-J., Harlos, K., Zhang, Z.-H., Baldwin, J.E., Schofield, C.J., Charnock, J.M., Garner, C.D., Hara, T., Terwisscha Van Scheltinga, A.C., Valegård, K., Viklund, J.A.C., Hajdu, J., Andersson, I., Danielsson, Å., and Bhikhabhai, R. 1999a. Studies on the active site of deacetoxycephalosporin C synthase. *J Mol Biol* **287:**943–960.

Lloyd, M.D., Merrit, K.D., Lee, V., Sewell, T.J., Wha-Son, B., Baldwin, J.E., Schofield, C.J., Elson, S.W., Baggaley, K.H., and Nicholson, N.H. 1999b. Product-substrate engineering by bacteria: studies on clavaminate synthase, a trifunctional dioxygenase. *Tetrahedron* **55:**10201–10220.

Lloyd, M.D., Lipscomb, S.J., Hewitson, K.S., Hensgenes, C.M., Baldwin, J.E., and Schofield, C.J. 2004. Controlling the substrate selectivity of deacetoxy/deacetylcephalosporin C synthase. *J Biol Chem*, In press.

Long, A.J., Clifton, I.J., Roach, P.L., Baldwin, J.E., Schofield, C.J., and Rutledge, P.J. 2003. Structural studies on the reaction of isopenicillin N synthase with the substrate analogue δ-(L-α-aminoadipoyl)-L-cysteinyl-D-α-aminobutyrate. *Biochem J* **372:**687–693.

Lukacin, R. and Britsch, L. 1997. Identification of strictly conserved histidine and arginine residues as part of the active site in *Petunia hybrida* flavanone 3ß-hydroxylase. *Eur J Biochem* **249:**748–757.

Lukacin, R., Groning, I., Pieper, U., and Matern, U. 2000a. Site-directed mutagenesis of the active site serine290 in flavanone 3β-hydroxylase from *Petunia hybrida*. *Eur J Biochem* **267:**853–860.

Lukacin, R., Gröning, I., Schiltz, E., Britsch, L., and Matern, U. 2000b. Purification of recombinant flavanone 3β-hydroxylase from Petunia hybrida and assignment of the primary site of proteolytic degradation. *Arch Biochem Biophys* **375:**364–370.

Lukacin, R., Wellman, F., Britsch, L., Martens, S., and Matern, U. 2003. Flavonol synthase from *Citrus unshiu* is a bifunctional dioxygenase. *Phytochem* **62:**287–292.

MacBeth, C.E., Golombek, A.P., Young, V.G., Jr., Yang, C., Kuczera, K., Hendrich, M.P., and Borovik, A.S. 2000. O_2 activation by non-heme iron complexes: a monomeric Fe(III)-oxo complex derived from O_2. *Science* **289:**938–941.

Mahon, P.C., Hirota, K., and Semenza, G.L. 2001. FIH-1: a novel protein that interacts with HIF-1α and VHL to mediate repression of HIF-1 transcriptional activity. *Genes Dev* **15:**2675–2686.

Mao, Y., Varoglu, M., and Sherman, D.H. 1999. Molecular characterization and analysis of the biosynthetic gene cluster for the antitumor antibiotic mitomycin C from *Streptomyces lavendulae* 2564. *Chem Biol* **6:**251–263.

Marsh, E.N., Chang, M.D.-T., and Townsend, C.A. 1992. Two isozymes of clavaminate synthase central to clavulanic acid formation: cloning and sequencing of both genes from *Streptomyces clavuligerus*. *Biochemistry* **31:**12648–12657.

Martens, S., Forkmann, G., Britsch, L., Wellmann, F., Matern, U., and Lukacin, R. 2003. Divergent evolution of flavonoid 2-oxoglutarate-dependent dioxygenases in parsley. *FEBS Lett* **544:**93–98.

Martens, S., Forkmann, G., Matern, U., and Lukacin, R. 2001. Cloning of parsley flavone synthase I. *Phytochem* **58:**43–46.

Martin, D.N., Proebsting, W.M., and Hedden, P. 1997. Mendel's dwarfing gene: cDNAs from the *Le* alleles and function of the expressed proteins. *Proc Natl Acad Sci USA* **94:**8907–8911.

Martinkus, K.J., Tann, C.-H., and Gould, S.J. 1983. The biosynthesis of the streptolidine moiety in streptothricin F. *Tetrahedron* **39:**3493–3505.

Masson, N., William, C., Maxwell, P.H., Pugh, C.W., and Ratcliffe, P.J. 2001. Independent function of two destructive domains in hypoxia-inducible factor-α chains activated by prolyl hydroxylation. *EMBO J* **20:**5197–5206.

Matsuda, J., Okabe, S., Hashimoto, T., and Yamada, Y. 1991. Molecular cloning of hyoscyamine 6β-hydroxylase, a 2-oxoglutarate-dependent dioxygenase, from cultured roots of *Hyoscyamus niger*. *J Biol Chem* **266:**9460–9464.

McGinnis, K., Ku, G.M., VanDusen, W.J., Fu, J., Garsky, V., Stern, A.M., and Friedman, P.A. 1996. Site-directed mutagenesis of residues in a conserved region of bovine aspartyl (asparaginyl) ß-hydroxylase: evidence that histidine 675 has a role in binding Fe^{2+}. *Biochemistry* **35:**3957–3962.

McGowan, S.J., Sebaihia, M., Porter, L.E., Stewart, G.S., Williams, P., Bycroft, B.W., and Salmond, G.P. 1996. Analysis of bacterial carbapenam antibiotic production genes reveals a novel β-lactam biosynthesis pathway. *Molec Microbiol* **22:**415–426.

McNeill, L.A., Hewitson, K.S., Claridge, T.D., Seibel, J.F., Horsfall, L.E., and Schofield, C.J. 2002a. Hypoxia-inducible factor asparginyl hydroxylase (FIH-1) catalyses hydroxylation at the β-carbon of asparagine-803. *Biochem J* **367:**571–575.

McNeill, L.A., Hewitson, K.S., Gleadle, J.M., Horsfall, L.E., Oldham, N.J., Maxwell, P.H., Pugh, C.W., Ratcliffe, P.J., and Schofield, C.J. 2002b. The use of dioxygen by HIF prolyl hydroxylase (PHD1). *Bioorg Med Chem Lett* **12:**1547–1550.

Mehn, M.P., Fujisawa, K., Hegg, E.L., and Que, L., Jr. 2003. Oxygen activation by nonheme iron(II) complexes: α-keto carboxylate versus carboxylate. *J Am Chem Soc* **124:**7828–7842.

Metcalf, W.W. and Wolfe, R.S. 1998. Molecular genetic analysis of phosphite and hypophosphite oxidation by *Pseudomonas stutzeri* WM88. *J Bacteriol* **180:**5547–5558.

Mihalik, S.J., Morrell, J.C., Kim, D., Sacksteder, K.A., Watkins, P.A., and Gould, S.J. 1997. Identification of *PAHX*, a Refsum disease gene. *Nature Genet* **17:**185–189.

Mihalik, S.J., Rainville, A.M., and Watkins, P.A. 1995. Phytanic acid α−oxidation in rat liver peroxisomes. Production of α-hydroxyphytanoyl-CoA and formate is enhanced by dioxygenase cofactors. *Eur J Biochem* **232:**545–551.

Min, J.-H., Yang, H., Ivan, M., Gertler, F., Kaelin, W.G., Jr., and Pavletich, N.P. 2002. Structure of an HIF-1α-pVHL complex: hydroxyproline recognition in signaling. *Science* **296:**1886–1889.

Min, W.-C., Begley, T.J., Myllyharju, J., and Kivirikko, K.I. 2000. Mechanistic studies on prolyl-4-hydroxylase: demonstration that the ferryl intermediate does not exchange with water. *Bioorgan Chem* **28:**261–265.

Minchenko, A., Leshchinsky, I., Opentanova, I., Sang, N., Srinivas, V., Armstead, V., and Caro, J. 2002. Hypoxia-inducible factor-1-mediated expression of the 6-phosphofructo-2-kinase/fructose-2,6-bisphosphate (*PFKFB3*) gene. Its possible role in the Warburg effect. *J Biol Chem* **277:**6183–6187.

Ming, L.-J., Que, L., Jr., Kriauciunas, A., Frolik, C.A., and Chen, V.J. 1990. Coordination chemistry of the metal binding site of isopenicillin N synthase. *Inorg Chem* **29:**1111–1112.

Ming, L.-J., Que, L., Jr., Kriauciunas, A., Frolik, C.A., and Chen, V.J. 1991. NMR studies of the active site of isopenicillin N

synthase, a non-heme iron(II) enzyme. *Biochemistry* **30:**11653–11659.

Mishina, Y. and He, C. 2003. Probing the structure and function of the *Escherichia coli* DNA alkylation repair AlkB protein through chemical cross-linking. *J Am Chem Soc* **125:**8730–8731.

Mishina, Y., Lee, C.-H.J., and He, C. 2004. Interaction of human and bacterial AlkB proteins with DNA as probed through chemical cross-linking studies. *Nucleic Acids Res* **32:**1548–1554.

Mori, H., Shibasaki, T., Uozaki, Y., Ochiai, K., and Ozaki, A. 1996. Detection of novel proline 3-hydroxylase activities in *Streptomyces* and *Bacillus* spp. by regio- and stereospecific hydroxylation of L-proline. *Appl Environ Microbiol* **62:**1903–1907.

Mori, H., Shibasaki, T., Yano, K., and Ozaki, A. 1997. Purification and cloning of a proline 3-hydroxylase, a novel enzyme which hydroxylates free L-proline to cis-3-hydroxy-L-proline. *J Bacteriol* **179:**5677–5683.

Mukherji, M., Kershaw, N.J., Schofield, C.J., Wierzbicki, A.S., and Lloyd, M.D. 2002. Utilization of sterol carrier protein-2 by phytanoyl-CoA 2-hydroxylase in the peroxisomal α oxidation of phytanic acid. *Chem Biol* **9:**597–605.

Mukherji, M., Schofield, C.J., Wierzbicki, A.S., Jansen, G.A., Wanders, R.J.A., and Lloyd, M.D. 2003. The chemical biology of branched-chain lipid metabolism. *Prog Lipid Res* **42:**359–376.

Mukherji, M., Chien, W., Kershaw, N.J., Clifton, I.J., Schofield, C.J., Wierzbicki, A.S., and Lloyd, M.D. 2001a. Structure-function analysis of phytanoyl-CoA 2-hydroxylase mutations causing Refsum's disease. *Human Molec Genet* **10:**1971–1982.

Mukherji, M., Kershaw, N.J., MacKinnon, C.H., Clifton, I.J., Wierzbicki, A.S., Schofield, C.J., and Lloyd, M.D. 2001b. "Chemical co-substrate rescue" of phytanoyl-CoA hydroxylase mutants causing Refsum's disease. *Chem Commun* 972–973.

Müller, I., Kahnert, A., Pape, T., Sheldrick, G.M., Meyer-Klaucke, W., Dierks, T., Kertesz, M., and Usòn, I. 2004. Crystal structure of the alkylsulfatase AtsK: insights into the catalytic mechanism of the Fe(II), α-ketoglutarate dependent dioxygenase superfamily. *Biochemistry* **43:**3075–3088.

Myllyharju, J. and Kivirikko, K.I. 1997. Characterization of the iron- and 2-oxoglutarate-binding sites of human prolyl 4-hydroxylase. *EMBO J* **16:**1173–1180.

Myllylä, R., Kuutti-Saolainen, E.-R., and Kivirikko, K.I. 1978. The role of ascorbate in the prolyl hydroxylase reaction. *Biochem Biophys Res Commun* **83:**441–448.

Myllylä, R., Majamaa, K., Günzler, V., Hanauske-Abel, H.N., and Kivirikko, K.I. 1984. Ascorbate is consumed stoichiometrically in the uncoupled reactions catalyzed by prolyl 4-hydroxylase and lysyl hydroxylase. *J Biol Chem* **259:**5403–5405.

Nagahama, K., Ogawa, T., Fujii, T., Tazaki, M., Goto, M., and Fukuda, H. 1991a. *L*-Arginine is essential for the formation *in vitro* of ethylene by an extract of *Pseudomonas syringae*. *J Gen Microbiol* **137:**1641–1646.

Nagahama, K., Ogawa, T., Fujii, T., Tazaki, M., Tanase, S., Morino, Y., and Fukuda, H. 1991b. Purification and properties of an ethylene-forming enzyme from *Pseudomonas syringae* pv. *phaseolica* PK2. *J Gen Microbiol* **137:**2281–2286.

Nagahama, K., Yoshini, K., Matsuoka, M., Tanase, S., Ogawa, T., and Fukuda, H. 1998. Site-directed mutagenesis of histidine residues in the ethylene-forming enzyme from *Pseudomonas syringae*. *J Ferm Bioeng* **85:**255–258.

Nakajima, J.-I., Yoshikaru, Y., Yamazaki, M., and Saito, K. 2001. Reaction mechanism from leucoanthocyanidin to anthocyanidin 3-glucoside, a key reaction for coloring in anthocyanin biosynthesis. *J Biol Chem* **276:**25797–25803.

Nickel, K., Suter, M.J.-F., and Kohler, H.-P.E. 1997. Involvement of two α-ketoglutarate-dependent dioxygenases in enantioselective degradation of (*R*)- and (*S*)-mecoprop by *Sphingomonas herbicidovorans* MH. *J Bacteriol* **179:**6674–6679.

O'Brien, J.R., Schuller, D.J., Yang, V.S., Dillard, B.D., and Lanzilotta, W.N. 2003. Substrate-induced conformational changes in *Escherichia coli* taurine/α-ketoglutarate dioxygenase and insight into the oligomeric structure. *Biochemistry* **42:**5547–5554.

Oehme, F., Ellinghaus, P., Kolkhof, P., Smith, T.J., Ramakrishnan, S., Hütter, J., Schramm, M., and Flamme, I. 2002. Overexpression of PH-4, a novel putative proline 4-hydroxylase, modulates activity of hypoxia-inducible transcription factors. *Biochem Biophys Res Commun* **296:**343–349.

Ogle, J.M., Clifton, I.J., Rutledge, P.J., Elkins, J.M., Burzlaff, N.I., Adlington, R.M., Roach, P.L., and Baldwin, J.E. 2001. Alternative oxidation by isopenicillin *N* synthase observed by X-ray diffraction. *Chem Biol* **8:**1231-1237.

Omura, S., Tomoda, H., Yamamoto, S., Tsukui, M., and Tanaka, H. 1984. Studies on two dioxygenases involved in the synthesis of tylosin in *Streptomyces fradiae*. *Biochim Biophys Acta* **802:**141–147.

Park, M.H., Wolff, E.C., and Folk, J.E. 1993. Hypusine: its post-translational formation in eukaryotic initiation factor 5A and its potential role in cellular regulation. *Biofactors* **4:**95–104.

Park, J.H., Wolff, E.C., Folk, J.E., and Park, M.H. 2003. Reversal of the deoxyhypusine synthesis reaction. Generation of spermidine or homospermidine from deoxyhypusine by deoxyhypusine synthase. *J Biol Chem* **278:**32683–32691.

Passoja, K., Myllyharju, J., Pirskanen, A., and Kivirikko, K.I. 1998a. Identification of arginine-700 as the residue that binds the C-5 carboxyl group of 2-oxoglutarate in human lysyl hydroxylase 1. *FEBS Lett* **434:**145–148.

Passoja, K., Rautavuoma, K., Ala-Kokko, L., Kosonen, T., and Kivirikko, K.I. 1998b. Cloning and characterization of a third human lysyl hydroxylase isoform. *Proc Natl Acad Sci USA* **95:**10482–10486.

Pavel, E.G., Zhou, J., Busby, R.W., Gunsior, M., Townsend, C.A., and Solomon, E.I. 1998. Circular dichroism and magnetic circular dichroism spectroscopic studies of the non-heme ferrous active site in clavaminate synthase and its interaction with α-ketoglutarate cosubstrate. *J Am Chem Soc* **120:**743–753.

Pekkala, M., Hieta, R., Kursula, P., Kivirikko, K.I. Wierenga, R.K., and Myllyharju, J. 2003. Crystallization of the proline-rich-peptide binding domain of human type I collagen prolyl 4-hydroxylase. *Acta Cryst* **D59:**940–942.

Pelletier, M.K. and Shirley, B.W. 1996. Analysis of flavanone 3-hydroxylase in *Arabidopsis* seedlings. *Plant Physiol* **111:**339–345.

Petersen, L., Olewinski, R., Salmon, P., and Conners, N. 2003. Novel proline hydroxylase activities in the pneumocandin-producing fungus *Glarea lozoyensis* responsible for the formation of *trans* 3- and *trans* 4-hydroxyproline. *Appl Microbiol Biotechnol* **62:**263–267.

Pirrung, M.C., Cao, J., and Chen, J.1998. Ethylene biosynthesis: processing of a substrate analog supports a radical mechanism for the ethylene-forming enzyme. *Chem Biol* **5:**49–57.

Pirrung, M.C., Kaiser, L.M., and Chen, J. 1993. Purification and properties of the apple fruit ethylene-forming enzyme. *Biochemistry* **32:**7445–7450.

Pirskanen, A., Kaimio, A.-M., Myllylä, R., and Kivirikko, K.I. 1996. Site-directed mutagenesis of human lysyl hydroxylase expressed in insect cells. Identification of histidine residues and an aspartic acid residue critical for catalytic activity. *J Biol Chem* **271:**9398–9402.

Poneleit, L.S. and Dilley, D.R. 1993. Carbon dioxide activation of 1-aminocyclopropane-1-carboxylate (ACC) oxidase in ethylene biosynthesis. *Postharvest Biol Technol* **3:**191–199.

Prescott, A.G. 1993. A dilemma of dioxygenases (or where biochemistry and molecular biology fail to meet). *J Exper Bot* **44:**849–861.

Prescott, A.G. and Lloyd, M.D. 2000. The iron(II) and 2-oxoacid-dependent dioxygenases and their role in metabolism. *Nat Prod Rep* **17:**367–383.

Prescott, A.G., Stamford, N.P.J., Wheeler, G., and Firmin, J.L. 2002. In vitro properties of a recombinant flavonol synthase from *Arabidopsis thaliana*. *Phytochem* **60:**589–593.

Price, J.C., Barr, E.W., Glass, T.E., Krebs, C., and Bollinger, J.M., Jr. 2003a. Evidence for hydrogen abstraction from C1 of taurine by the high-spin Fe(IV) intermediate detected during oxygen activation by taurine:α-ketoglutarate dioxygenase (TauD). *J Am Chem Soc* **125:**13008–13009.

Price, J.C., Barr, E.W., Tirupati, B., Bollinger, J.M., Jr., and Krebs, C. 2003b. The first direct characterization of a high-valent iron intermediate in the reaction of an α-ketoglutarate-dependent dioxygenase: a high-spin Fe(IV) complex in taurine/α-ketoglutarate dioxygenase (TauD) from *Escherichia coli*. *Biochemistry* **42:**7497–7508.

Proshlyakov, D.A., Henshaw, T.F., Monterosso, G.R., Ryle, M.J., and Hausinger, R.P. 2004. Direct detection of oxygen intermediates in the non-heme Fe enzyme taurine/α-ketoglutarate dioxygenase. *J Am Chem Soc* **126:**1022–1023.

Puistola, U., Turpeenniemi-Hujanen, T.M., Myllylä, R., and Kivirikko, K. 1980. Studies on the lysyl hydroxylase reaction. 1. Initial velocity kinetics and related aspects. *Biochim Biophys Acta* **611:**40–50.

Randall, C.R., Zang, Y., True, A.E., Que, L., Jr., Charnock, J.M., Garner, C.D., Fujishima, Y., Schofield, C.J., and Baldwin, J.E. 1993. X-ray absorption studies of the ferrous active site of isopenicillin N synthase and related model complexes. *Biochemistry* **32:**6664–6673.

Rao, N.V. and Adams, E. 1978. Partial reaction of prolyl hydroxylase. $(Gly\text{-}Gly\text{-}Pro)_n$ stimulates α-ketoglutarate decarboxylation without prolyl hydroxylase. *J Biol Chem* **253:**6327–6330.

Risteli, J., Tryggvason, K., and Kivirikko, K.I. 1977. Prolyl 3-hydroxylase: partial purification of the enzyme from rat kidney cortex. *Eur J Biochem* **73:**485–492.

Roach, P.L., Clifton, I.J., Fülöp, V., Harlos, K., Barton, G.J., Hajdu, J., Andersson, K., Schofield, C.J., and Baldwin, J.E. 1995. Crystal structure of isopenicillin *N* synthase is the first from a new structural family of enzymes. *Nature (London)* **375:**700–704.

Roach, P.L., Clifton, I.J., Hensgens, C.M.H., Shibata, N., Schofield, C.J., Hajdu, J., and Baldwin, J.E. 1997. Structure of isopenicillin *N* synthase complexed with substrate and the mechanism of penicillin formation. *Nature (London)* **387:**827–830.

Rocklin, A.M., Tierney, D.L., Kofman, V., Brunhuber, N.M.W., Hoffman, B.M., Christoffersen, R.E., Reich, N.O., Lipscomb, J.D., and Que, L., Jr. 1999. Role of the nonheme Fe(II) center in the biosynthesis of the plant hormone ethylene. *Proc Natl Acad Sci USA* **96:**7905–7090.

Roelfes, G., Lubben, M., Chen, K., Ho, R.Y.N., Meetsma, A., Genseberger, S., Hermant, R.M., Hage, R., Mandal, S.K., Young, V.G., Jr., Zang, Y., Kooijman, H., Spek, A.L., Que, L., Jr., and Feringa, B.L. 1999. Iron chemistry of a pentadentate ligand that generates a metastable Fe^{III}-OOH intermediate. *Inorg Chem* **38:**1929–1936.

Roelfes, G., Lubben, M., Hage, R., Que, L., Jr., and Feringa, B.L. 2000. Catalytic oxidation with a non-heme iron complex that generates a low-spin Fe^{III}OOH intermediate. *Chem Eur J* **6:**2152–2159.

Rohde, J.-U., In, J.-H., Lim, M.H., Brennessel, W.W., Bukowski, M.R., Stubna, A., Münck, E., and Que, L., Jr. 2003. Crystallographic and spectroscopic characterization of a nonheme Fe(IV)=O complex. *Science* **299:**1037–1039.

Rüetschi, U., Nordin, I., Odelhög, B., Jörnvall, H., and Lindstedt, S. 1993. γ-Butyrobetaine hydroxylase. Structural characterization of the *Pseudomonas* enzyme. *Eur J Biochem* **213:**1075–1080.

Ryle, M.J. and Hausinger, R.P. 2002. Non-heme iron oxygenases. *Curr Opinion Chem Biol* **6:**193–201.

Ryle, M.J., Koehntop, K.D., Liu, A., Que, L., Jr., and Hausinger, R.P. 2003a. Interconversion of two oxidized forms of TauD, a non-heme iron hydroxylase: evidence for bicarbonate binding. *Proc Natl Acad Sci USA* **100:**3790–3795.

Ryle, M.J., Liu, A., Muthukumaran, R.B., Ho, R.Y.N., Koehntop, K.D., McCracken, J., Que, L., Jr., and Hausinger, R.P. 2003b. O_2- and α-ketoglutarate-dependent tyrosyl radical formation in TauD, an α-keto acid-dependent non-heme iron dioxygenase. *Biochemistry* **42:**1854–1862.

Ryle, M.J., Padmakumar, R., and Hausinger, R.P. 1999. Stopped-flow kinetic analysis of *Escherichia coli* taurine/α-ketoglutarate dioxygenase: interactions with α-ketoglutarate, taurine, and oxygen. *Biochemistry* **38:**15278–15286.

Saari, R.E. and Hausinger, R.P. 1998. Ascorbic acid-dependent turnover and reactivation of 2,4-dichlorophenoxyacetic acid/α-ketoglutarate dioxygenase using thiophenoxyacetic acid. *Biochemistry* **37:**3035–3042.

Saari, R.E., Hogan, D.A., and Hausinger, R.P. 1999. Stereospecific degradation of the phenoxypropionate herbicide dichlorprop. *J Molec Catalysis B* **6:**421–428.

Sabourin, P.J. and Bieber, L.L. 1982. The mechanism of α-ketoisocaproate oxygenase. Formation of β-hydroxyisovalerate from α-ketoisocaproate. *J Biol Chem* **257:**7468–7471.

Saito, K., Kobayashi, M., Gong, Z., Tanaka, Y., and Yamazaki, M. 1999. Direct evidence for anthocyanidin synthase as a 2-oxoglutarate-dependent oxygenase: molecular cloning and functional expression of cDNA from a red forma of *Perilla fructescens*. *Plant J* **17:**181–189.

Sami, M., Brown, T.J.N., Roach, P.L., Schofield, C.J., and Baldwin, J.E. 1997. Glutamine-330 is not essential for activity in isopenicillin N synthase from *Aspergillus nidulans*. *FEBS Lett* **405:**191–194.

Samson, S.M., Belagaje, R., Blankenship, D.T., Chapman, J.L., Perry, D., Skatrud, P.L., VanFrank, R., Abraham, E.P., Baldwin, J.E., Queener, S.W., and Ingolia, T.D. 1985. Isolation, sequence determination and expression in *Escherichia coli* of the isopenicillin N synthetase gene from *Cephalosporium acremonium*. *Nature (London)* **318:**191–194.

Sauvaire, Y., Petit, P., Broca, C., Manteghetti, M., Baissac, Y., Fernandez-Alverez, J., Gross, R., Roye, M., Leconte, A., Gomis, R., and Ribes, G. 1998. 4-Hydroxyisoleucine: a novel amino acid potentiator of insulin secretion. *Diabetes* **47:**206–210.

Schofield, C.J., Baldwin, J.E., Byford, M.F., Clifton, I.J., Hensgens, C., and Roach, P.L. 1997. Proteins of the penicillin biosynthesis pathway. *Curr Opinion Struct Biol* **7:**857–864.

Schofield, C.J. and Zhang, Z. 1999. Structural and mechanistic studies on 2-oxoglutarate-dependent oxygenases and related enzymes. *Curr Opinion Struct Biol* **9:**722–731.

Schomburg, F.M., Bizzell, C.M., Lee, D.J., Zeevaart, J.A.D., and Amasino, R.M. 2003. Overexpression of a novel class of gibberellin 2-oxidases decreases gibberellin levels and creates dwarf plants. *The Plant Cell* **15:**151–163.

Scott, R.A., Wang, S., Eidsness, M.K., Kriauciunas, A., Frolik, C.A., and Chen, V.J. 1992. X-ray absorption spectroscopic studies of the high-spin iron(II) active site of isopenicillin N synthase: evidence for Fe-S interaction in the enzyme-substrate complex. *Biochemistry* **31:**4596–4601.

Sedgwick, B. and Lindahl, T. 2002. Recent progress on the Ada response for inducible repair of DNA alkylation damage. *Oncogene* **21:**8886–8894.

Senda, T., Sugiyama, K., Narita, H., Yamamoto, T., Kimbara, K., Fukuda, M., Sato, M., Yano, K., and Mitsui, Y. 1996. Three-dimensional structures of free form and two substrate complexes of an extradiol ring-cleavage type dioxygenase, the BphC enzyme from *Pseudomonas* sp. strain KKS102. *J Mol Biol* **255:**735–752.

Seo, J.-A., Proctor, R.H., and Plattner, R.D. 2001. Characterization of four clustered and coregulated genes associated with fumonisin biosynthesis in *Fusarium verticillioides*. *Fungal Genet Biol* **34:**155–165.

Serre, L., Sailland, A., Sy, D., Boudec, P., Rolland, A., Pebay-Peyroula, E., and Cohen-Addad, C. 1999. Crystal structure of *Pseudomonas fluorescens* 4-hydroxyphenylpyruvate dioxygenase: an enzyme involved in the tyrosine degradation pathway. *Structure* **7:**977–988.

Shaffer, P.M., Cairns, J.R., Dorman, D.C., and Lott, A.M. 1984. Separation and characterization of pyrimidine deoxyribonucleoside 2′-hydroxylase and thymine 7-hydroxylase from *Aspergillus nidulans*. *Int J Biochem* **16:**429–434.

Shaffer, P.M., McCroskey, R.P., Palmatier, R.D., Midgett, R.J., and Abbott, M.T. 1968. The cell-free conversion of a deoxyribonucleoside to a ribonucleoside without detachment of the deoxyribose. *Biochem Biophys Res Commun* **33:**806–811.

Shaw, J.-F., Chou, Y.-S., Chang, R.-C., and Yang, S.F. 1996. Characterization of the ferrous ion binding sites of apple 1-aminocyclopropane-1-carboxylate oxidase by site-directed mutagenesis. *Biochem Biophys Res Commun* **225:**697–700.

Shibasaki, T., Mori, H., Chiba, S., and Ozaki, A. 1999. Microbial proline 4-hydroxylase screening and gene cloning. *Appl Environ Microbiol* **65:**4028–4031.

Simaan, A.J., Banse, F., Mialane, P., Boussac, A., Un, S., Kargar-Grisel, T., Bouchoux, G., and Girerd, J.J. 1999. Characterization of a non-heme mononuclear peroxoiron(III) intermediate by UV vis and EPR spectroscopy and mass spectrometry. *Eur J Inorg Chem* **6:**993–999.

Smith, J.J. and John, P. 1993. Activation of 1-aminocyclopropane-1carboxylate oxidase by bicarbonate/carbon dioxide. *Phytochem* **32:**1381–1386.

Solomon, E.I., Brunold, T.C., Davis, M.I., Kemsley, J.N., Lee, S.-K., Lehnert, N., Neese, F., Skulan, A.J., Yang, Y.-S., and Zhou, J. 2000. Geometric and electronic structure/function correlations in non-heme iron enzymes. *Chem Rev* **100:**235–349.

Sono, M., Roach, M.P., Coulter, E.D., and Dawson, J.H. 1996. Heme-containing oxygenases. *Chem Rev* **96:**2841–2887.

Springob, K., Nakajima, J.I., Yamazaki, M., and Saito, K. 2003. Recent advances in the biosynthesis and accumulation of anthocyanins. *Nat Prod Rep* **20:**288–303.

Stenflo, J., Holme, E., Lindstedt, S., Chandramouli, N., Huang, L.H.T., Tam, J.P., and Merrifield, R.B. 1989. Hydroxylation of aspartic acid in domains homologous to the epidermal growth factor precursor is catalyzed by a 2-oxoglutarate-dependent dioxygenase. *Proc Natl Acad Sci USA* **86:**444–447.

Streber, W.R., Timmis, K.N., and Zenk, M.H. 1987. Analysis, cloning, and high level expression of 2,4-dichlorophenoxyacetate monooxygenase gene *tfdA* of *Alcaligenes eutrophus* JPM134. *J Bacteriol* **169:**2950–2955.

Stubbe, J. 1985. Identification of two α-ketoglutarate-dependent dioxygenases in extracts of *Rhodotorula glutinis* catalyzing deoxyuridine hydroxylation. *J Biol Chem* **260:**9972–9975.

Swiegers, J.H., Vaz, F.M., Pretorius, I.S., Wanders, R.J.A., and Bauer, F.F. 2002. Carnitine biosynthesis in *Neurospora crassa*: identification of a cDNA coding for ε-*N*-trimethyllysine hydroxylase and its functional expression in *Saccharomyces cerevisiae*. *FEMS Microbiol Lett* **210:**19–23.

Tan, D.S.H. and Sim, T.-S. 1996. Functional analysis of conserved histidine residues in *Cephalosporium acremonium* isopenicillin N synthase by site-directed mutagenesis. *J Biol Chem* **271:**889–894.

Tett, V.A., Willetts, A.J., and Lappin-Scott, H.M. 1997. Biodegradation of the chlorophenoxy herbicide (*R*)-(+)-mecoprop by *Alcaligenes denitrificans*. *Biodegradation* **8:**43–52.

Thomas, S.G., Phillips, A.L., and Hedden, P. 1999. Molecular cloning and functional expression of gibberellin 2-oxidases, multifunctional enzymes involved in gibberellin deactivation. *Proc Natl Acad Sci USA* **96:**4698–4703.

Thornburg, L.D., Lai, M.-T., Wishnok, J.S., and Stubbe, J. 1993. A non-heme iron protein with heme tendencies: an investigation of the substrate specificity of thymine hydroxylase. *Biochemistry* **32:** 14023–14033.

Thornburg, L.D. and Stubbe, J. 1989. Mechanism-based inhibition of thymine hydroxylase. *J Am Chem Soc* **111:**7632–7633.

Thornburg, L.D. and Stubbe, J. 1993. Mechanism-based inactivation of thymine hydroxylase, an α-ketoglutarate-dependent dioxygenase, by 5-ethynyluracil. *Biochemistry* **32:**14034–14042.

Thrower, J.S., Blalock, R. III, and Klinman, J.P. 2001. Steady-state kinetics of substrate binding and iron release in tomato ACC oxidase. *Biochemistry* **40:**9717–9724.

Tiedje, J.M. and Alexander, M. 1969. Enzymatic cleavage of the ether bond of 2,4-dichlorophenoxyacetate. *J Agric Food Chem* **17:**1080–1084.

Tiow-Suan, S. and Tan, D.S.H. 1994. Histidine-272 of isopenicillin N synthase of *Cephalosporium acremonium*, which is possibly involved in iron binding, is essential for its catalytic activity. *FEMS Microbiol Lett* **120:**241–248.

Trewick, S.C., Henshaw, T.F., Hausinger, R.P., Lindahl, T., and Sedgwick, B. 2002. Oxidative demethylation by *Escherichia coli* AlkB directly reverts DNA base damage. *Nature* **419:**174–178.

Tryggvason, K., Majamaa, K., Risteli, J., and Kivirikko, K.I. 1979. Partial purification and characterization of chick-embryo prolyl 3-hydroxylase. *Biochem J* **183:**303–307.

Tryggvason, K., Risteli, J., and Kivirikko, K.I. 1976. Separation of prolyl 3-hydroxylase and 4-hydroxylase activities and the 4-hydroxyproline requirement for synthesis of 3-hydroxyproline. *Biochem Biophys Res Commun* **76:**275–281.

Tuderman, L., Myllylä, R., and Kivirikko, K.I. 1977. Mechanism of prolyl hydroxylase reaction. 1. Role of co-substrates. *Eur J Biochem* **80:**314–348.

Turnbull, J.J., Nagle, M.J., Seibel, J.F., Welford, R.W.D., Grant, G.H., and Schofield, C.J. 2003. The C-4 stereochemistry of leucocyanidine substrates for anthocyanidin synthase affects product selectivity. *Bioorg Med Chem Lett* **13:**3853–3857.

Turnbull, J.J., Nakajima, J.I., Welford, R.W., Yamazaki, M., Saito, K., and Schofield, C.J. 2004. Mechanistic studies on three 2-oxoglutarate dependent oxygenases of flavonoid biosynthesis: anthocyanidin synthase, flavonol synthase, and flavaonone 3b hydroxylase. *J Biol Chem* **279:**1206–1216.

Udenfriend, S. and Cardinale, G. 1982. α-Ketoglutarate-coupled dioxygenases. In *Oxygenases and Oxygen Metabolism*, pp. 99–110, M. Nozaki, S. Yamamoto, Y. Ishimura, M.J. Coon, L. Ernster, and R.W. Estabrook, Eds., Academic Press, New York.

Valegård, K., Terwisscha van Scheltinga, A.C., Dubus, A., Ranghino, G., Öster, L.M., Hajdu, J., and Andersson, I. 2004. The structural basis of cephalosporin formation in a mononuclear ferrous enzyme. *Nat Struct Biol* in press.

Valegård, K., Terwisscha van Scheltinga, A.C., Lloyd, M.D., Hara, T., Ramaswamy, S., Perrakis, A., Thompson, A., Lee, W.-J., Baldwin, J.E., Schofield, C.J., Hajdu, J., and Andersson, I. 1998. Structure of a cephalosporin synthase. *Nature (London)* **394:**805–809.

Valtavaara, M., Papponen, H., Pirttila, A.M., Hiltunen, K., Helander, H., and Myllylä, R. 1997. Cloning and characterization of a novel human lysyl hydroxylase isoform highly expressed in pancreas and muscle. *J Biol Chem* **272:**6831–6834.

Valtavaara, M., Szpirer, C., Szpirer, J., and Myllylä, R. 1998. Primary structure, tissue distribution, and chromosomal localization of a novel isoform of lysyl hydroxylase (lysyl hydroxylase 3). *J Biol Chem* **273:**12881–12886.

Vaz, F.M., Ofman, R., Westinga, K., Back, J.W., and Wanders, R.J.A. 2001. Molecular and biochemical characterization of rat *N*-trimethyllysine hydroxylase, the first enzyme of carnitine biosynthesis. *J Biol Chem* **276:**33512–33517.

Vaz, F.M., van Gool, S., Ofman, R., Ijlst, L., and Wanders, R.J.A. 1998. Carnitine biosynthesis: identification of the cDNA encoding human γ-butyrobetaine hydroxylase. *Biochem Biophys Res Commun* **250:**506–510.

Vaz, F.M. and Wanders, R.J.A. 2002. Carnitine biosynthesis in mammals. *Biochem J* **361:**417–429.

Vazquez-Flota, F., De Carolis, E., Alarco, A.-M., and De Luca, V. 1997. Molecular cloning and characterization of desacetoxyvindoline-4-hydroxylase, a 2-oxoglutarate dependent-dioxygenase involved in the biosythesis of vindoline in *Catharanthus roseus* (L.) G. Don. *Plant Molec Biol* **34:**935–948.

Veijola, J., Koivunen, P., Annunem, P., Pihlajaniemi, T., and Kivirikko, K.I. 1994. Cloning, Baculovirus expression, and characterization of the α subunit of prolyl 4-hydroxylase from the nematode *Caenorhaditis elegans*. This α subunit forms an active αβ dimer with the human protein disulfide isomerase/β subunit. *J Biol Chem* **269:**26746–26753.

Verhoeven, N.M., Schor, D.S.M., ten Brink, H.J., Wanders, R.J.A., and Jakobs, C. 1997. Resolution of the phytanic acid α-oxidation pathway: identification of pristanal as product of the decarboxylation of 2-hydroxyphytanoyl-CoA. *Biochem Biophys Res Commun* **237:**33–36.

Wada, A., Ogo, S., Watanabe, Y., Mukai, M., Kitagawa, T., Jitsukawa, K., Masuda, H., and Einaga, H. 1999. Synthesis and characterization of novel alkylperoxo mononuclear iron(III) complexes with a tripodal pyridylamine ligand: a model for peroxo intermediates in reactions catalyzed by non-heme iron enzymes. *Inorg Chem* **38:**3592–3593.

Wang, Q., VanDusen, W.J., Petroski, C.J., Garsky, V.M., Stern, A.M., and Friedman, P.A. 1991. Bovine liver aspartyl β-hydroxylase. Purification and characterization. *J Biol Chem* **266:**14004–14010.

Warn-Cramer, B.J., Macrander, L.A., and Abbott, M.T. 1983. Markedly different ascorbate dependencies of the sequential α-ketoglutarate dioxygenase reactions catalyzed by an essentially homogeneous thymine 7-hydroxylase from *Rhodotorula glutinis*. *J Biol Chem* **258:**10551–10557.

Watanabe, M., Sumida, N., Murakami, S., Anzai, H., Thompson, C.J., Tateno, Y., and Murakami, T. 1999. A phosphonate-induced gene which promotes *Penicillium*-mediated bioconversion of *cis*-propenylphosphonic acid to fosfomycin. *Appl Environ Microbiol* **65:**1036–1044.

Watkins, P.A., Howard, A.E., and Mihalik, S.J. 1994. Phytanic acid must be activated to phytanoyl-CoA prior to its α-oxidation in rat liver peroxisomes. *Biochim Biophys Acta* **1214:**288–294.

Wei, Y.-F., Carter, K.C., Wang, R.-P., and Shell, B.K. 1996. Molecular cloning and functional analysis of a human cDNA encoding an *Escherichia coli* AlkB homolog, a protein involved in DNA alkylation damage repair. *Nucl Acids Res* **24:**931–937.

Welford, R.W.D., Schlemminger, I., McNeill, L.A., Hewitson, K.S., and Schofield, C.J. 2003. The selectivity and inhibition of AlkB. *J Biol Chem* **278:**10157–10161.

Wellman, F., Lukacin, R., Moriguchi, T., Britsch, L., Schiltz, E., and Matern, U. 2002. Functional expression and mutational analysis of flavonol synthase from *Citrus unshiu*. *Eur J Biochem.* **269:**4134–4142.

Wellman, F., Matern, U., and Lukacin, R. 2004. Significance of C-terminal sequence elements for *Petunia* flavanone 3β-hydroxylase activity. *FEBS Lett* **561:**149–154.

Westendorf, A., Müller, A., and Babel, W. 2003. Purification and characterization of the enantiospecific dioxygenases from *Delftia acidovorans* MC1 initiating the degradation of phenoxypropionate and phenoxyacetate herbicides. *Acta Biotechnol* **23:**3–17.

White, A.K. and Metcalf, W.W. 2002. Isolation and biochemical characterization of hypophosphite/2-oxoglutarate dioxygenase. A novel phosphorus-oxidizing enzyme from *Pseudomonas stutzeri* WM88. *J Biol Chem* **277:**38262–38271.

Whiting, A.K., Que, L., Jr., Saari, R.E., Hausinger, R.P., Fredrick, M.A., and McCracken, J. 1997. Metal coordination environment of a Cu(II)-substituted α-keto acid-dependent dioxygenase that degrades the herbicide 2,4-D. *J Am Chem Soc* **119:**3413–3414.

Wierzbicki, A.S., Lloyd, M.D., Schofield, C.J., Feher, M.D., and Gibberd, F.B. 2002. Refsum's disease: a peroxisomal disorder affecting phytanic acid α-oxidation. *J Neurochem* **80:**727–735.

Wilmouth, R.C., Turnbull, J.J., Welford, R.W.D., Clifton, I.J., Prescott, A.G., and Schofield, C.J. 2002. Structure and mechanism of

anthocyanidin synthase from *Arabidopsis thaliana*. *Structure* **10:**93–103.

Wu, H., de Graaf, B., Mariani, C., and Cheung, A.Y. 2001. Hydroxyproline-rich glycoproteins in plant reproductive tissues: structure, functions and regulation. *Cell Molec Life Sci* **58:**1418–1429.

Yin, X., O'Hare, T., Gould, S.J., and Zabriskie, T.M. 2003. Identification and cloning of genes encoding viomycin biosynthesis from *Streptomyces vinaceus* and evidence for involvement of a rare oxygenase. *Gene* **312:**215–224.

Zhang, J.H., Quigley, N.B., and Gross, D.C. 1995. Analysis of *syrB* and *syrC* genes of *Pseudomonas syringae* pv. *syringae* indicates that syringomycin is synthesized by a template mechanism. *J Bacteriol* **177:**4009–4020.

Zhang, Z., Barlow, J.N., Baldwin, J.E., and Schofield, C.J. 1997. Metal-catalyzed oxidation and mutagenesis studies on the iron(II) binding site of 1-aminocyclopropane-1-carboxylate oxidase. *Biochemistry* **36:**15999–16007.

Zhang, Z., Ren, J., Stammers, D.K., Baldwin, J.E., Harlos, K., and Schofield, C.J. 2000. Structural origins of the selectivity of the trifunctional oxygenase clavaminic acid synthase. *Nat Struct Biol* **7:**127–133.

Zhang, Z., Ren, J.-S., Harlos, K., McKinnon, C.H., Clifton, I.J., and Schofield, C.J. 2002. Crystal structure of a clavaminate synthase-Fe(II)-2-oxoglutarate-substrate-NO complex: evidence for metal centred rearrangements. *FEBS Lett* **517:**7–12.

Zhou, J., Gunsior, M., Bachmann, B.O., Townsend, C.A., and Solomon, E.I. 1998. Substrate binding to the α-ketoglutarate-dependent non-heme iron enzyme clavaminate synthase 2: coupling mechanism of oxidative decarboxylation and hydroxylation. *J Am Chem Soc* **120:**13539–13540.

Zhou, J., Rocklin, A.M., Lipscomb, J.D., Que, L., Jr., and Solomon, E.I. 2002. Spectroscopic studies of 1-aminocyclopropane-1-carboxylic acid oxidase: molecular mechanism and CO_2 activation in the biosynthesis of ethylene. *J Am Chem Soc* **124:**4602–4609.

Zhou, J., Kelly, W.L., Bachmann, B.O., Gunsior, M., Townsend, C.A., and Solomon, E.I. 2001. Spectroscopic studies of substrate interactions with clavaminate synthase 2, a multifunctional α-KG-dependent non-heme iron enzyme: correlation with mechanisms and reactivities. *J Am Chem Soc* **123:**7388–7398.